



Master of Urban Climate and Sustainability (MURCS)

Exploring the triadic relation of urban form, wind, and air quality at
street level: A case of City of London, UK.

Kiran Ashok Apsunde

August 2020

Exploring the triadic relation of urban form, wind, and air quality at
street level: A case of City of London, UK.

Submitted in partial fulfilment for the requirements of
Master of Urban Climate & Sustainability (MUrCS) by:

Kiran Ashok Apsunde

S1839382

Glasgow Caledonian University, UK;
LAB University of Applied Sciences, Finland;
University of Huelva, Spain

Supervisors: Prof R Emmanuel, Dr J.A Dueñas Díaz, Dr J Fletcher

August 2020

Declaration

This dissertation is my own original work and has not been submitted elsewhere in fulfilment of the requirements of this or any other award.

Kiran Ashok Apsunde

August 2020

Abstract

The triadic relation on urban form, air quality and the wind environment at street level in a dense setting of the City of London is investigated through detailed characterisation of the urban form, wind simulation and statistical analysis in conjunction with AQ data observations for the period June – December 2018. While there are a plethora of broad level indicators describing urban morphology and form at neighbourhood and city levels, this study has taken a detailed approach towards identifying the street level canyon and canopy related metrics that influence the urban wind environment and ambient air quality. While it has tried out some of the existing metrics, the study has also introduced a set of new parameters that may further aid in understanding the triadic relation. For over 826 canyons mapped in the study area, the study has analysed about forty-two (42) urban form and morphological metrics to understand the influence of urban form on the wind environment.

Additionally, for sixty-three (63) canyons with AQ observations, sixty-four (64) wind and urban form related metrics were analysed for their statistical significance as predictors using the exploratory regression approach. Out of the 42 metrics used to investigate the influence of urban form on wind pattern, twenty-two (22) are found to have a statistical significance of greater than 50%. Moreover, out of the sixty-four (64) variables used towards investigating the role of wind and urban form metrics on AQ, ten (10) are found to exhibit a statistical significance of greater than 50%.

Amongst the newly introduced parameters Canyon Normality, Topographic Openness, Global solar Radiation, Effective Frontal Area, Wind Effect, Node Exposure and traffic Z-score are identified as statically significant predictors with a strong influence on the wind environment and consequently, the ambient air quality.

Dedication

Last few months have been difficult. Finishing this report has not been easy either. Many of us around the world have been through tough times, and some of us have even lost dear ones.

This piece of work is dedicated to all the health workers and families who have lost their dear ones during these unfortunate times of COVID-19.

Acknowledgements

The completion of my dissertation work would not have been possible without the support of many people. I would like to express my deepest gratitude to my guides and advisors, *Prof Rohinton Emmanuel* and *Dr José Antonio Dueñas Díaz*. Without your motivation, directions, support and insightful feedback in my research, this dissertation journey would have not been the same.

I would like to express my deepest appreciation to *Dr Julie Fitcher* for introducing me to the study area, for providing me with valuable data related to the City of London area, and for her guidance throughout the process.

I would also like to extend my greatest appreciation to all the *MURCS Academic Staff* and *Program Board*, for offering me this unique opportunity and making this Erasmus+ journey a positive and memorable one.

Further, I would like to thank my friend Megi for all the support, care, and company throughout my MURCS journey. I would also like to thank the entire MURCS 2018 batch, for all the wonderful memories we shared together. It has indeed been a great intercultural experience.

Finally, I am tremendously grateful to my family for their company, moral support and all the help they gave me when I needed it most. I thank my dear parents, *Suman* and *Ashok Apsunde* for their unconditional support throughout my years living away from home and particularly their understanding and encouragement for finishing my dissertation studies. I am particularly grateful to my elder brothers, *Jagdish* and *Ganesh*, for their understanding, support, and encouragement during my studies.

Table of Contents

Declaration.....	i
Abstract.....	ii
Dedication.....	iii
Acknowledgements.....	iv
Abbreviations:.....	x
1 Introduction	1
1.1 Rationale	1
1.2 Research questions	2
1.3 Aim and Objectives	2
1.4 Outline of the methodology	2
1.5 Disposition	3
2 Literature Review	4
2.1 Urbanisation, Sustainability and Human Wellbeing	4
2.2 Urban form and air quality.....	5
2.3 City of London (UK).....	6
3 Research Method.....	8
3.1 Research Philosophy and Approach.....	8
3.2 Overall framework	8
3.3 Data collection	9
3.4 Study area delineation	10
3.5 Data preparation.....	10
3.5.1 Air Quality (AQ) Data.....	10
3.5.2 Building Footprint and Height.....	11
3.5.3 Digital Surface Model (Elevation)	12
3.5.4 Elevation data consistency check	12
3.5.5 Meteorological Parameters	13
3.6 Characterisation of Urban Form	14
3.6.1 Geometric Descriptors	15
3.6.2 Terrain and Climate-Related Properties:	21
3.7 Traffic Hotspot Analysis and Node Exposure	23
3.7.1 Hotspot Analysis.....	23
3.7.2 Node Exposure	24
3.8 Wind Simulation & Metrics.....	25

3.9	Exploratory regression analysis and correlation matrix	27
4	Results and Analysis.....	29
4.1	Air Quality Observations	29
4.2	Study Region Meteorological Profile	32
4.2.1	Temperature and Rain	32
4.2.2	Cloud Cover	33
4.2.3	Wind Profile	34
4.3	Build Footprint Data and Lidar DSM Consistency Check	35
4.3.1	Building Footprint and Height Data	35
4.3.2	Lidar DSM Data	37
4.3.3	Consistency Check – OS Building Height and Lidar DSM Height.....	38
4.4	Urban Form Characteristics	38
4.4.1	Street Canyon Metrics	38
4.4.2	Canyon Normality	42
4.4.3	Urban Canopy Metrics	43
4.4.4	Terrain and Climate Metrics	49
4.5	Traffic Activity Intensity Hotpot.....	54
4.6	Wind Simulation and Metrics	55
4.6.1	Wind Speed Metrics.....	57
4.6.2	Wind Direction Metrics.....	59
4.6.3	Turbulence Intensity Metrics.....	60
4.6.4	Wind Effect – Direct and Indirect (WEDI)	61
4.7	Exploratory Regression, Variable Significance and Correlation Matrix	63
4.7.1	Urban form and the Wind Environment.....	63
4.7.2	Air Quality, Urban Form and the Wind Environment	65
5	Discussion on Results and Reflections	68
5.1	Seasonal Variation in Air Quality	68
5.2	Influence of Canyon Orientation.....	68
5.3	Key Findings - Performance of Urban Morphological and Geometrical metrics	69
5.3.1	Canyon Normality (CN)	69
5.3.2	Effective FAD (EFAD)	69
5.3.3	Topographic Openness (TO).....	69
5.3.4	Global Solar Radiations (GSR)	70
5.3.5	Wind Effect Index.....	70
5.3.6	Z-score and JN/Node Exposure	70
5.3.7	Road Width	71

5.3.8	Plan Area Density (PAD).....	71
5.4	Limitations.....	72
6	Conclusion.....	73
7	Recommendation for future studies.....	74
8	Bibliography	75
9	Appendices.....	79
9.1	List of Metrics and Abbreviations	79
9.2	Predictors used for filling data gaps.....	81
9.3	Air Quality Observations - Data Used for the Study	82
9.4	Urban form and the Wind Environment.....	84

List of Tables:

TABLE 3.1. DATA SOURCES	10
TABLE 3.2. CHARACTERISTICS OF THE THREE IDENTIFIED STATIONS	13
TABLE 3.3. URBAN CANYON METRICS	16
TABLE 3.4. CN CLASSES	18
TABLE 3.5. STANDARD DEVIATION BASED HOTSPOT CLASSIFICATION	24
TABLE 3.6. WIND SIMULATION OUTCOMES	26
TABLE 3.7. METRICS COMPUTED FOR CHARACTERISING THE WIND BEHAVIOUR	26
TABLE 3.8. STATISTICAL TEST CRITERIA ADAPTED FOR IDENTIFYING OLS	27
TABLE 4.1. CLUSTER-WISE SHARE OF PREDICTED DATA VALUES	30
TABLE 4.2. CLUSTERS-WISE CONCENTRATION OF NO ₂	30
TABLE 4.3. STATISTICAL SUMMARY OF THE NO ₂ CONCENTRATION BY CLUSTER	32
TABLE 4.4. MONTHLY METEOROLOGICAL PARAMETERS (2018)	33
TABLE 4.5. SUNSHINE- HOURS BASED CLOUD COVER OF THE STUDY REAGION	34
TABLE 4.6. WIND CHARACTERISTICS BY SEASONS	34
TABLE 4.7. WIND CHARACTERISTICS FROM 3 MAIN STATIONS	34
TABLE 4.8. VARIABLE OF HIGHTS (A) AND CLASSIFICATION OF BUILDING HIGHT (D)	36
TABLE 4.9. DSM DESCRIPTIVE STATISTICS	37
TABLE 4.10. STATISTICAL SUMMARY OF THE TWO DATASETS	38
TABLE 4.11. STATISTICAL SUMMARY OF CANYON METRICS	39
TABLE 4.12. CANYON NORMALITY CLASSIFICATION	42
TABLE 4.13. STATISTIC SUMMARY OF CANYON NORMALITY	43
TABLE 4.14. STATISTICAL URBAN CANOPY METRICS (GRID AND CANOPY LEVEL)	43
TABLE 4.15. STATISTICAL SUMMARY OF THE TERRAIN AND CLIMATE-RELATED METRICS	49
TABLE 4.16. WIND METRICS FOR 6M HEIGHT	56
TABLE 4.17. WIND METRICS FOR 12M TO 6M HEIGHT	56
TABLE 4.18. THE BEST OLS MODELS	67

List of Figures:

FIGURE 2.1. MAP - CITY OF LONDON	7
FIGURE 3.1. FRAMEWORK ADAPTED FOR THE STUDY	9
FIGURE 3.2. MONITORING POINTS AND CLUSTERS	11
FIGURE 3.3. WEATHER STATION LOCATION	13
FIGURE 3.4. CORE CANYON PARAMETERS (CERC,2015)	15
FIGURE 3.5. BUILDING DISTANCE TOLERANCE (CERC,2015)	16
FIGURE 3.6. ILLUSTRATION – PLAN AREA DENSITY AND FRONTAL AREA DENSITY (CERC,2015)	18
FIGURE 3.7. ILLUSTRATION ON FRONTAL ADVANTAGE	20
FIGURE 3.8. UPWIND AND DOWNWIND FAD NEIGHBOURS	20
FIGURE 3.9. CANOPY GRID -CANYON SPATIAL JOIN APPLICATION	21
FIGURE 3.10. STANDARD DEVIATION BASED HOTSPOT CLASSIFICATION	24
FIGURE 3.11. NODE EXPOSURE SCORE	25
FIGURE 4.1. SEASONAL CHANGE IN THE CONCENTRATION OF NO ₂ BY CLUSTERS	31
FIGURE 4.2. SPATIAL DISTRIBUTION OF NO ₂	31
FIGURE 4.3. TEMPERATURE AND RAINFALL PROFILE OF THE STUDY REGION	33
FIGURE 4.4. SEASONAL CLOUD COVER OF THE STUDY REGION	34
FIGURE 4.5. WIND SPEED IN THE STUDY REGION	35
FIGURE 4.6. BUILDING HEIGHT DISTRIBUTION MAP (B) / PIE CHART (C)	36
FIGURE 4.7. LIDAR DSM MAP	37
FIGURE 4.8. HEIGHT CONSISTENCY CHECK: DSM VS BUILDING DATA	38
FIGURE 4.9. CANYON ASPECT RATIO MAP: HWR AVERAGE	40

FIGURE 4.10. LENGTH WIDTH RATIO (LWR) MAP.....	40
FIGURE 4.11. HEIGHT DIFFERENCE (HD) MAP.....	41
FIGURE 4.12. HEIGHT DIFFERENCE- LEFT TO RIGHT (HDLR) MAP.....	41
FIGURE 4.13. CANYON NORMALITY DISTRIBUTION.....	42
FIGURE 4.14. CANYON NORMALITY MAP.....	42
FIGURE 4.15. MEAN FAD VALUES OF NEIGHBOURING CELLS.....	44
FIGURE 4.16. PLAN AREA DENSITY MAP.....	45
FIGURE 4.17. CANYON PLAN AREA MAP.....	45
FIGURE 4.18. FRONTAL AREA DENSITY MAP.....	46
FIGURE 4.19. CANYON FRONTAL AREA MAP.....	46
FIGURE 4.20. EFFECTIVE FRONTAL AREA MAP.....	47
FIGURE 4.21. CANYON EFFECTIVE FRONTAL AREA.....	47
FIGURE 4.22. BUILDING VOLUME DENSITY MAP.....	48
FIGURE 4.23. AVERAGE BUILDING VOLUME MAP.....	48
FIGURE 4.24. OPENNESS VALUE MAP.....	50
FIGURE 4.25. CANYON OPENNESS MEAN VALUE MAP.....	50
FIGURE 4.26. GLOBAL SOLAR RADIATION MAP.....	51
FIGURE 4.27. CANYON SOLAR RADIATION MAP.....	52
FIGURE 4.28. WIND EFFECT (DIRECT) MAP.....	53
FIGURE 4.29. WIND EFFECT (DIRECT) MAP.....	53
FIGURE 4.30. TRAFFIC HOTSPOT ANALYSIS MAP.....	54
FIGURE 4.31. TRAFFIC HOTSPOT CANYON MAP (Z-SCORE).....	55
FIGURE 4.32. WIND SIMULATION OUTPUT (WIND VECTORS).....	55
FIGURE 4.33. WIND SPEED MAP.....	57
FIGURE 4.34. AVERAGE CANYON WIND SPEED MAP.....	58
FIGURE 4.35. VERTICAL SPEED FLUX MAP.....	58
FIGURE 4.36. WIND DIRECTION RASTER MAP.....	59
FIGURE 4.37. VERTICAL DIRECTION FLUX MAP.....	60
FIGURE 4.38. CANYON TURBULENCE INTENSITY MAP.....	61
FIGURE 4.39. WIND EFFECT (DIRECT +INDIRECT) MAP.....	62
FIGURE 4.40. WIND EFFECT (DIRECT+ INDIRECT) (WEDI) MAP.....	62
FIGURE 4.41. VARIABLE RELATIONSHIP CONSISTENCY (LEFT).....	63
FIGURE 4.42. VARIABLE STATISTICAL SIGNIFICANCE & CORRELATION (RIGHT).....	63
FIGURE 4.43. VARIABLE RELATIONSHIP CONSISTENCY – HIGH NORMALITY (LEFT).....	64
FIGURE 4.44. VARIABLE RELATIONSHIP CONSISTENCY – MEDIUM NORMALITY (MIDDLE).....	64
FIGURE 4.45. VARIABLE RELATIONSHIP CONSISTENCY – LOW NORMALITY (RIGHT).....	64
FIGURE 4.46. VARIABLE SIGNIFICANCE BY NORMALITY CLASS.....	65
FIGURE 4.47. VARIABLE RELATIONSHIP CONSISTENCY (LEFT).....	66
FIGURE 4.48. VARIABLE STATISTICAL SIGNIFICANCE AND CORRELATION (RIGHT).....	66
FIGURE 5.1. PAD MAP SAMPLING.....	71

Abbreviations:

AQ – Air Quality

BLWR – Built Length-Width Ratio

CC – Canyon Coverage

CEDA – Centre for Environmental Data Analysis

CFD – Computational Fluid Dynamics

CN – Canyon Normality

DSM – Digital Surface Model

FAD – Frontal Area Density

GDP – Gross Domestic Product

GEP – Google Earth Pro

GSR – Global Solar Radiation

HD – Height Difference

HDLR – Height Difference – *Left to Right*

HWR – Height Width Ratio

HWR_Δ – Height Width Ratio Difference

LAEI – London Atmospheric Emissions Inventory

LWR – Length Width Ratio

MIDAS – Met Office Integrated Data Archive System

NLA – New London Architecture

NO₂ – Nitrogen Dioxide

OLS – Ordinary Least Squared

OS – Ordnance Survey

PAD – Plan Area Density

PM₁₀ – Particulate matter 10 micrometers or less in diameter

PM_{2.5} – Particulate matter 2.5 micrometers or less in diameter

SO₂ – Sulfur dioxide

SVF – Sky View Factor

TO – Topographic Openness

UK – United Kingdom

EU – European Union

1 Introduction

1.1 Rationale

Cities generate over 80% of the world's GDP and are the economic and social centres of the world (*The World Bank, 2019*). Today, over 50% of the global population lives in cities (*United Nations, 2015*). Following the current trends, by 2050, it is anticipated that nearly 70% of the world's population will be residing in cities (*The World Bank, 2019*). If managed well, urbanisation can contribute to sustainable and climate-resilient growth. However, the rate and scale of urbanisation present cities with a plethora of physical, socio-economic, and environmental challenges. Exacerbation of heat stress due to UHI alongside air, water, land, and noise pollution are already posing severe risks to human health and wellbeing in urban settings. With changing climate and increasing inequality in socioeconomic conditions within the cities, the vulnerability of the urban population is anticipated to increase significantly. Recognising this, a great emphasis has been laid on sustainable urban development in recent years. The United Nations Sustainable Development Goal (SDG) 11 aims specifically at making cities and human settlements safe, resilient, and sustainable (*United Nations, 2015*). Over the last two decades, the significance of urban form in the quest for sustainable development has seen a gradual recognition globally (*Marquez & Smith, 1999*). Owing to some positive influences on thermal comfort and energy consumption, there appears to be a consensus towards 'compact' urban form as a key to urban sustainability (*Emmanuel & Steemers, 2018*). However, studies indicate that although compact cities may decrease the operational energy consumption to some extent, they tend to have poor air quality with high concentrations of pollutants like NO₂, PM₁₀, PM_{2.5} and SO₂ (*Cárdenas Rodríguez, Dupont-Courtade & Oueslati, 2016*). Thus, there are significant shortcomings and oversights in terms of impacts and consequences of compact form on local microclimates and what this means for energy demand, thermal comfort, air quality and health and wellbeing (*Emmanuel & Steemers, 2018*). Extensive research has been done on the effects of urban form on local climate, thermal comfort, and energy consumption over the past five decades. However, despite its recognition among researchers, there is dearth of research examining the dynamic relationship between built forms and overlying climate on air quality. While a number of studies analysing cities at a broad scale have emerged in the recent years, the degree to which urban form impacts air quality at street level; and urban form metrics that are pivotal in altering the ambient air quality and the wind environment are yet to gain wider attention. Acknowledging this, the proposed study aims at characterising the urban setting using a set of parameters and demonstrating the role of urban form in modifying the background air quality conditions. The overarching goal of the study is to further the understanding on the subject and identify urban form metrics that may potentially

inform the development of a broad planning framework that incorporates 'Built Form' driven effects on public realm while guiding urban development in a climate-sensitive manner.

1.2 Research questions

Through an integrated use of numerical modelling, spatial modelling and statistical analysis, the study aims to answer the following questions:

- a. What are the critical morphological and geometrical parameters used for characterising the urban form?
- b. What are the most influential urban form parameters at street level with regards to wind flow and air quality in the urban areas?
- c. What are the AQ trend in the study region, and how are they interconnected with the built form?

1.3 Aim and Objectives

The overall aim of this study is to examine the influence of urban form on the wind environment and the background air quality and identify the potential metrics that may facilitate the development of a planning framework intended towards guiding urban development in a climate-sensitive manner.

The aforementioned aim shall be attained through the following key objectives:

1. Develop an understanding of the chosen urban setting by characterising it for its geometrical, spatial, thermal, and meteorological metrics using primary and secondary data.
2. Simulate, explore, and characterise the wind behaviour within the study area.
3. Conduct geospatial modelling to map the city's pollution profile and to identify the pollution hotspots.
4. Devise and adopt a new set of indicators that may potentially facilitate in exploring the triadic relation.
5. Explore spatially and statistically the relationships between urban form metrics, wind pattern and air quality parameters.

1.4 Outline of the methodology

The study intends to investigate the triadic relation on urban form, air quality and the wind environment at the street level in a dense setting of the City of London through a detailed approach that entails characterisation of the urban form using secondary data, understand air quality and emission activity trends, wind simulation and statistical analysis. Using a set of tools, the method intends to measure the

urban form metrics, simulate wind environment, and finally explore their statistical interaction with the observed air quality. Tools like ArcGIS 10.8, SAGA GIS, WindNinja, Urban Canopy Tool Urban Canyon Tools, etc. are proposed for the study.

1.5 Disposition

This dissertation is structured into seven main chapters:

Chapter 1 starts by briefly introducing the topic to the reader by identifying the problems, scope, aims and objectives of the dissertation.

Chapter 2 presents an overall review of literature indicating state of the art.

Chapter 3 provides an outline of the Methodological Framework, following with the approach on data collection, preparation, and a presentation of all the indicators and method used for the analysis.

Chapter 4 offers the analysis conducted and results obtained from the indicators considered and created. The chapter concludes with an analysis of Exploratory Regression, Variable Significance and Correlation Matrix.

Chapter 5 presents the discussion on results and reflections and concludes with key findings of the dissertation.

Chapter 6 consists of a brief summary of the conclusions.

Chapter 7 provides the recommendations for future studies, following two previews chapters.

2 Literature Review

2.1 Urbanisation, Sustainability and Human Wellbeing

Being the economic and social centres of the world, urban areas have a crucial role to play in sustainable development and tackling climate change. Housing over 4 billion people, i.e. over half the world's population, cities are not only the primary consumers of natural resources but also the major producer of pollution and waste. Today, cities consume close to 2/3 of the world's energy and account for more than 70% of global greenhouse gas emissions (*The World Bank, 2019*). However, despite being the source of the problem, cities are also a site of the solution, and if designed and managed well, they can significantly contribute towards a reduction in degradation of natural resources and the environment (*Marquez & Smith, 1999*).

Triggered by the publication of the United Nations' report "Our Common Future" in 1987, Sustainable development has been high on the agenda of urban planners for a quarter of a century. Towards this end, the importance of urban form in the quest for sustainable development has been increasingly recognised. Though an outcome of physical planning practices, a city's urban form is a product of its social and economic activity patterns. The urban form essentially refers to the land-use patterns, infrastructure and all other physical forms of developments that facilitate human activities and their interactions. (*Marquez & Smith, 1999; Næss, 2014*).

Current urban development comes with a high rate of conversion of natural areas and farmland into urbanised land, causing severe implications to the urban and peri-urban ecosystems and human wellbeing. Thus, combating urban sprawl has been a priority for urban planners and researchers aiming to promote sustainability in the urban context. The role of densification of urban areas has long been a topic of hot discussion among planners and environmentalists. Several studies have concluded that dense urban structures are favourable in order to reduce greenhouse gas emissions from transport, limit energy consumption in buildings and protect farmland and natural areas in the surroundings of the city. (*Næss, 2014*). Thus, there appears to be a consensus towards compact urban form as a key to urban sustainability (*Emmanuel & Steemers, 2018*). In 1990, the European Commission promoted the "compact city" as the most sustainable model for urban development (*Marquez & Smith, 1999; Næss, 2014*). However, a considerable body of international literature has highlighted the tensions between compact urban development strategies and public health. Several studies have concluded that population living in inner-city districts, i.e. dense areas of the city, are more exposed to air pollution, noise and traffic accidents than their suburban counterparts (*Næss, 2014*). A study encompassing 249

large urban zones in the European Union showed that cities that are dense, highly constructed and fragmented suffer from higher concentrations of NO₂, PM₁₀ and SO₂ (Cárdenas Rodríguez, Dupont-Courtade & Oueslati, 2016). With changing climate and unprecedented rates of urbanisation, cities will be presented a plethora of physical, socio-economic, and environmental challenges. Risks posed to human wellbeing due to UHI induced heat stress, air and noise pollution are likely to be severe in the years to come. Towards this end, due consideration should be given towards incorporating the implications of compactness on sustainable and climate-sensitive urban design.

2.2 Urban form and air quality

“The adverse effects of air pollution are realised globally. Pollutants such as particulate matters, ozone, oxides of nitrogen and hydrocarbons, destroy tissues in people, animals and plants and also impair respiratory functions. The impacts extend beyond human health and encompass issues such as damage to agriculture and forestry, disruption to natural ecosystems, degradation of building materials and the aesthetic aspects of the environment (for instance, visibility). The costs of air pollution, from health and other damages, coupled with public concern, are thus prompting governments to seek better urban air quality.” (Marquez & Smith, 1999).

The dynamics of urban air environment are complicated. It has been argued that urban form, through its direct and indirect effects on travel behaviour, land cover, urban wind flow, and spatial distribution of land use, can significantly alter the urban air quality (Chen Lu & Yi Liu, 2016; Clark, Millet & Marshall, 2011). The relationship between urban form and air quality has attracted attention from many urban planners and environmentalists; thus, understanding the influences of the urban form of air quality may be a crucial factor for understanding the dynamics of urban air environment (Chen Lu & Yi Liu, 2016). Although a widely under-researched area, a few studies have attempted exploring the interaction between urban form and air quality at different scales. Using indices like compact ratio index, the fractal dimension index and Boyce-Clark shape index to characterise the urban morphology, Lu & Liu (2016), conducted a macro-level study to capture the influence of urban form on air quality in 287 cities of China. They found that cities with high compact ratio and cities that are **H-** or **X-** shaped showed relatively lower levels of SO₂ and NO₂ concentration. Although in contradiction with the popular argument - *where compact cities are said to have relatively poor air quality* - this influence was by and large attributed to the reduction in urban traffic and improved industrial efficiency incurred through compactness. Clark, Millet & Marshall (2011), used city shape, road density, jobs-housing imbalance, population density, and population centrality to characterise the form of 111 cities in USA and found that population density and

population centrality were the strongest predictors of air quality. Higher population densities strongly correlated with higher concentration levels, whereas higher population centrality strongly correlated with lower concentration levels. The study offered an insight into the potential air quality trade-offs between population centrality and population density. Cities are composed of a wide array of units. These studies, owing to their scale, considered cities as single units. Consequently, the influences of urban form on air quality within the cities could not be understood.

Krüger, Minella & Rasia (2011), conducted a neighbourhood scale study in Curitiba, Brazil to understand the influence of urban form on pollution dispersion and found that wind speed and direction has a significant influence on pollution dispersion in urban street canyons. Street canyons with relatively higher wind speeds performed better at pollutant dispersion in comparison to those with low wind speeds. Further, the dispersion was found to be better under northerly wind conditions than easterly conditions. The study, however, predominantly focussed on wind parameters and lacked establishing relationships between morphological or geometrical parameters and air pollution. Several studies have used a set of urban geometry parameters to understand the corresponding implications on thermal comfort and energy consumption (For instance, see *Chatzipoulka & Nikolopoulou, 2018*). Although this study did not explore the link between urban form and air quality, some of the metrics used are widely adopted for air pollution studies in urban areas. In 2014, *Edussuriya et al.* highlighted that street-level pollution is a multidimensional problem and deals with a large number of complex variables other than its source. The study analysed about 21 variables, of which only nine variables were found significant. This study, however, lacked wind simulation and was based only on statistical correlations between the urban form metrics and air quality. To fully understand the phenomena, it is essential to identify the critical parameters in action in an urban environment that affect air dispersion (*Edussuriya et al., 2011*). Since then, several studies have emerged; however, most of these studies are limited to isolated cuboids and do not reflect the real-world urban environment. Therefore, this study is the first attempt to investigate the triadic relationship of a real-world case thoroughly. Further, the study investigates around 64 variables, representing the urban canyons at great detail – including geometrical parameters on either side of the canyons.

2.3 City of London (UK)

Exposure to pollutants like particulate matter (PM_{2.5}), Ozone and NO₂ is responsible for over half a million premature death across Europe (*Neslen, 2019*). The UK happens to be the fourth most affected country in the EU with at least 40,000 early deaths from lung and heart disease (*Carrington, 2019; Neslen, 2019*). Air quality in major cities of the UK – especially London - is of growing concern. Located in the heart of London, the City of London, houses over 7,500 residents and 24,000 business. With a

working population of over 510,000, the city witnesses a massive influx of population on a daily basis. By 2036, the working population in the city is projected to increase to 640,000. The City of London Corporation (City Corporation) is the governing body of the city. (*City of London Corporation, 2019*).

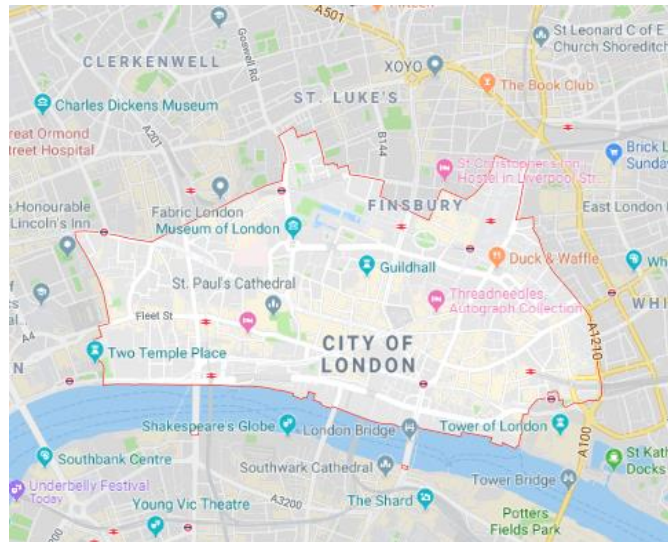


Figure 2.1. Map - City of London (Google, 2020)

As in most areas of central London, the City of London suffers from high levels of NO_2 , $\text{PM}_{2.5}$ and PM_{10} owing to which it has been declared an Air Quality Management Area. The quality of air in the city of London is heavily influenced by the emissions generated in Greater London and other surrounding areas. It is estimated that over 75% of particle pollution and 40% NO_2 emissions measured in the city of London originates outside the city boundary. Stationary and mobile combustion - *primarily associated with buildings and road traffic* - is the primary local source of pollution. Despite several measures from the City Corporation, maintaining healthy air quality continues to be a challenge. Owing to the high density of working population in the city, a range of health impacts have been registered. High concentration levels have resulted in increased hospital admissions for those suffering from respiratory and cardiovascular diseases. (*City of London Corporation, 2019*).

Irrespective of the source of pollution, the dense urban form of the city might have some role to play in the city's air quality problem. Given this context, the City of London would serve as a good case study to explore the dynamics between urban form and ambient air quality.

3 Research Method

This chapter presents an outline of the Methodological Framework, following with the approach on data collection, preparation, and a presentation of all the indicators and method used for deducing and analysing them.

3.1 Research Philosophy and Approach

Giving the nature of the study, Interpretivism/constructivism best describes this dissertation. As defined by Patel (2015), "*Interpretivism/constructivism describes that the reality needs to be interpreted and is used to discover the underlying meaning of event and activities*".

The research moves between Deductive and Inductive *Research*. For instance, after exploring existing literature, it is to be highlighted that little to none of the existing theory has studied the triadic relation on form, wind and air quality at the street canyon level nor are there studies that have investigated and explored further whether the change in orientation triggers a change in the influence of urban form metrics on either wind behaviour or air quality. Therefore, based on the existing literature, new observations and metrics have been proposed in order to further the current understanding on the subject.

For this research, a case study method is used to investigate the triadic relation on urban, air quality and the wind environment at street level in a dense setting of the City of London. The research takes place in a specific context and follows the strategic approach of a case study that investigates a contemporary phenomenon within its context with unclear evident boundaries between the phenomenon and its context (*Gillham 2000; Yin,2014*).

3.2 Overall framework

Literature suggests that there seems to be a correlation between the urban form, wind environment and air pollution. While the different form may trigger changes in wind metrics, certain wind velocities, and turbulence conditions may contribute to the removal of pollutants (*Yang, Shi, Shi, et al., 2020*). Thus, a framework based on this understanding has been considered for this study. Figure 3.1 schematically outlines the approach adopted within the broader framework.

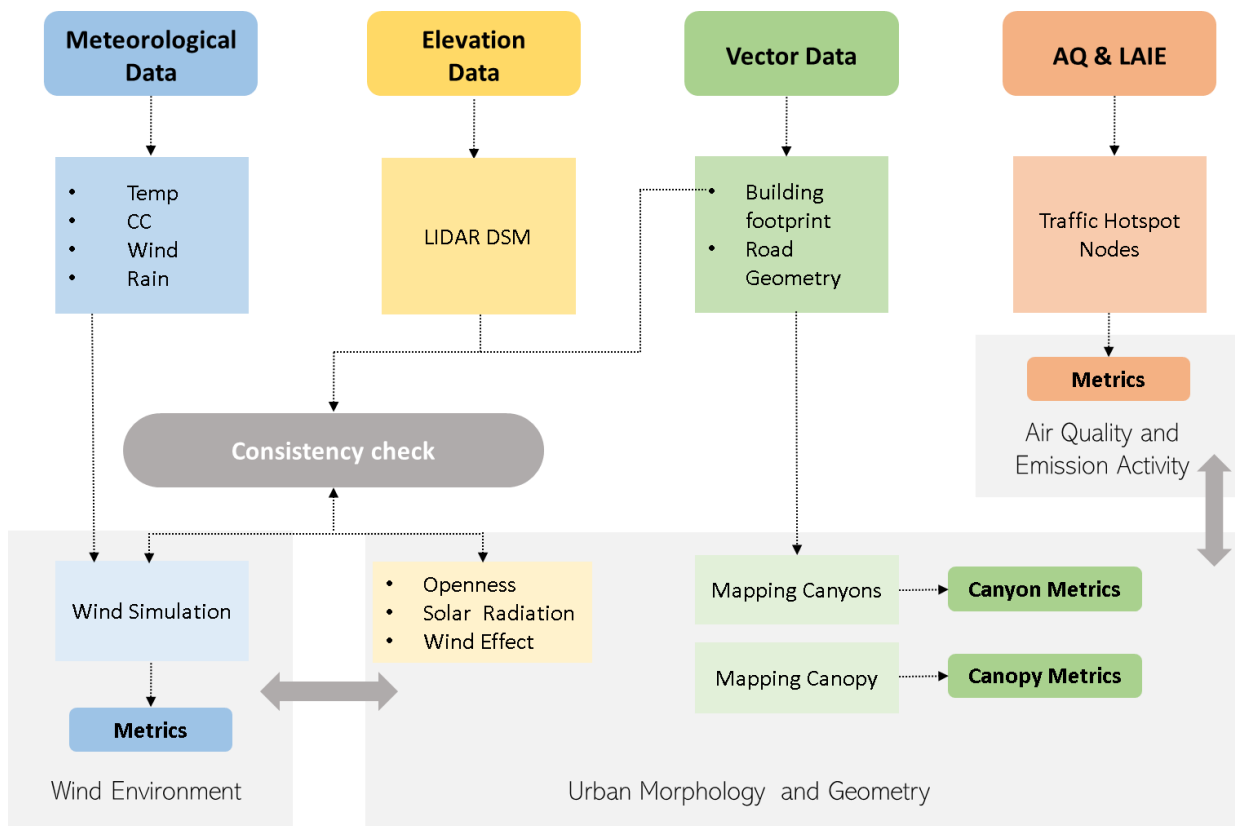


Figure 3.1. Framework adapted for the study

“Good air quality is a valuable asset as far as the health of urban ecosystems, and human wellbeing is concerned. However, maintaining healthy air quality is challenging in urban settings where dense human population exist in confined spaces like buildings and street canyons, often in close proximity to multiple sources of air pollution. Air quality in urban settings is governed by the **strength and density of emission sources**, the **ability of the atmosphere to mix and advect air pollutants**, and **removal of air pollutants**.” (Oke, Mills, Christen & Voogt, 2017). Acknowledging these factors, the study broadly encompasses the following methodological stages to reach its intended objectives:

- *Characterisation of urban morphology and geometry*
- *Emission intensity hotspot assessment and AQ analysis*
- *Simulating the wind environment within the study area.*
- *Exploring the interrelationship between urban form, wind environment and air pollution.*

3.3 Data collection

A summary of the data used for this study is presented in the table below.

Table 3.1. Data Sources

DATA	YEAR	REMARKS	SOURCE
Elevation data	2009-2015	Secondary data 0.5m resolution	Lidar DSM
AQ	2018	Primary data	Dr. Julie Fitcher Field Observation
Road	2019	Secondary data	Ordnance Survey (OS)
Building Footprint	2019	Secondary data	Ordnance Survey (OS)
Met Data	2018	Secondary data	MIDAS

3.4 Study area delineation

Due to the diversity in its urban form that has led to a creation of a series of extreme and diverse urban microclimates, the city of London is considered a perfect monitoring study area to improve our understanding on the effects of built form on the wider environment. An Urban Climate Walking tour was availed with the help of Dr. J. Fitcher, to explore the influence of building forms on the various urban climate effects and further its influence on the dispersion of heat and pollution. The walk along its route entails a network of air quality monitoring points - data from which has been used for this study. Thus, a radius of 900m from the centre of the climate walking tour, covering all monitoring points, has been demarcated as the study area or the core analysis area for this exercise (*Figure 3.2*). For certain modelling tasks, an additional 20%, i.e. 360m buffer, has been considered to avoid errors along the periphery.

3.5 Data preparation

This section elaborates on the steps taken towards overcoming data gaps and preparing the data for the subsequent step.

3.5.1 Air Quality (AQ) Data

Spanning over eight (08) clusters in the City of London area, the acquired AQ monitoring data representing a network of eighty-two (82) Nitrogen Dioxide (NO₂) observation points, corresponds to the period between February 2018 (R1) to February 2019 (R12) (*Figure 3.2*). However, the raw data comprises of significant temporal gaps. In order to overcome the effects of missing data, the timeframe with the least data gaps, i.e. June to December 2018, has been preferred for this study. For the identified timeframe, only observation points with temporal data coverage equal to or greater than (\geq) 80% of the

timeframe have been retained. In order to fill the remnant data gaps, a combinatorial approach entailing cluster wise correlation matrix and geographical proximity has been deployed. In other words, observation points within the respective clusters were cross-correlated, and the observation points exhibiting high correlation and geographic proximity are used as predictors for data filling. On certain occasions, observation points from the neighbouring clusters have also been considered for the combinatorial method. The rationale behind this approach is to avoid excessive data filling and to retain the representativeness of the field observations.

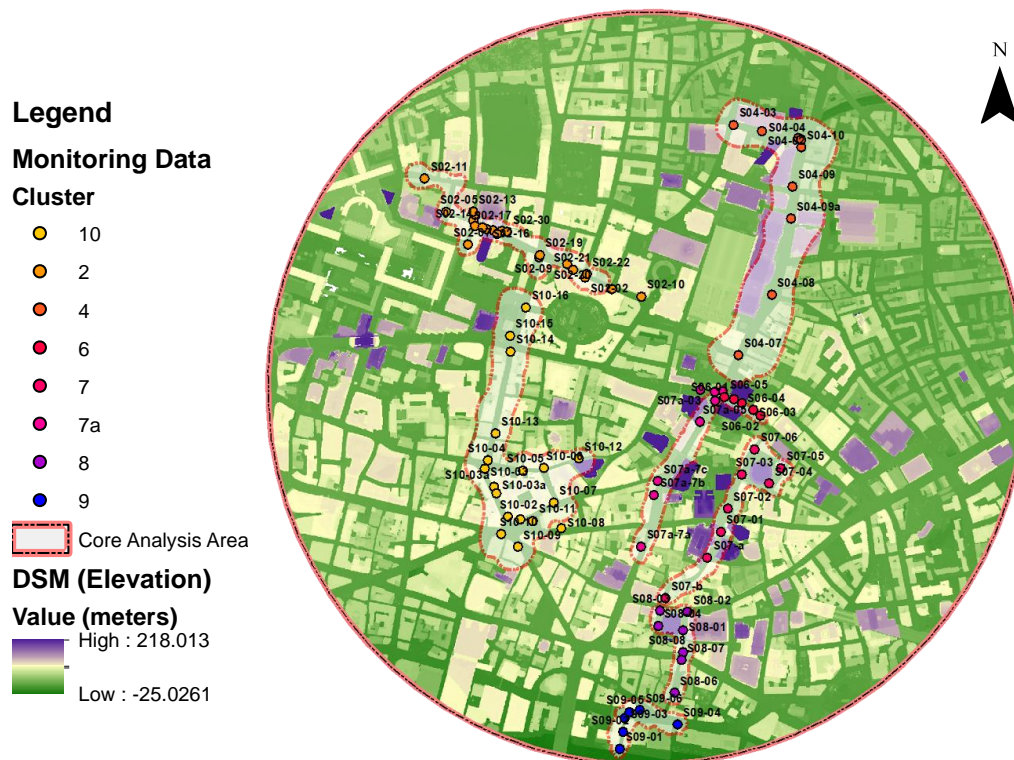


Figure 3.2. Monitoring Points and Clusters

3.5.2 Building Footprint and Height

The building footprint and height data is a crucial input towards computing the urban morphological parameters discussed in the subsequent steps. While studying the interaction between urban form and AQ, it is essential to ensure that the building data corresponds to the state of built form during the AQ monitoring timeframe. This ensures that the computation of the corresponding urban morphological parameters is not influenced due to outdated data, and thus allows for a better understanding of the interaction between built form and AQ. Thus, using satellite images on the Google Earth Pro (GEP) platform in conjunction with the New London Architecture (NLA) database on new constructions, the

OS Building Footprint and Height Data (2019) has been validated prior to its application in the study. Using ArcGIS 10.8 and GEP, new buildings are included while the demolished ones are excluded. An additional buffer of 20% was adopted to avoid computational errors on the edge/periphery of the study area.

3.5.3 Digital Surface Model (Elevation)

The surface data obtained in the form of 1 km x 1 km Lidar Digital Surface Model (Lidar DSM) images of 0.5m resolution, corresponds to the acquisition period 2009-2015. The data represents the elevations of the surface of the Earth, including features like trees, buildings, bridges, etc. Considering the fine resolution of the surface data, it has been preferred for the wind and solar simulations discussed in later parts of this report. However, before its application, the data has been validated and rectified using the updated Building Footprint and Height data as references. Towards this end, tools like *Create a Constant Raster*, *Raster Calculator*, *Conditional Function*, and *Mosaic to New Raster* available in the ArcGIS environment are applied in combination.

3.5.4 Elevation data consistency check

As it can be inferred from Section 3.4.2 and Section 3.4.3, two different sources of elevation data have been used for this study viz. Remotely Sensed Data (Lidar DSM) and Observed Data (OS Building Height). The latter is applied towards computing urban morphological parameters while the former serves as input towards simulating the wind behaviour, solar insolation and topographic openness in the study area. This implies that owing to the difference in data acquisition methods; the respective elevation values may vary across the two datasets, which in turn may influence the respective metrics derived from the two datasets. Thus, the two datasets have been checked for consistency, and the degree of similarity between them is highlighted prior to investigating the influence of urban morphological parameters on wind behaviour. For checking the consistency across the two datasets, Buildings heights for the study area and the 20% buffer area, are extracted using Lidar DSM data. These DSM based heights are then compared with the OS Building Height data.

3.5.5 Meteorological Parameters

Meteorological parameters like wind speed, wind direction, temperature and cloud cover required for the wind simulation exercise are derived from the acquired meteorological datasets. The following subsections entail more details on the data preparation approach adopted at this stage.

3.5.5.1 Wind

The UK Met Office’s MIDAS database accessed on the Centre for Environmental Data Analysis (CEDA) portal, offers data for nine (09) stations within the Greater London region. However, only three of these stations provide wind observations corresponding to the chosen timeframe of this study, i.e. June 2018 to December 2018. Characteristics of the three identified stations have been included in *Table 3.2*. The stations are situated at a radial distance ranging from 15 to 26 kilometres from the site centre in the westward direction.

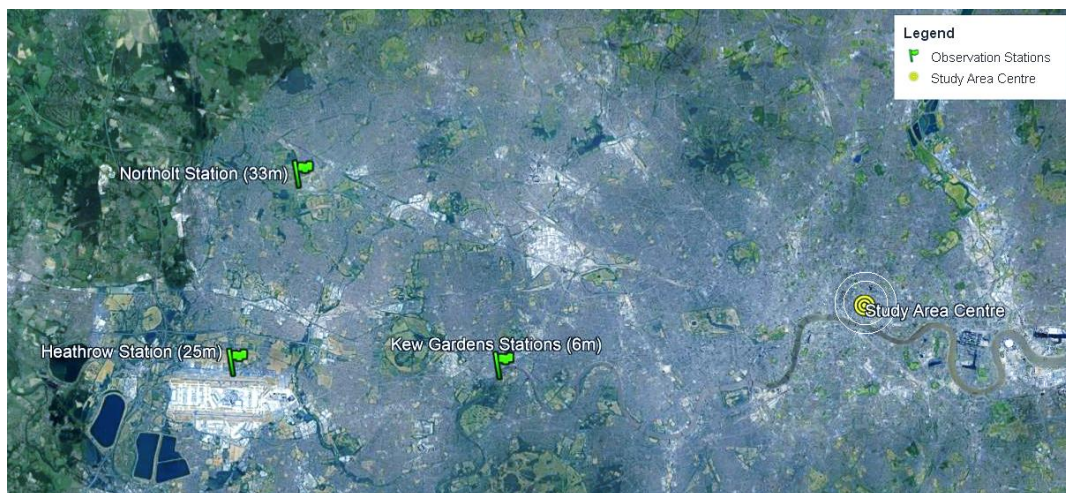


Figure 3.3. Weather Station Location (Google, 2020)

Table 3.2. Characteristics of the three identified stations

Station Name	Latitude	Longitude	Measurement Height (m)	Distance to Site centre (Km)	Time-frame
Heathrow	51.479	-0.451	25	25.87	June to December (2018)
Northolt	51.549	-0.417	33	23.5	
Kew Gardens	51.482	-0.294	6	15.03	

As the table indicates, the height of measurements for respective weather stations is variable. Thus, before deriving the seasonal and overall mean values of wind speed in the study area, the observations for Heathrow and Kew Gardens stations have been transposed to 33 m using the power law equation:

$$U_Z = V_G \left(\frac{Z}{Z_G} \right)^\alpha$$

Where, V_G = Observed Velocity at height Z_G ; Z = height at which the velocity is to be computed (33m); and α = Surface roughness factor which has been assumed as 0.28 given the suburban areas that surround the observation stations (*Erell, Pearlmutter and Williamson, 2015*).

3.5.5.2 Temperature and Rainfall

At this stage, the monthly, seasonal and overall values of parameters such as maximum temperature (T_{max}), minimum temperature (T_{min}), rainfall, and the number of Rainy days are computed using the weather data acquired from Accuweather Archives for the study timeframe. Days with rainfall greater than or equal to (\geq) 0.5mm have been considered as Rainy days.

3.5.5.3 Cloud Cover

Cloud cover estimation using sunshine hours has shown significant consistency with the field-based observations (*Hoyt, 1977*). Thus, owing to the lack of data availability on cloud cover for the study area, the cloud cover has been estimated using the sunshine hours data sourced from the CEDA portal and the possible daily sunshine hour for the respective month. Towards this end, the following equation has been applied for cloud cover estimation:

$$CC_x = \left(1 - \frac{SH_{Observed}}{SH_{Possible}}\right) \times 100$$

Here,

CC_x = Percentage Cloud Cover for Month 'X'

$SH_{Observed}$ = Observed Mean Daily Sunshine Hours

$SH_{Possible}$ = Total Possible Daily Sunshine Hours or Day Length

3.6 Characterisation of Urban Form

Williams et al. (2000) describe the urban form as “morphological attributes of an urban area at all scales”. As closely seen related to scale, it includes different spatial features such as city, neighbourhood, urban block, street, and individual buildings. These, are elements that influence in analysing, measuring and understanding and shaping the urban form (*Dempsey et al., 2010*). Further, the UK Government defines urban form as “the physical characteristics that make up built-up areas, including the shape, size, density and configuration of settlements” (*Foresight Government Office for Science, 2014*).

Despite the heterogeneity of the urban canopy in almost any real city, it is useful to describe the built form and the spaces in between in terms of quantifiable measures that express its properties that influence the micro-scale climate (*Erell, Pearlmutter and Williamson, 2015*). For this study, the urban

form has been primarily described using geometrical parameters pertaining to street canyons and urban canopy. Additional metrics based on terrain and climatic factors have also been incorporated. This section of the report discusses the approach adopted towards computing the aforesaid urban form parameters.

3.6.1 Geometric Descriptors

3.6.1.1 Street Canyon Parameters

“In street canyons, the concentration of pollutants is high due to the presence of (ground level) vehicular and anthropogenic emissions and to the weak air ventilation caused by a recirculating motion between the buildings. The proximity between emitters (vehicles, chimneys) and receptors makes these regions extremely vulnerable to health risks” (Fellini et al., 2020). Street canyon refers to the linear space such as a street or passage which is bounded on both sides by vertical elements such as the walls of adjacent buildings (Erell, Pearlmutter and Williamson, 2015). The ADMS Street Canyon Tool, an ArcGIS based tool by CERC, has been used to map the street canyons and to calculate the core parameters describing them. The street canyon tool uses road network, building geometry and building height as critical inputs for the mapping and computation process. On both sides of the mapped street canyons, the tool computes the following core parameters: Canyon Heights (Maximum, Minimum, and Average), Canyon Width, Canyon Length, and Built Length (Figure 3.4).

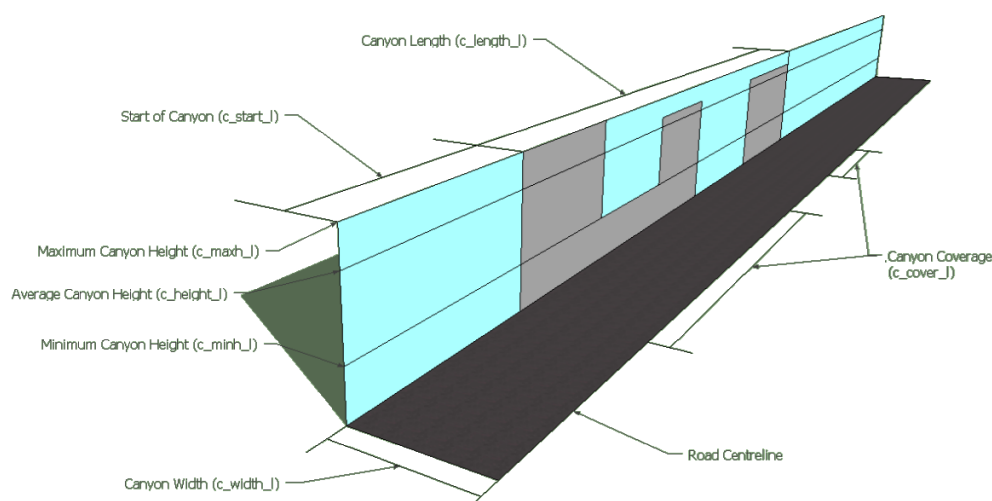


Figure 3.4, Core Canyon Parameters (CERC,2015).

For this study, the road network sourced from Ordnance Survey data, and the updated building footprint and height data day have been used for computing the aforesaid core parameters. It should be noted that while mapping the street canyons following input factors, as suggested for London in the user guide, are applied:

Maximum distance to the nearest building: This defines the distance from the road centreline the tool will search to find suitable base buildings. A 50m distance has been used for this study.

Building distance tolerance: This factor is a combination of a proportion of the minimum distance - from the road centreline to the nearest building - and a constant distance. As suggested in the tool user guide, for London, the adopted proportion is 0.3 while the constant distance is 14m.

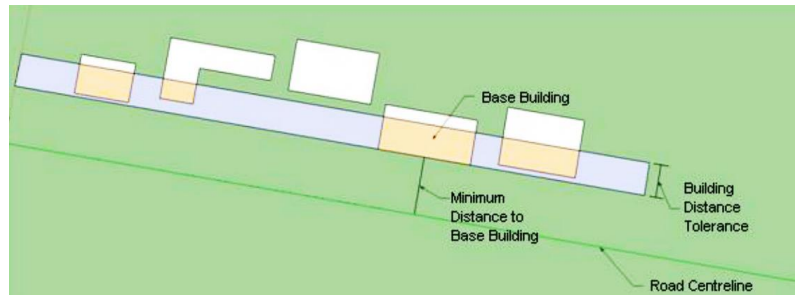


Figure 3.5. Building Distance Tolerance (CERC,2015).

Using the core parameters, the following metrics were derived:

Table 3.3. Urban Canyon Metrics.

Metric Name	Definition	Formula
Height-Width Ratio (HWR) OR Aspect Ratio <i>[Left Side, Right Side and Average]</i>	Ration between the average height of adjacent vertical elements (facades) and the average width of the space between them. (Evyatar Erell, Pearlmutter and Williamson, 2015)	$HWR = \frac{Canyon\ Height_{Left,Right,Avg}}{Canyon\ Width}$
HWR Difference (HWR _Δ)	Arithmetic difference between the left-side aspect ratio and the right-side aspect ratio.	$HWR_{\Delta} = HWR_{Left} - HWR_{Right}$
Length-Width Ratio (LWR)	Ratio between the average length of the mapped canyons and the average width of the space between the adjacent vertical elements.	$LWR = \frac{Canyon\ Length_{Average}}{Canyon\ Width}$
Canyon Coverage (CC)	Ratio between the average length of vertical elements (Built Length) on either sides and the length of mapped canyons.	$CC = \frac{Built\ Length_{Average}}{Canyon\ Length_{Average}}$
Built Length-Width Ratio (BLWR)	Product of CC and LWR. May also be interpreted as effective LWR.	$BLWR = CC \times LWR$
Height Difference – Left to Right (HDLR)	Arithmetic difference between the average height of vertical elements on the left and right sides of the canyons.	$HDLR = Avg.Height_{Left} - Avg.Height_{Right}$
Height Difference (HD)	Arithmetic difference between mean maximum height of the vertical elements and the average height of vertical elements in canyons. (Yang et al., 2020)	$HD = Max.Height_{Avg.} - Avg.Height$

3.6.1.2 Canyon Normality

Of the many urban design parameters, canyon orientation has been used in several urban microclimate studies (*Chatzipoulka et al., 2016*). Canyon orientation refers to the angle between a line running North-South and the central street axis running along its length and is often measured in a clockwise direction (*Erell, Pearlmutter and Williamson, 2015*). Studies have identified substantial differences in the wind pattern of streets that are parallel and perpendicular to the incident wind direction (*Jareemit & Srivanit, 2019*). This implies that the orientation of canyons with respect to the incident wind flow is crucial in understanding how the interaction between urban form and wind may differ with changes in either the canyon orientation or the wind direction or both. Considering this, Canyon Normality (CN), a measure which is a function of both canyon and wind orientations with respect to North. With values ranging from 0 to 1, the purpose of CN is to indicate the degree of normality between the longitudinal canyon axis and the incident wind flow.

Canyon Normality has been computed as follows:

$$CN = |\sin[\theta_{wind} - \theta_{canyon}]|$$

Here,

θ_{wind} = Wind Orientation w.r.t North.

θ_{canyon} = Canyon Orientation or Street Bearing w.r.t North.

A CN value of zero (0) indicates that the wind flows parallel to the canyon axis, while a value of one (1), indicates perpendicular wind flow. In other words, when the difference in the wind and canyon orientations results in perpendicular (normal) angles (90° or 270°), the CN value becomes 1. Similarly, when the difference is either 0° or 180° degrees, the CN value becomes zero.

The wind and canyon orientation values range from 0° to 360°, covering all four quadrants on an X-Y plane. Thus, in order to avoid negative values of CN, the absolute sine function [modulus] has been incorporated in the expression.

CN values have been computed for all the mapped canyons in the preceding step. Further, based on the corresponding CN values for 0°, 30°, 60° and 90° difference in wind and canyon orientations, the mapped canyons have been grouped into three normality classes as shown in the table below:

Table 3.4. CN classes

Normality Class	Wind and Canyon Angle Difference Range (degrees)	CN Value
High	> 60 - ≤ 90	> 0.87 - ≤ 1.00
Medium	> 30 - ≤ 60	> 0.50 - ≤ 0.87
Low	≥ 0.0 - ≤ 30	≥ 0.00 - ≤ 0.50

3.6.1.3 Urban Canopy Properties

When wind approaches an urban area composed of densely packed buildings, its profile gets altered. The presence of buildings drastically adds on to the surface roughness owing to which wind flows relatively low in magnitude to the upwind flow are observed. A set of geometric measures are used to characterise the surface roughness of urban areas. Amongst these, average canopy height, plan area density or floor area ratio, and frontal area density are found considerably useful in urban pollution studies and thus are most widely adopted (*for instance, see Wong & Nichol, 2013; Edussuriya et al., 2014; Li et al., 2019; and Yang et al., 2020*).

The ADMS Urban Canopy Tool, an ArcGIS based tool by CERC, has been used to compute the canopy related metrics for the study area. The urban canopy tool uses road network, canyon or road width, building geometry, building height, and wind direction as key inputs for the computation process. For a defined grid resolution, the tool computes the following core parameters: *Plan Area Density (PAD)*, *Frontal Area Density (FAD)*, and *Average Canopy Height (H)*.

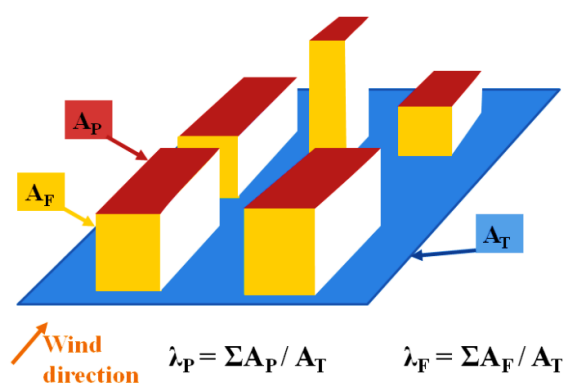


Figure 3.6. Illustration – Plan Area Density and Frontal Area Density (CERC,2015).

Plan area density is defined as the density of building coverage on the ground, and as shown in *Figure 3.6*, it is expressed as the ratio between the sum of planar areas of buildings within a cell (grid) to the total horizontal or plan area. The values of PAD ranges from zero (0) to one (1). On the other hand, frontal area density is a three-dimensional measure of urban density and is expressed as the ratio of the

total frontal area of buildings perpendicular to a specified wind direction to the total horizontal or plan area within a grid cell. FAD may have values greater than 1. Average canopy height refers to the average height of buildings within a grid cell. (CERC,2015; Erell, Pearlmutter and Williamson, 2015).

Urban canopy metrics are generally used for assessing the intra-city variabilities and thus are computed at a neighbourhood scale with cell size ranging from 200 – 500m (Chatzipoulka & Nikolopoulou, 2018; Badach et al., 2020). However, given the street or canyon level focus of this study, the urban canopy tool has been executed at a much finer resolution of 25m. In the case of FAD, the wind direction output has been further aggregated at 50m and 75m resolutions.

Based on the obtained values of PAD, FAD, and H, the following metrics are considered in addition:

- I. **Built Volume:** This metric is a measure of the total building volume within a grid cell. For this study, the built volume is obtained by multiplying PAD with the average canopy height (H).
- II. **Effective Frontal Area:** As cited earlier, the study area is heterogeneous in its built landscape. Tall towers surround many of the AQ observation points in the study area. Thus, it is essential to capture the influence these buildings may have on their immediate surrounding.

Yang et al. (2020) used 'Height Difference (HD)' and identified a non-linear relevance with AQ. While increased height may form strong angular winds and promote overall air circulation, it is also like to generate fugitive emissions. Tall buildings may deflect upper airflow to the surface and facilitate pollutant dispersion on the lee side. However, this may also cause the formation of low wind zones in areas behind tall buildings. This explains the non-linear relevance of HD with AQ.

In this study, a new metric, Effective Frontal Area, has been adopted. It is a function of the frontal area density in a specified wind direction and frontal advantage. It is expressed as:

$$Eff. \lambda_{Frontal} = \{\lambda_{F.Adv.}\} + \{\lambda_{Frontal.}\}$$

Here, $\lambda_{F.adv.}$ = Frontal Advantage; $\lambda_{Frontal}$ = Frontal Area observed within the grid cell of interest.

The Frontal Advantage is a measure based on the frontal area of grid cells surrounding the cell of interest in all 8 directions. (Figure 3.8). Frontal advantage uses the FAD values of neighbouring cells and identifies whether a grid cell is advantaged or disadvantaged due to its position. Frontal advantage is negative when the mean FAD value on the upwind side is higher than the downwind side, and vice-versa.

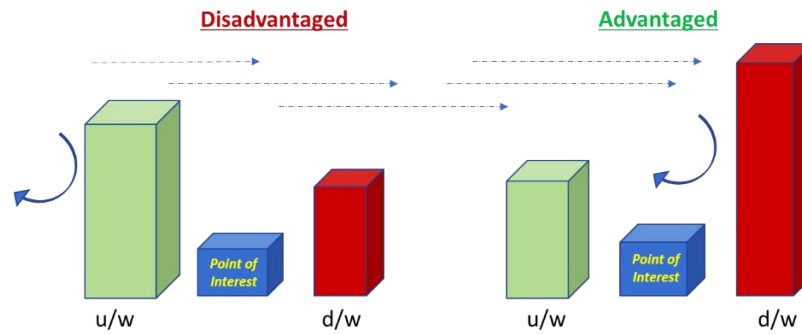


Figure 3.7. Illustration on Frontal Advantage.

Negative values indicate that a cell is disadvantaged i.e. it falls on the leeward side of big buildings and potentially has low access to indirect winds that may result due to downward deflection of wind by tall buildings surrounding the cell in the downwind side. Positive values imply that irrespective of whether the cell of interest lies in the leeward side or not, it potentially has access to direct and/or indirect flows resulting due to deflection by surrounding buildings. Thus, it is advantaged due to its positioning.

Frontal advantage ($\lambda_{F.Adv.}$) for dominant wind direction in the region, i.e. South-Southwest, has been computed as follows:

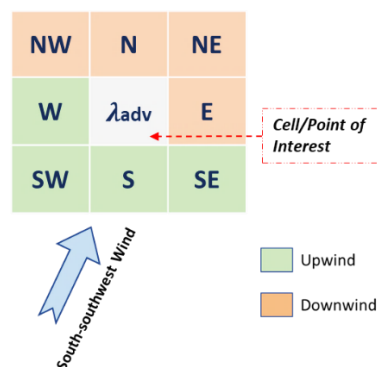


Figure 3.8. Upwind and Downwind FAD neighbours.

$$\lambda_{F.Adv.} = \left\{ \frac{\lambda_{NW} + \lambda_N + \lambda_{NE} + \lambda_E}{4} \right\} - \left\{ \frac{\lambda_{SW} + \lambda_S + \lambda_{SE} + \lambda_W}{4} \right\}$$

Here, λ_{NW} = FAD of North-Western grid cell; λ_N = FAD of Northern grid cell; and so on.

The FAD values for surrounding cells have been identified in ArcGIS by applying the ‘*Calculate Adjacent Field*’ cartography tool on the output derived from the ADMS Urban Canopy Tool.

As can be understood, all urban canopy metrics are computed at the grid level. Thus, in order to transfer their values to adjoining canyons, the ‘*Spatial Join*’ function in ArcGIS has been applied. As shown in *Figure 3.10*, Spatial Join identifies grids intersecting with adjoining canyons and attributes the mean grid values to the Canyons they intersect with.

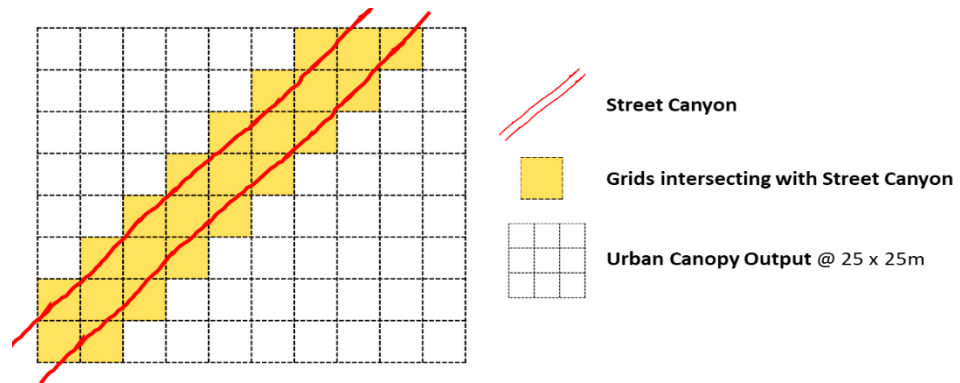


Figure 3.9. Canopy Grid -Canyon Spatial Join Application

3.6.2 Terrain and Climate-Related Properties:

3.6.2.1 Topographic Openness (TO)

Sky View Factor (SVF), a factor describing the degree of openness of a point to the sky, is being widely used as a measure of built environment complexity in urban microclimate studies (*Chatzipoulka et al., 2016*). SVF is closely related to the canyon aspect ratio (H/W); however, some points may exhibit similar SVF values despite the variations in the composition of an urban setting (*Krüger et al., 2011*). It should be noted that SVF, as a measure, is unidirectional. This could be significant for urban microclimate studies where the vertical movement of heat is crucial. However, urban air pollution is directly influenced by the wind movement, which is fluid, i.e. multi-directional in nature. In fact, the presence of buildings tends to enhance this multi-directionality, and thus pollutants are transported and dispersed in both vertical and horizontal directions. Acknowledging this, Topographic Openness (TO), a multi-

directional measure expressing the degree of dominance or enclosure of a location on an irregular surface (Yokoyama et al., 2002), has been adopted for this study. In other words, TO is a measure of how open a point is in both horizontal and vertical directions. TO is measured either in degrees or radians.

Using the updated Lidar DSM Elevation data as input, Topographic Openness of the study area has been computed for 8 directions between 0 – 360° at an interval of 45° in SAGA GIS.

3.6.2.2 Wind Effect (Direct)

The irregularity of the urban terrain adds on to the complexity of airflow in built-up areas (Erell, Pearlmutter and Williamson, 2015). Air pollution is directly affected by wind environmental factors (Yang, Shi, Shi, et al., 2020). Thus, exposure to wind, or the lack of it, may considerably alter the local air quality in urban areas. The 'Wind Effect' is a dimensionless index (Boehner & Antonic, 2009) wherein values below 1 indicate wind shadowed area while values above 1 indicate wind-exposed areas. The Wind Effect Index is computed with regards to the specified direction, which might either be constant or varying in space.

Using the updated Lidar DSM Elevation data in conjunction with the mean (constant) wind direction observed during the study period, June to December 2019, the wind exposure pattern for the study area is derived. When a constant wind direction is used, the resulting exposure map does not reflect the indirect exposure that may occur due to deflection from surround elements. Thus, the wind effect computed at this stage is termed as Direct Wind Effect Index.

This step is repeated later after deriving a detailed wind map of the study area based on wind simulation exercise. Since the wind direction raster offers varying flow directions, including surface deflections, the latter outcome of wind effect index is termed as Direct & Indirect Wind Effect Index.

3.6.2.3 Global Solar Radiation (Insolation)

Emerging studies indicate that the differential heating of canyon elements such as canyon floor, windward and leeward sides influence the removal of pollutants from urban canyons. Depending on the canyon element receiving more heat, rotating cells that are either conducive or unfavourable for pollution dispersion are formed (Fellini et al., 2020). When canyon wind is low and radiant loads are intense, the influence of differential heating on air circulation and pollution dispersion is more substantial. When winds are strong, advection dominates even under strong radiant load conditions, and thus the influence of differential heating is relevant only to a minor extent (Erell, Pearlmutter and Williamson, 2015).

In order to capture the influence of differential heating on canyons of the study area, Area Solar Radiation simulation tool within the ArcGIS environment has been executed under a uniform sky condition from 1st June to 31st December 2018, fortnightly. The georeferenced surface data in the form Lidar DSM Elevation model has served as the core input for this simulation. The outcome of this step, i.e. the obtained Global Solar Radiation (WH/m²) represents both direct and diffused surface heating. It should be noted, however, that the study does not take into consideration the material properties of the built form, and thus areas with relatively high solar insolation are assumed to be the ones getting more heated. This, however, need not be the case on the ground.

3.7 Traffic Hotspot Analysis and Node Exposure

3.7.1 Hotspot Analysis

Traffic activity is the primary source of pollution in the study area. The London Atmospheric Emissions Inventory (LAEI), an initiative by the Greater London Authority, offers emissions estimation of key pollutants like NO_x, PM₁₀, PM_{2.5} and CO₂. The inventory takes into consideration traffic flow by vehicle type and other contributing activities. Thus, owing to temporally non-uniform traffic data, the LAEI – NO₂ data (2016) has been considered for identifying the activity-based hotspots in the study area.

Juxtaposing the road geometry and the LAEI-NO₂ raster dataset, values are extracted at an interval of 10 m across the road network within the study area. These points, termed as *incident points or weighted features*, are used for creating a map of statistically significant hot and cold spots using the Getis-Ord Gi* statistics based Hot-spot Analysis tool in ArcGIS. With reference to the local means, the tool assigns a Z-score value to all the incident points, indicating their respective standard deviation. Based on the Z-score ranges shown in the illustrations below, and the side of the distribution the incident points fall on, they incident points are classified into Hot Spots and Cold Spots at varying confidence level.

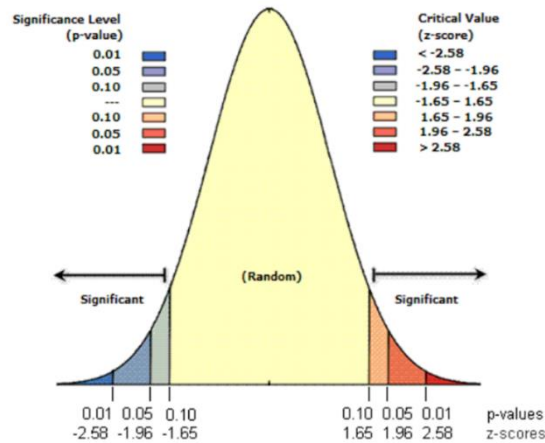


Figure 3.10. Standard deviation based Hotspot classification

Table 3.5. Standard deviation based Hotspot classification

z-score (Standard Deviations)	p-value (Probability)	Confidence level
< -1.65 or > +1.65	< 0.10	90%
< -1.96 or > +1.96	< 0.05	95%
< -2.58 or > +2.58	< 0.01	99%

It should be noted that the data used for hotspot analysis does not correspond to the study period - *June to December 2018* - but to the year 2016. Since there has not been any significant change in the traffic pattern within the study area in recent years, the hotspot distribution is still considered relevant to the study period. However, given the dynamic nature of traffic flows, this may still fall short of representing the actual traffic activities, the fluctuations therein, and the consequent implications on air quality observed during the study period.

3.7.2 Node Exposure

The way traffic functions around nodes (junctions) - *high accumulation and slow movement* - often creates pockets of higher pollution concentrations the locations of which may shift owing to the traffic dynamics and airflows around junctions (Gokhale, 2011). Several AQ observation points are located on nodes of some form (Figure 3.11). Thus, in order to capture the influence of nodes on AQ observations, a simplistic approach wherein all the observation points are given a 'node exposure score' (Figure 3.11) depending on the type of node and number of road segments they are exposed to. This further facilitates in ensuring that poor AQ resulting due to proximity to nodes is not misattributed to urban form metrics.






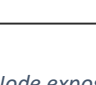
	4
	3
	2
	1
	1
	0

Figure 3.11. Node exposure score.

3.8 Wind Simulation & Metrics

Apart from affecting people’s physiological comfort in daily life, the urban wind environment plays a pivotal role in the dispersion of air pollution in urban areas (Yang, Shi, Shi, et al., 2020). However, the built environment’s heterogeneity in form and the consequent surface roughness greatly influences the urban wind environment. Thus, understanding the interaction between urban spatial form and the wind is of paramount importance. Towards this end, wind simulation exercises based on the principles of Computational Fluid Dynamics (CFD) are key. Wind simulation exercises help in deepening our understanding of the wind behaviour in urban areas while further facilitating in deciphering the urban form factors or metrics that act as strong manipulators of wind flow.

For this study, wind simulation exercise, i.e. computation of spatially varying wind field, is performed using WindNinja, a computer program that is specifically designed to simulate the effect of terrain on wind flow. WindNinja uses elevation data in conjunction with the domain mean meteorological parameters to simulate wind behaviour and is composed of two solver types viz. Conservation of mass and Conservation of mass and momentum. The former serves as a simplified form of CFD and thus is suitable for simulating complex terrain datasets at a very high resolution, while the latter is more complex and computationally demanding. Given the complexity of the urban surface model data, and the fine resolution of computation alongside the scale of simulation, the conservation of mass solver has been preferred. Further, to avoid potential computational errors along the study area boundary, an additional buffer of 20% (360 m) has been applied to the main study area. The updated Lidar DSM

Elevation data has been deployed as the terrain input for wind simulation, and for the meteorological parameters, the mean meteorological values observed during June to December 2018 (Section 3.4.5), have been used. To account for diurnal winds, the time of simulation where the observed temperature and traffic activity are generally high, has been considered. Acknowledging that the atmospheric stability can have a dramatic impact on surface wind flow, the simulation is run under a non-neutral atmospheric stability environment. Here, it should be noted that WindNinja uses a simplified approach wherein surface heat flux is computed to approximate the atmospheric stability.

Spatially distributed wind vectors of varying speed and direction are the key output of the simulation exercise. Two runs, at 6m and 12m height from the ground level, have been undertaken to arrive at the wind speed and direction pattern across the study area at 3m spatial resolution.

Using *Spatial Join* function in ArcGIS, the outcomes of the simulation are aggregated at the canyon level to obtain the following wind parameters shown in the table below.

Table 3.6. Wind Simulation Outcomes

Wind Parameter	Height	
	6m	12m
Average Speed	√	√
SD. Speed	√	√
Average Direction	√	√
SD. Direction	√	√

As cited earlier, the urban wind environment directly influences the local air quality. Thus, any change in the wind metrics along the horizontal and vertical plane may indicate the state of pollution dispersion. Referring to the Eddy Covariance or Eddy Flux principle, higher the deviation in wind metrics larger is the influence on the gas or pollution concentration. Acknowledging this, additional metrics on vertical and horizontal fluctuations in wind behaviour have been computed.

Table 3.7. Metrics computed for characterising the wind behaviour.

Wind Metric	Plane	Description	Calculation method
Turbulence Intensity (@ 6m and 12m)	Horizontal	Turbulence intensity is defined as the ratio of standard deviation of fluctuating wind velocity to the mean wind speed, and it represents the intensity of wind velocity fluctuation.	$TI = \frac{\sigma_u}{\bar{u}}$
Wind Speed Flux	Vertical	Change in wind speed per meter height.	$Flux = \frac{x_6 - x_{12}}{6}$ <p>Here, X6 = Value at 6m; X12 = Value at 12m.</p>
Wind Direction Flux	Vertical	Change in wind direction per meter height.	
SD Speed Flux	Vertical	Change in SD of wind speed per meter height.	
SD Direction Flux	Vertical	Change in SD of wind direction per meter height.	
Turbulence Intensity Flux	Vertical	Change in Turbulence Intensity per meter height.	

*SD = Standard Deviation

3.9 Exploratory regression analysis and correlation matrix

At this stage, the triadic relationship between urban form, wind flow, and air quality at street level has been explored statistically. Using exploratory regression method, the significant variables and the nature of relationship with dependent (response) variables such as wind flow and air quality has been identified. Later, using Pearson's correlation matrix the strength of the relationship, i.e. the degree of influence of the independent (predictor) variables have been presented. This approach takes inspiration from *Edussuriya et al., (2014)* where Principal Component Analysis (PCA) and Spearman's Rank correlation are deployed in conjunction to understand the relationship between street-level pollution and urban form.

The Exploratory Regression tool in ArcGIS has been used for this study. The tool evaluates all possible combinations of the input candidate explanatory variables (potential predictors) and looks for Ordinary Least Squared (OLS) multi-linear models that best explain the dependent (response) variable within the context of user-specified criteria. Additionally, the tool provides a summary of Variable Significance wherein the statistical significance and the consistency and nature relationship of the explanatory variable with the dependent variable is indicated. Strong predictors will be consistently significant (% Significant), and the relationship will be stable (primarily negative or primarily positive).

For this study, following statistical test criteria have been adopted towards identifying the best OLS models through Exploratory Regression:

Table 3.8. Statistical test criteria adapted for identifying OLS

Adjusted R ² threshold	≥0.5
coefficient p-values	<0.05
coefficient VIF values	<7.5
Jarque-Bera p-value	<0.1
Spatial Autocorrelation p-value	<0.1

Exploratory Regression & Correlation analysis has been performed twice in this study.

- I. **Urban Form and the Wind Environment:** Firstly, the analysis is conducted to understand the influence of urban form on wind speed (dependent variable) across all the canyons in the study area. Later, to understand whether change canyon orientation or wind direction affects variable significance, the same has been repeated for respective Canyon Normality classes. At this stage, altogether 42 explanatory variables have been deployed for significance testing and OLS model search. This is followed by Pearson's correlation analysis to explain the strength or degree of influence of respective variables.

II. Air Quality, Urban Form and the Wind Environment: Since the AQ observation point does not cover the entire spatial extent of the study area, only canyons with AQ observations are considered for exploring the triadic interaction. Here, AQ is treated as the dependent variable, while variables pertaining to the wind and urban form are considered as explanatory variables. At this stage, about 64 explanatory variables have been deployed for significance testing and OLS model search. This is followed by Pearson's correlation analysis to explain the strength or degree of influence of respective variables.

4 Results and Analysis

This chapter presents the results and the analysis conducted for the study. It is structured in 6 sections: Air Quality Observations, Study Region Meteorological Profile, Build Footprint Data and Lidar DSM Consistency Check, Wind Simulation and Metrics and lastly, Exploratory Regression, Variable Significance and Correlation Matrix.

Further, the chapter demonstrates the fulfilment of the following objectives:

1. Simulate, explore, and characterise the wind behaviour within the study area.
2. Conduct geospatial modelling to map the city's pollution profile and to identify the pollution hotspots.
3. Devise & Adopt a new set of indicators that may potentially facilitate in exploring the triadic relation.
4. Explore spatially and statistically the relationships between urban form metrics, wind pattern and air quality parameters.

4.1 Air Quality Observations

Out of eighty-two (82) observation points across the study area, sixty-five (65) points satisfy the selection criteria outlined in the Air Quality Data preparation section. In other words, about 79.3% of the observation network in the study area has been applied for this study. Across the sixty-five (65) observation points, a total of 390 air quality observations during from June to December 2018, have been obtained. Out of these, thirty-three (33), i.e. about 8.5% of the observations have been predicted using the combinatorial approach entailing cluster wise correlation matrix and geographical proximity – *details of which have been provided in Appendix 9.2*. Cluster-wise assessment (*Table 4.1*) indicates that clusters 6 and 8 have the highest share of predicted values. Since predictions are not free from errors, the share of predicted observations should be taken into consideration while reading the air quality trends in the study area.

Table 4.1. Cluster-wise share of predicted data values

Cluster Name	Observation Points	Total Observations (June to December 2018)	Predicted Observations	% of Total
2	14	84	6	7.14
4	8	48	2	4.17
6	3	18	4	22.22
7	6	36	3	8.33
7a	6	36	2	5.56
8	7	42	6	14.29
9	6	36	2	5.56
10	15	90	8	8.89
ALL	65	390	33	8.46

The study period extends over two seasons viz. Summer (*June – September*) and Autumn (*September – December*). The air quality trend in the study area indicates that as the study area progresses from Summer to Autumn, the overall air quality worsens, i.e. NO₂ concentration values increase. While two clusters (6 & 7a) witness enhanced air quality in Autumn, there is an overall increase of 5.62% in NO₂ concentration across the monitoring network. Among the clusters witnessing an increase in NO₂ concentration, clusters 4,6,7a and 10 are the most affected. These clusters also exceed the overall study area mean concentration of 59.29 ug/m³. All clusters, except for cluster 7 in Summer, have mean concentration values exceeding the UK and EU limit of 40 ug/m³.

While the Summer values of NO₂ are considerably low, it is observed that the variation in concentration i.e. the standard deviation of NO₂ in Summer (19.67) across the study area is significantly higher than in Autumn (15.5). This holds true even at the cluster level, where high variability in concentration is witnessed during summer.

Table 4.2. Clusters-wise concentration of NO₂

Cluster Name	Summer	Autumn	Overall	% Change - Seasonal
2	49.22	55.58	52.40	12.92
4	59.20	65.22	62.21	10.16
6	78.10	69.98	74.04	-10.39
7	39.25	44.88	42.07	14.34
7a	87.04	74.70	80.87	-14.18
8	40.72	46.64	43.68	14.55
9	52.23	54.55	53.39	4.45
10	66.33	71.86	69.10	8.33
ALL	57.66	60.91	59.29	5.62

Unit: ug/cu.m

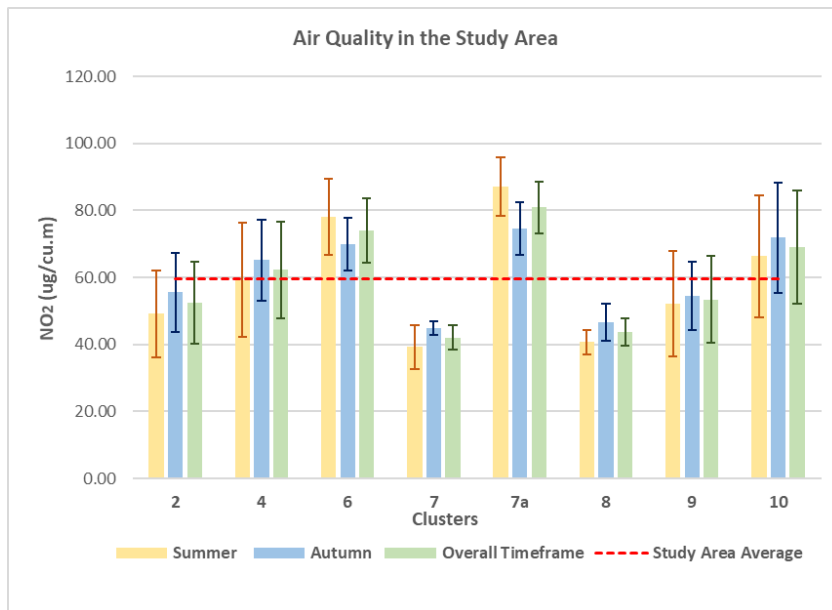


Figure 4.1. Seasonal change in the concentration of NO₂ by clusters.

Spatial distribution of air quality indicates that the NO₂ concentration spikes around street nodes and junctions – especially around Bank of England (A) area and the intersection between Camomile Street and Bishopgate Street (B) (Figure 4.2). Clusters with pedestrian streets or the ones located away from busy roads, exhibit lower NO₂ concentration values. For example, see cluster 2 in the North-West; and clusters 7, 8 and 9 in the East and South.

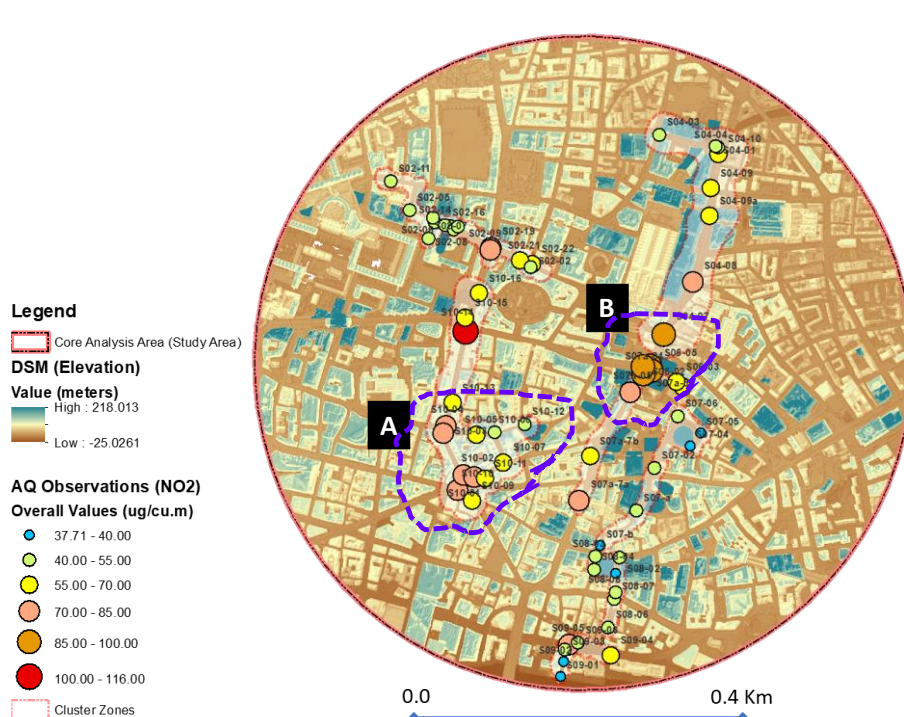


Figure 4.2. Spatial distribution of NO₂.

Table 4.3. Statistical summary of the NO₂ concentration by cluster.

Cluster Name	Observation Points	Timeframe	NO ₂ Concentration (ug/cu.m)				
			Minimum	Maximum	Range	Mean	Standard Deviation
2	14	Summer	35.49	78.91	43.42	49.22	12.98
		Autumn	44.53	82.28	37.75	55.58	11.81
		Overall	40.01	80.51	40.50	52.40	12.29
4	8	Summer	37.85	90.25	52.40	59.20	16.99
		Autumn	45.62	82.77	37.15	65.22	12.07
		Overall	41.74	86.51	44.78	62.21	14.32
6	3	Summer	69.73	94.22	24.49	78.10	11.40
		Autumn	64.38	81.00	16.62	69.98	7.79
		Overall	67.15	87.61	20.46	74.04	9.59
7	6	Summer	32.27	50.08	17.81	39.25	6.52
		Autumn	40.91	46.60	5.69	44.88	1.92
		Overall	38.51	47.73	9.22	42.07	3.56
7a	6	Summer	70.52	95.54	25.02	87.04	8.81
		Autumn	63.50	84.73	21.23	74.70	7.87
		Overall	67.01	89.66	22.65	80.87	7.70
8	7	Summer	34.88	44.60	9.72	40.72	3.71
		Autumn	39.25	55.06	15.81	46.64	5.64
		Overall	37.71	49.04	11.33	43.68	3.97
9	6	Summer	33.58	77.18	43.60	52.23	15.72
		Autumn	41.82	69.64	27.83	54.55	10.22
		Overall	38.55	73.41	34.86	53.39	12.92
10	15	Summer	38.39	116.54	78.14	66.33	18.22
		Autumn	43.20	115.31	72.11	71.86	16.50
		Overall	40.80	115.92	75.13	69.10	16.85

4.2 Study Region Meteorological Profile

4.2.1 Temperature and Rain

For June – December 2018, the mean observed temperature in the study region is about 13.3° C. As expected; there is a drastic change in the temperature profile as the study region progresses from Summer to Autumn. The mean temperature in Summer months is about 16.83° C, while that in Autumn months is 9.93° C (*Figure 4.3*). On the other hand, the rainfall tends to increase as we move from Summer to Autumn. The average monthly rainfall (111.6 mm) and the number of rainy days (15.5) in Autumn are almost twice the values observed in Summer. From June to December 2018, the average monthly rainfall in the region is about 85.64mm, while the average number of rainy days per month is 12 days. July is the

warmest month of the study period, while December happens to be the coldest. On the other hand, June is the driest month of the study period, while November is the wettest (*Table 4.4*).

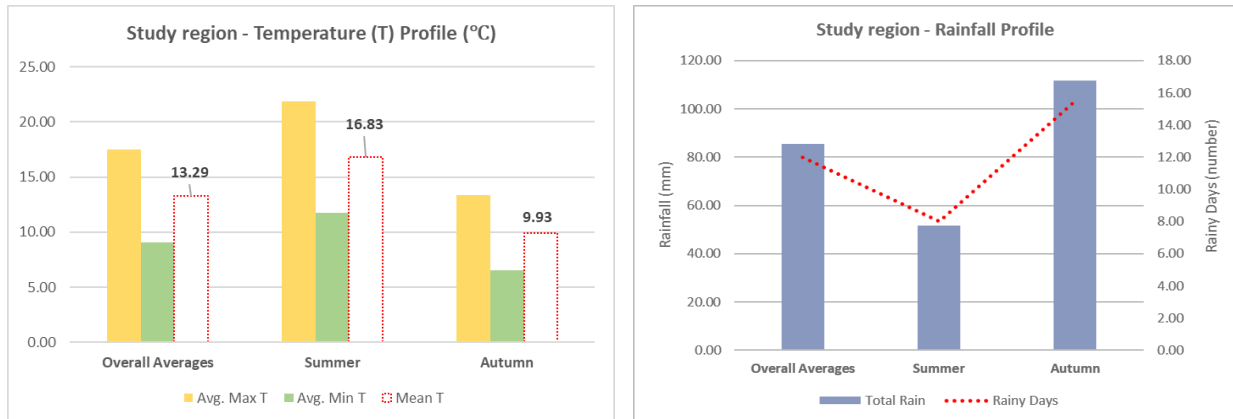


Figure 4.3. Temperature and rainfall profile of the study region.

Table 4.4. Monthly Meteorological Parameters (2018)

Months 2018	Avg. Max T (°C)	Avg. Min T(°C)	Mean T(°C)	Total Rain (mm)	Rainy Days
June	21.53	11.17	16.35	1.50	3.00
July	25.74	14.03	19.89	37.60	5.00
August	21.84	12.32	17.08	114.00	14.00
September	18.43	9.53	13.98	53.30	10.00
October	15.03	7.03	11.03	79.60	15.00
November	10.47	5.30	7.88	190.30	18.00
December	9.35	4.32	6.84	123.20	19.00
Overall Averages	17.49	9.10	13.29	85.64	12.00
Summer	21.89	11.76	16.83	51.60	8.00
Autumn	13.32	6.55	9.93	111.60	15.50

4.2.2 Cloud Cover

Ranging from 45.45% to 83.75% during the study period, the mean sunshine-hour based cloud cover in the region, as observed at Heathrow Station, is 61.48%. While July is the sunniest month in the region, December tends to be the most overcast month of the study period (*Table 4.5*). The average cloud cover in Summer is 52.88% while during Autumn is 68.10% (*Figure 4.4*).

Heathrow Station			%Cloud
Sunshine hours	Day Length (hour)	Non-Sun hours	
8.00	16.00	8.00	50.00
9.00	16.50	7.50	45.45
6.00	16.00	10.00	62.50
6.50	14.00	7.50	53.57
4.50	11.00	6.50	59.09
2.40	10.00	7.60	76.00
1.30	8.00	6.70	83.75
Overall Averages			61.48
Summer			52.88
Autumn			68.10

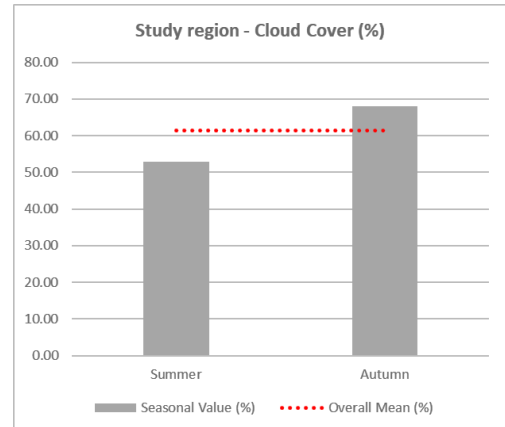


Table 4.5. Sunshine- hours based cloud cover of the Study region.

Figure 4.4. Seasonal Cloud Cover of the Study region.

4.2.3 Wind Profile

The observations averages across the chosen weather stations in the study region indicate that the autumn months witness a higher wind velocity in comparison to the summer months (Figure 4.5). Across the entire study period, the mean velocity has been observed to be about 13.48 km/h. The mean incident direction calculated based on hourly wind observations from June to December 2018 is 193.66° with respect to North. The same tends to lean more towards south-southwest in Summer (195.85°), and towards South (191.47°) in Autumn (Table 4.6 and Table 4.7).

Table 4.6. Wind characteristics by seasons.

Timeframe	Direction	Speed(Km/h)
Summer	195.85	13.02
Autumn	191.47	13.94
Overall	193.66	13.48

Table 4.7. Wind characteristics from 3 main Stations.

Station	Heathrow		Northolt		Kew Garden	
	Direction	Speed(km/h)	Direction	Speed(km/h)	Direction	Speed (km/h)
Summer	194.82	14.45	201.59	12.91	191.14	11.70
Autumn	187.18	15.63	196.50	13.58	190.73	12.62
Overall	191.00	15.04	199.05	13.24	190.93	12.16

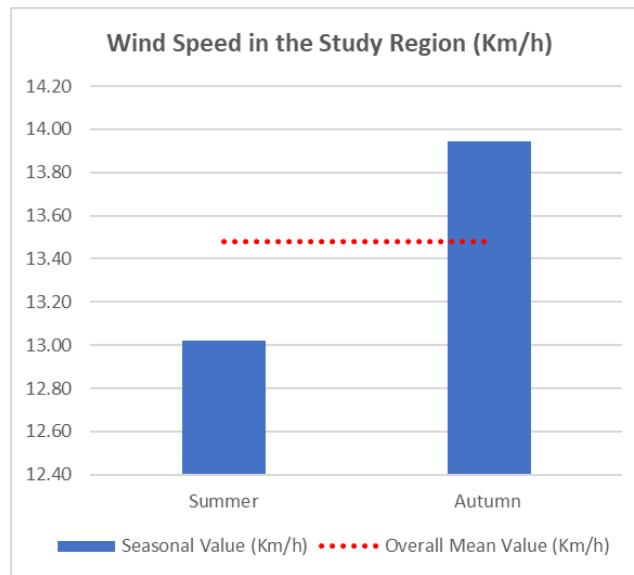


Figure 4.5. Wind Speed in the Study Region.

4.3 Build Footprint Data and Lidar DSM Consistency Check

4.3.1 Building Footprint and Height Data

The updated building footprint and height data are presented in the Map below (Figure 4.6). It is observed that the height of buildings or other vertical elements in the study area range from 5.5m to 241.1m. With a mean height of 36.22m, there are around 4471 buildings in the study area.

A standard deviation-based height distribution indicates that about 82.4% (3684) buildings in the study area are lower than 45.2m in their height. Buildings with the height ranging from 27.3m to 45.2m ($n=2441$) constitute the largest share of buildings (54.6%) in the study area. There are about 100 towers in the study area that are taller than 80m (Table 4.8d). Most of these towers (shown in red) are in close proximity to each other - especially near the study area centre - and are clustered along the Bishopgate Street (indicated with a purple dotted line in the Map). Buildings ranging in height from 45.2 to 63 m constitute only 13.38% ($n=598$) of the total number of buildings in the study area. However, despite the low share in numbers, owing to their large size, they have significant spatial coverage across the study area (see buildings shown in orange colour).

(a)

Variable (Height)	Value (m)
Minimum:	5.5
Maximum:	241.1
Range:	235.6
Mean:	36.22
Standard Deviation:	17.86

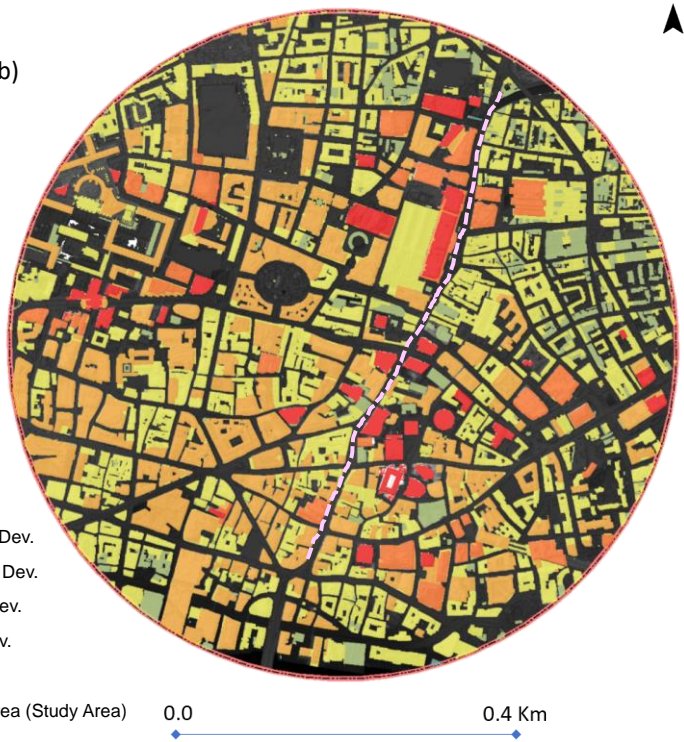
(b)

Legend

Height (m)

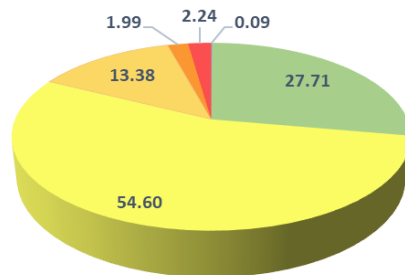
- < -1.5 Std. Dev.
- 1.5 - -0.50 Std. Dev.
- 0.50 - 0.50 Std. Dev.
- 0.50 - 1.5 Std. Dev.
- 1.5 - 2.5 Std. Dev.
- > 2.5 Std. Dev.

 Core Analysis Area (Study Area)



(c)

Building Height Distribution (%)



■ ≤ 9.5 ■ > 9.5 - ≤ 27.3 ■ > 27.3 - ≤ 45.2 ■ > 45.2 - ≤ 63 ■ > 63 - ≤ 80.9 ■ > 80.9

(d)

Height Class (m)	Std. Dev. Class	Number	% Total
≤ 9.5	< -1.5 SD	4	0.09
> 9.5 - ≤ 27.3	-1.5 - -0.50 SD	1239	27.71
> 27.3 - ≤ 45.2	-0.50 - 0.50 SD	2441	54.60
> 45.2 - ≤ 63	0.50 - 1.5 SD	598	13.38
> 63 - ≤ 80.9	1.5 - 2.5 SD	89	1.99
> 80.9	> 2.5 SD	100	2.24
Total Buildings/Vertical Elements		4471	100

Figure 4.6. Building height distribution Map (b) / Pie Chart (c)

Table 4.8. Variable of hights (a) and Classification of building hight (d)

4.3.2 Lidar DSM Data

The updated Lidar DSM data has been presented below. As per the surface data, the elevation in the site – including building heights, trees, and other structures – ranges from -7.5 to 218 m. The mean Urban Form Characteristics



Figure 4.7. Lidar DSM Map

Parameter	Value (m)
Minimum	-7.5
Maximum	218
Range	225.5
Std. Deviation	21.74
Mean	32.03

Table 4.9. DSM Descriptive statistics

4.3.3 Consistency Check – OS Building Height and Lidar DSM Height

Elevations for about 8903 buildings in the study area and buffer zone are extracted using the Lidar DSM data. The scatter plot between the OS building height data and the DSM derived building heights exhibits that two datasets follow a highly consistent pattern, and that a very strong linear relation exists between them ($R^2 = 0.98$) (Figure 4.8). The mean building height and standard deviation values across the two datasets are almost identical. The linear model between the datasets entail a prediction error of ± 2.16 m – which is about 6.6% of the OS Building Height mean (32.68 m). This error has been considered acceptable and is assumed to have spread across the study area evenly (Table 4.10).

Table 4.10. Statistical summary of the two datasets.

Data Type	Number of Buildings	Mean (m)	Std. Deviation	Coefficient Correlation (R)	Standard Error
Building Height Data	8903	32.68	15.25	0.99	2.16
DSM Heights		31.44	13.34		

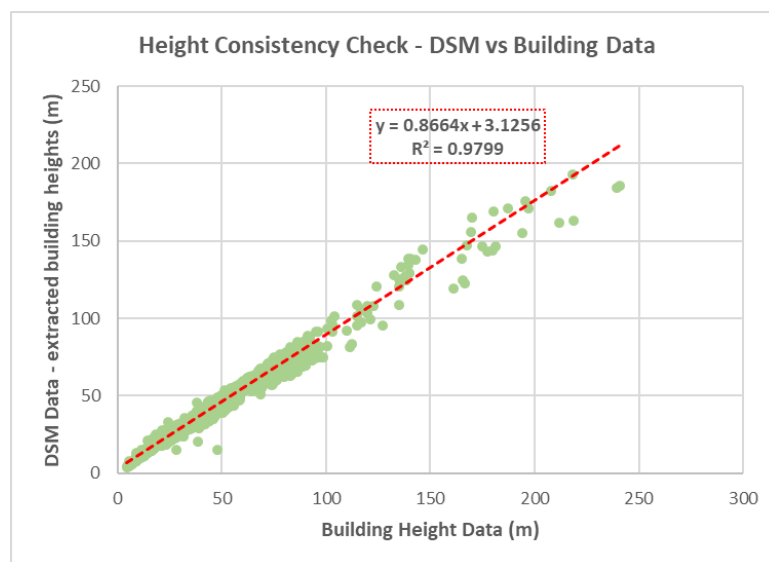


Figure 4.8. Height Consistency Check: DSM vs Building Data.

4.4 Urban Form Characteristics

4.4.1 Street Canyon Metrics

The outputs of the street canyon metrics are presented in Table 4.11. Additionally, the spatial distribution of a select few metrics has been presented in the maps to follow.

Results indicated that the average canyon height across the study area is 45.22m, while the mean canyon length is about 52.95m. The mean HWR in the study area is 3.34, and the canyon coverage is 0.95 on an average (Figure 4.9). Besides indicating that the canyons throughout the study area remain heavily sheltered from the wind and natural light, this also suggests that the urban form surrounding the canyons is dense and of a complex nature. The mean Length-width ratio for the study area is about 4.26. In general, high LWR values are observed in narrow internal streets that are surrounded by large buildings (Figure 4.10).

There is significant variability in the vertical elements along the mapped canyons. The deviation of the average maximum canyon height from the mean height is 8.73m, which is considerably high (Figure 4.11). In general, the right side of the canyon is taller than the left side by 0.78m (Figure 4.12). However, the standard deviation value indicates that there is a massive variability in the elevational differences between the two sides. Much of these variations in building heights root from the clusters of tall towers near the study area centre.

Table 4.11. Statistical Summary of Canyon Metrics

Descriptor	Left		Right		Overall	
	Mean	Std.Dev	Mean	Std.Dev	Mean	Std.Dev
Width	-				18.17	11.80
Avg. Height	44.83	21.09	45.61	22.00	45.22	21.55
Min. Height	34.08	18.34	33.73	16.65	33.90	17.49
Max. Height	48.83	24.93	50.33	27.84	49.58	26.39
Length	52.98	38.34	52.93	37.84	52.95	38.09
Built Length	49.21	34.90	49.20	34.50	49.21	34.70
CC	-				0.95	0.09
HWR	3.30	2.20	3.39	2.41	3.34	2.05
HWR Difference	-				-0.09	2.09
LWR	-				4.26	3.98
BLWR	-				4.02	3.77
HDLR	-				-0.78	25.93
HD	-				8.73	16.50

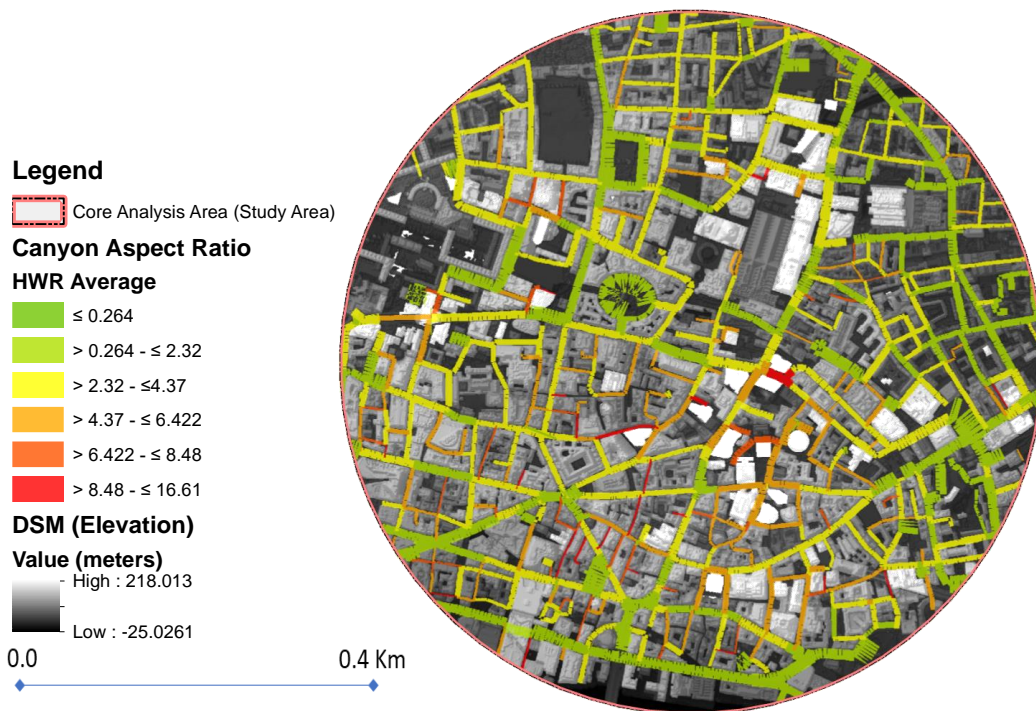


Figure 4.9. Canyon Aspect Ratio Map: HWR Average

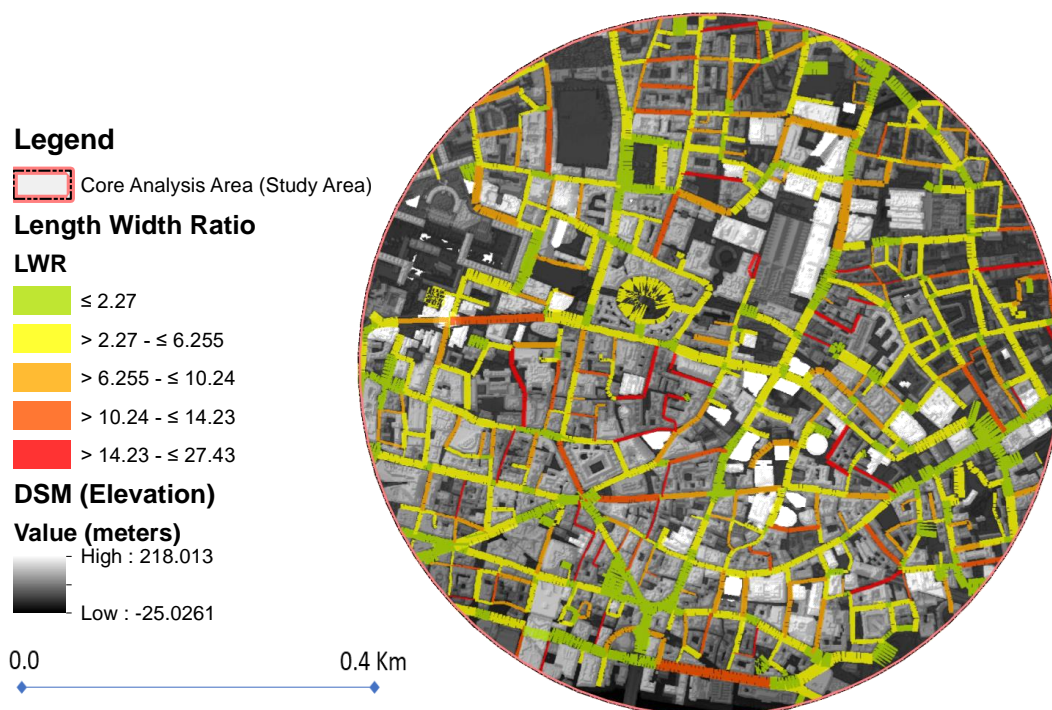


Figure 4.10.Length Width Ratio (LWR) Map

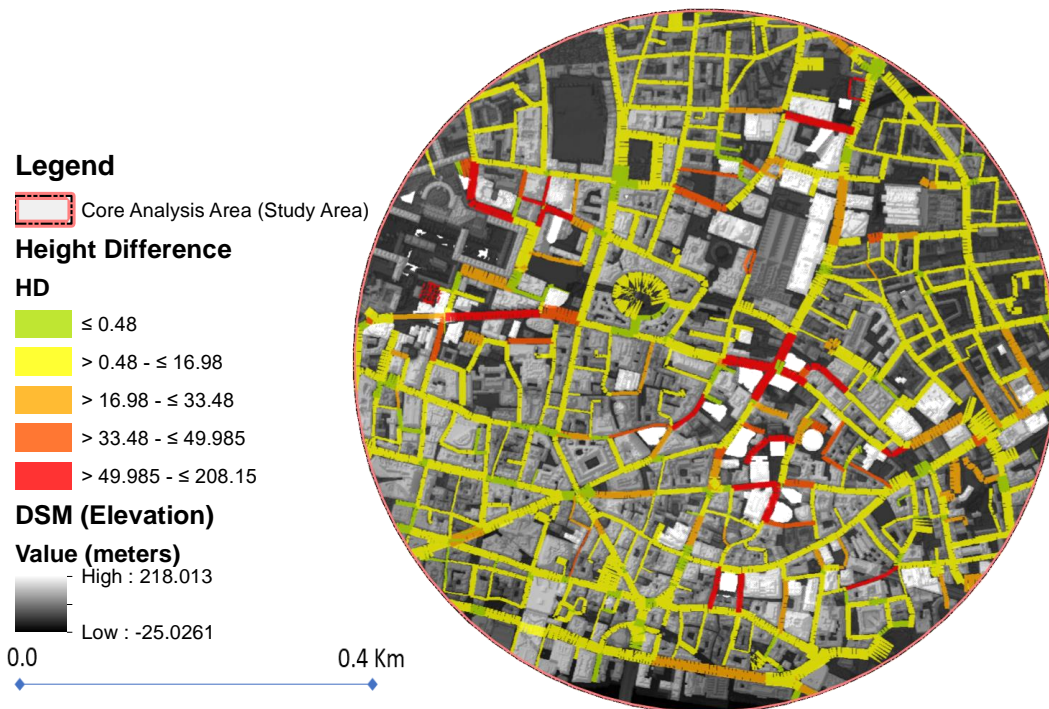


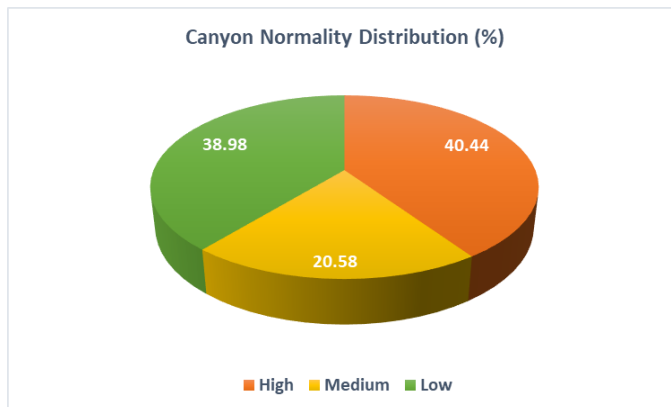
Figure 4.11. Height Difference (HD) Map



Figure 4.12. Height Difference- Left to Right (HDLR) Map

4.4.2 Canyon Normality

The Canyon Normality assessment shows that the study area is mostly composed of canyons that either highly or mildly (low) normal to the incident wind direction. Out of the 826 identified canyons, 334 (40.44%) exhibit high normality, while 322 (38.92%) exhibit low normality. Moderately normal canyons which are about 170 in number (20.58%) are a minority (*Figure 4.13 and Table 4.12*). Spatial distribution of canyons by normality class is presented in *Figure 4.14*.



Normality Class	Angle Range	Number of Canyons	% of Total
High	> 60 - ≤ 90	334	40.44
Medium	> 30 - ≤ 60	170	20.58
Low	≥ 0.0 - ≤ 30	322	38.98
Total Canyons		826	100

Figure 4.13. Canyon Normality Distribution

Table 4.12. Canyon Normality Classification



Figure 4.14. Canyon Normality Map

The seasonal variations in the wind direction have a slight influence on the Canyon Normality values. As the wind direction leans more towards the South in Autumn, the average CN values of highly normal and moderately normal canyons show an overall increase of 0.38% and 0.19%, respectively (Table 4.13). However, the same for canyons classified under the low normality class witness an overall decline (-2.68%). Across the study region, there is an overall decline in the CN values. This indicates that Canyon Normality, in general, is slightly higher in summer than in Autumn. In other words, wind flow in Summer observes more surface roughness or dissipation or potential wind deflection than in Autumn.

Table 4.13. Statistic summary of Canyon Normality

Normality Class	Timeframe	Canyon Normality (CN)					% Change in Mean CN (Summer to Autumn)
		Minimum	Maximum	Range	Mean	Std. Deviation	
High	Summer	0.853	1.000	0.147	0.968	0.035	0.380
	Autumn	0.848	1.000	0.152	0.972	0.033	
	Overall	0.868	1.000	0.132	0.971	0.033	
Medium	Summer	0.472	0.882	0.411	0.708	0.105	0.190
	Autumn	0.468	0.884	0.416	0.710	0.111	
	Overall	0.502	0.866	0.364	0.709	0.105	
Low	Summer	0.002	0.531	0.529	0.184	0.138	-2.679
	Autumn	0.002	0.523	0.521	0.179	0.131	
	Overall	0.002	0.498	0.496	0.179	0.133	

4.4.3 Urban Canopy Metrics

A statistical summary of the urban canopy metrics obtained at both, grid and canopy levels, are presented in the table below (Table 4.14)- alongside maps illustrating the spatial distribution of some urban canopy metrics.

Table 4.14. Statistical Urban canopy metrics (grid and canopy level).

Descriptor	Canopy Values - Study Area		Canyon Values	
	Mean	Std.Dev	Mean	Std.Dev
PAD	0.54	0.30	0.446	0.135
FAD - Summer (25m)	2.680	1.73	2.446	0.910
FAD - Autumn (25m)	2.626	1.71	2.400	0.904
FAD - Overall Timeframe (25m)	2.653	1.72	2.423	0.907
FAD - Overall Timeframe (50m)	2.646	1.308	2.563	0.895
FAD - Overall Timeframe (75m)	2.652	1.080	2.604	0.806
Built Volume	26.04	21.07	20.271	8.907
Effective FAD (Overall @25m)	2.672	2.130	2.360	1.082
FAD - Overall North (25m)	2.663	1.718	2.417	0.876
FAD - Overall Northwest (25m)	2.666	1.717	2.677	0.996
FAD - Overall West (25m)	2.653	1.723	2.646	0.992
FAD - Overall Southwest (25m)	2.637	1.734	2.628	1.033
FAD - Overall South (25m)	2.640	1.731	2.554	1.106
FAD - Overall Southeast (25m)	2.641	1.731	2.803	1.285
FAD - Overall East (25m)	2.655	1.724	2.682	1.126
FAD - Overall Northeast (25m)	2.664	1.720	2.602	0.994
Avg. Canopy Height	44.915	24.013	43.489	14.594

Results indicate that across the study area, the Plan Area Density is about 0.54 i.e. 54% of the land area is covered by buildings. The same along the canyons is about 0.446. PAD values are high in pockets where the streets are narrow, and buildings are either densely packed or have high ground coverage.

The Frontal Area Density (FAD) value is 2.653 across the study area at canopy grid level (25 x 25m), while the same along the canyons is about 2.423. As seen in *Figure 4.15*, FAD values are higher in areas where tall buildings are present. Since FAD is a function of wind direction, the value changes as the study area progress from Summer to Autumn. A similar pattern, as observed for canyon normality in the preceding section, is observed in the case of FAD values. The values at both canopy grid and canyon levels, witness a decline of 2% on an average. This substantiates the understanding that surface roughness or flow dissipation or wind deflection is potentially higher in Summer than in Autumn.

The overall FAD values of neighbouring grid cells at the canyon level are presented in the figure below. As the figure illustrates (*Figure 4.15*), on an average basis, the grid cells in the surrounding 8 directions have higher FAD values than the central cells. Grid cells, mainly in the South-East, East, North-West, West, and South-West, have values much higher than the central grid. The Effective FAD, which takes into consideration the difference between upwind and downwind frontal areas, is 2.36 at the canyon level across the study area. Since, Effective FAD takes, frontal advantage into consideration, the spatial distribution across the site (*Figure 4.18*) is more discrete in comparison to the PAD distribution.

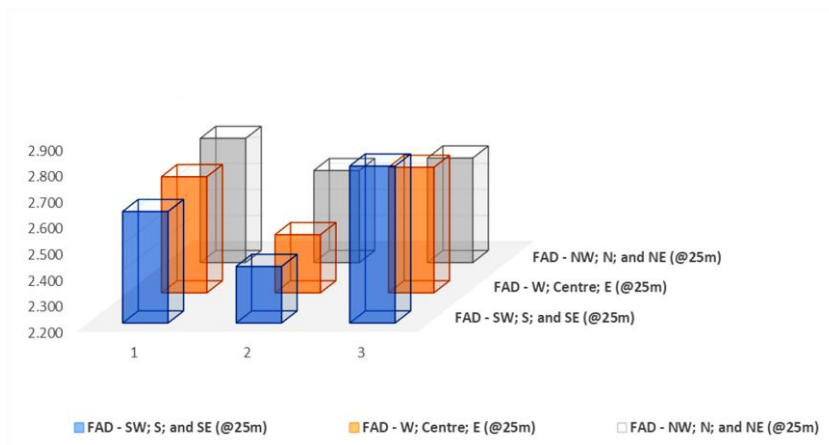


Figure 4.15. Mean FAD Values of neighbouring cells.

The Built Volume Density, which is a function of PAD and canopy height, is 26.04 m³/m² across the study area. While the same at the canopy level is about 20.28 m³/m². Similar to the spatial trend observed in FAD, canopy grids with tall buildings exhibit very high built volume density values— *especially in clusters 6, 7a, 7, 8 and 4.*

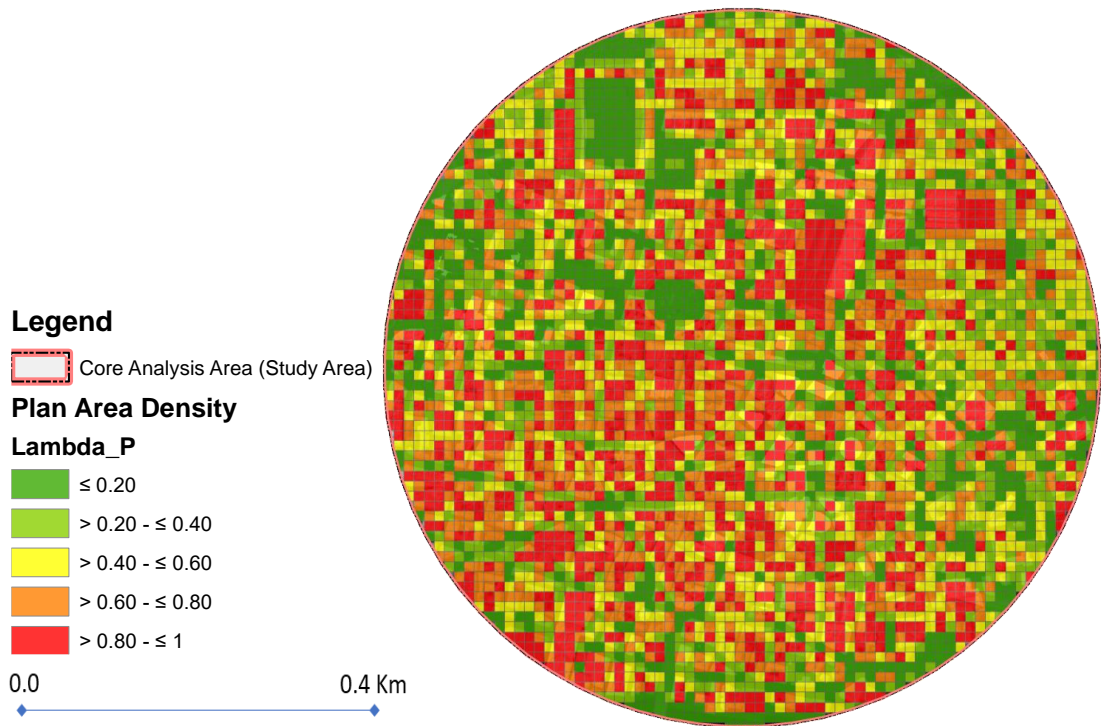


Figure 4.16. Plan Area Density Map

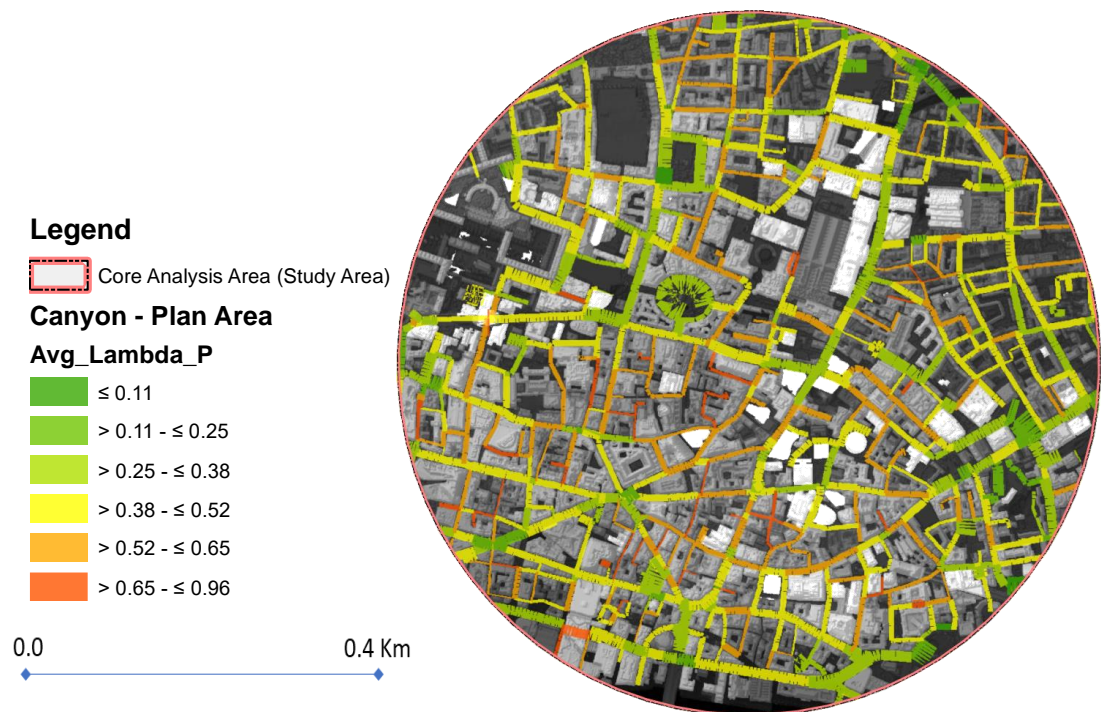


Figure 4.17. Canyon Plan Area Map

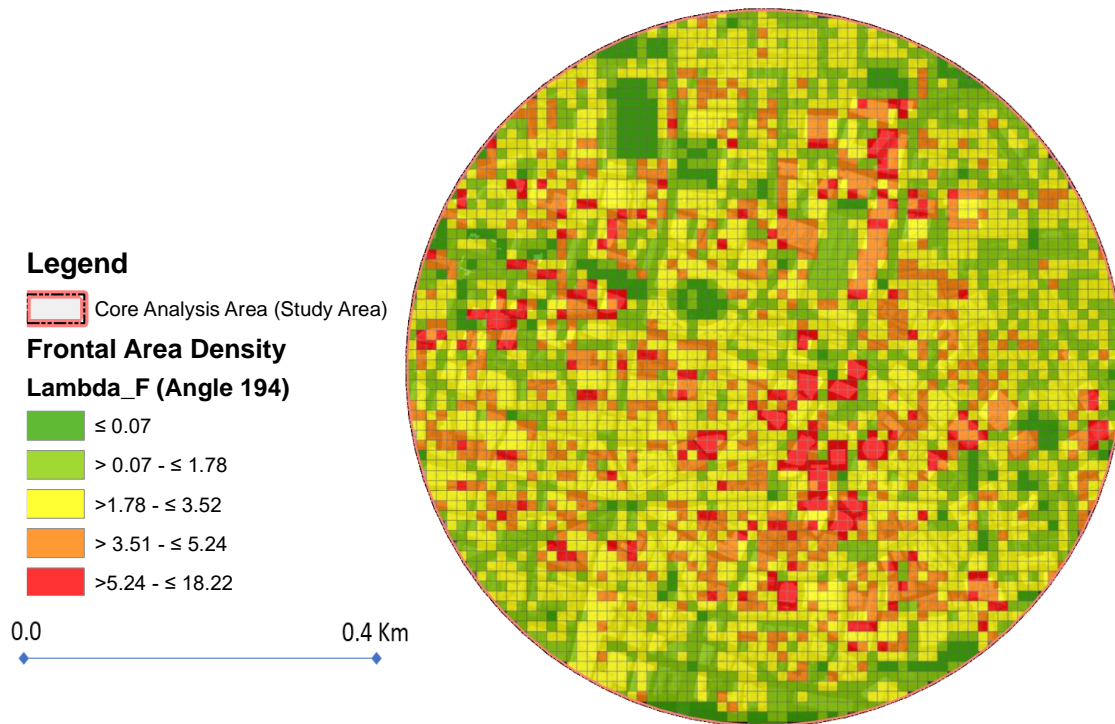


Figure 4.18. Frontal Area Density Map

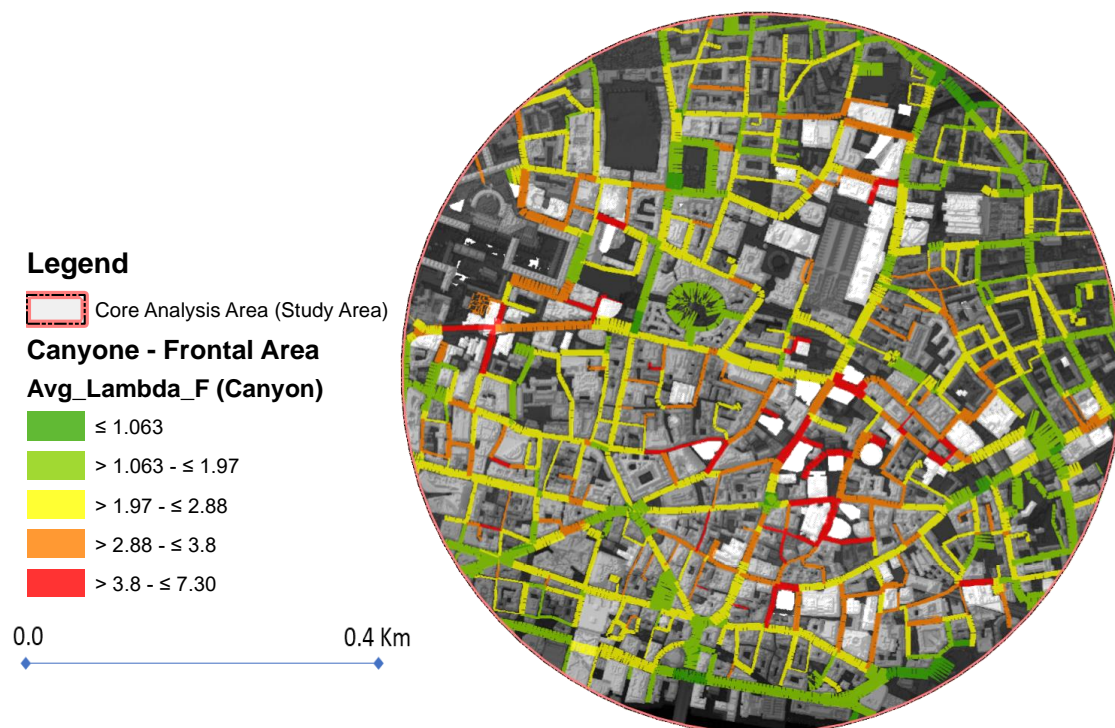


Figure 4.19. Canyon Frontal Area Map

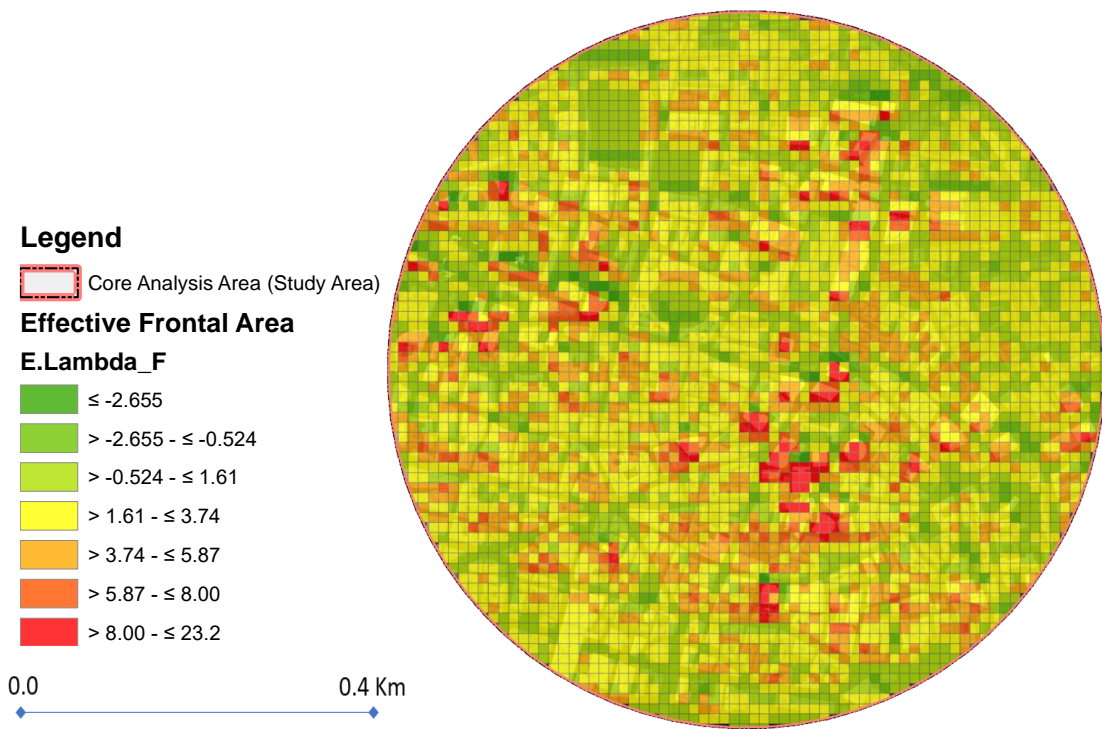


Figure 4.20. Effective Frontal Area Map

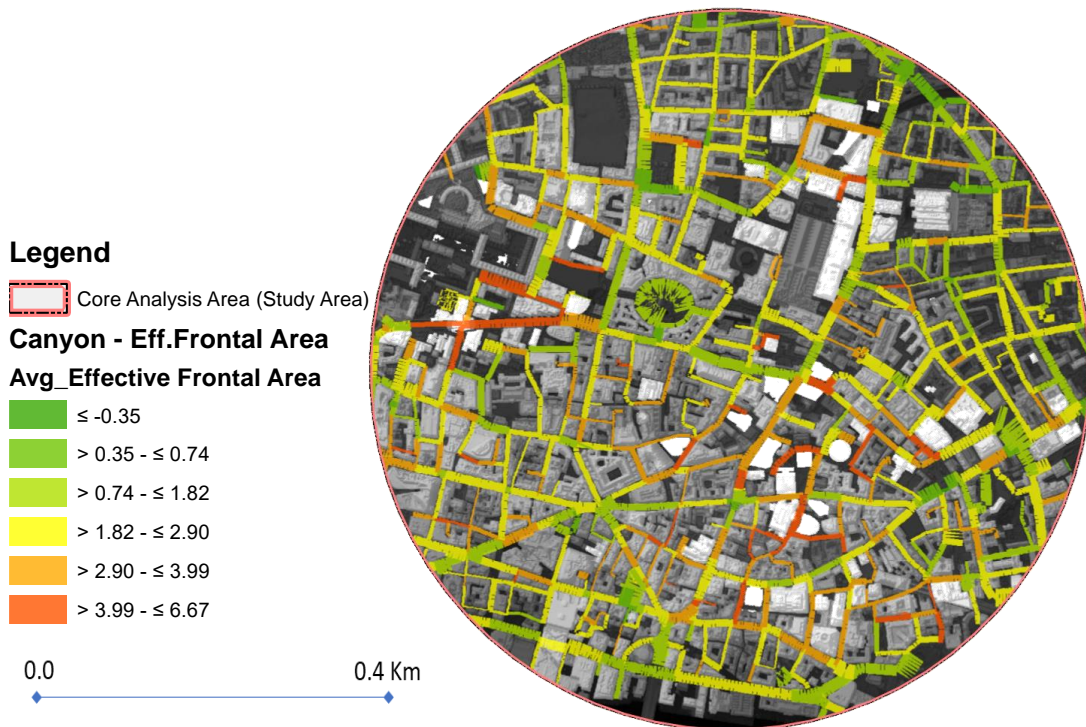


Figure 4.21. Canyon Effective Frontal Area

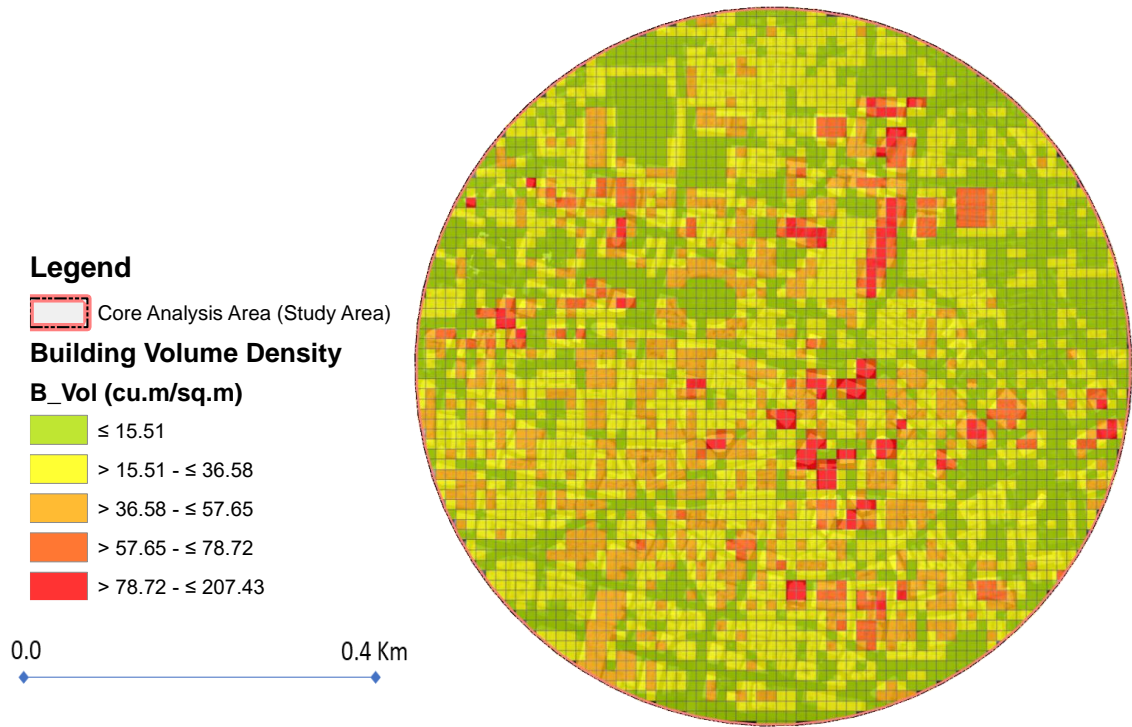


Figure 4.22. Building Volume Density map



Figure 4.23. Average Building Volume Map

4.4.4 Terrain and Climate Metrics

A statistical summary of the terrain and climate related metrics viz. Topographic Openness, Global Solar Radiation (Insolation), and Wind Effect is illustrated in the table below.

Table 4.15. Statistical summary of the terrain and climate-related metrics.

Canyon Descriptors	Normality Class	Statistical Parameters				
		Minimum	Maximum	Range	Mean	Std. Dev.
Openness	High	17.21	81.54	12036.76	36.04	8.93
	Medium	18.62	62.00	6671.99	39.25	8.27
	Low	0.00	63.44	11123.56	34.55	9.51
	ALL	0.00	81.54	81.54	36.12	9.20
Solar Radiations (KWH/sq.m)	High	63.09	546.32	67134.30	201.00	86.03
	Medium	59.71	415.05	40809.52	240.06	80.38
	Low	0.00	475.59	67766.85	210.46	80.93
	ALL	0.00	546.32	546.32	212.72	84.18
Wind Effect (Direct)	High	0.80	1.11	292.26	0.88	0.04
	Medium	0.82	1.00	151.53	0.89	0.03
	Low	0.00	1.17	289.94	0.90	0.06
	ALL	0.00	1.17	1.17	0.89	0.05

4.4.4.1 Topographic Openness (TO)

The mean Topographic Openness across the study area canyons is observed to be 36.12° (degrees). On average, canyons grouped under medium normality class, have higher openness values, while the ones with low normality have relatively low openness value. In general, narrow streets and spaces between buildings, i.e. enclosed spaces have lower openness values, and building roofs, wide roads, and open spaces have higher TO values. The spatial distribution of TO across the study area and canyons is illustrated in *Figure 4.24*.

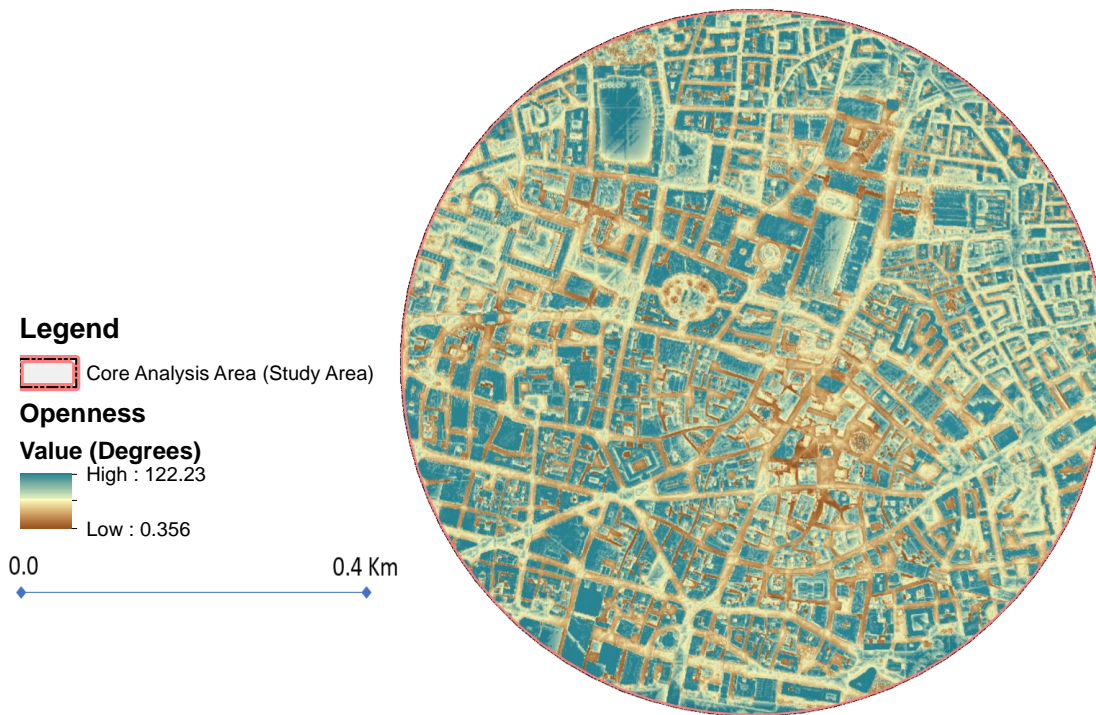


Figure 4.24. Openness Value Map

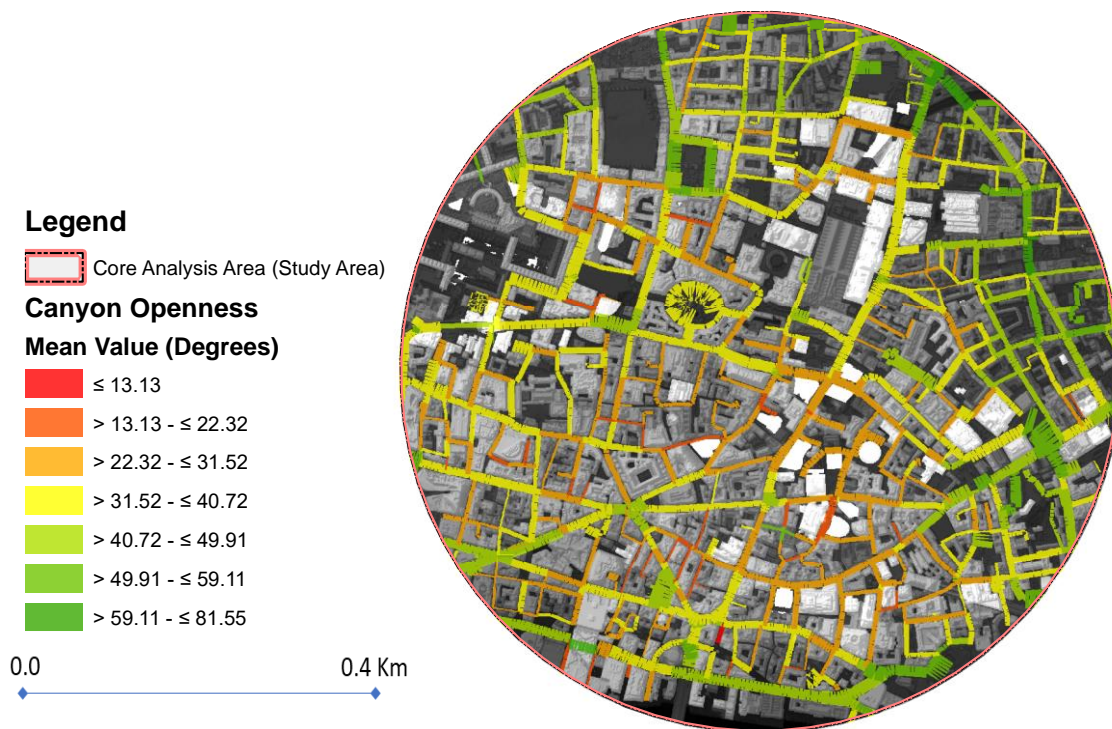


Figure 4.25. Canyon Openness Mean Value Map

4.4.4.2 Global Solar Radiation (Insolation) (GSR)

The Solar insolation output for the study area suggests that under a uniform sky condition, the global radiations range from 0.410 to 585.40 KWH/m². Across the canyons in the study area, the mean solar insolation is about 212.72 KWH/ m². Canyons grouped under moderate normality receive more solar radiations in comparison to other normality classes.

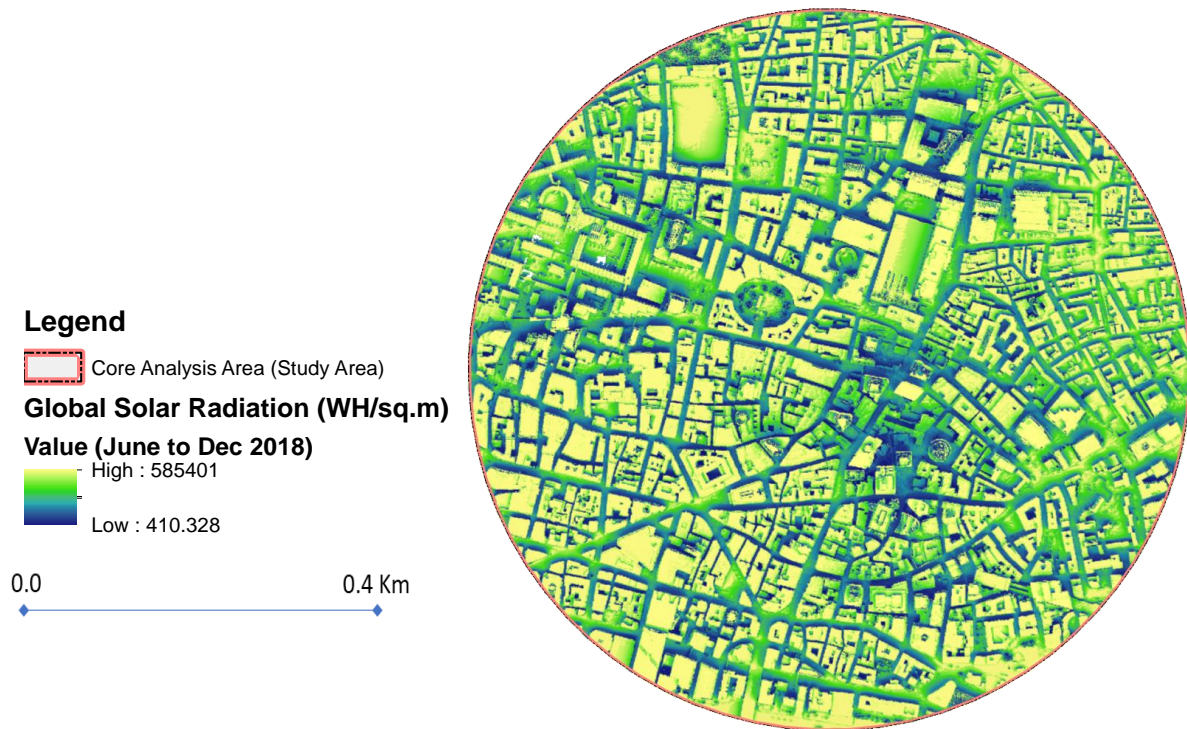


Figure 4.26. Global Solar Radiation Map

Overall, canyons shadowed by tall towers in the study area exhibit poor solar insolation (Figure 4.27). A significant portion of the study area covering clusters 6, 7, and 7a is heavily shadowed due to the presence of tall towers. On the other hand, significantly higher solar radiation values are observed in the North-East section of the study area, where the relatively low building heights allow for more solar penetration. Additionally, the distribution GSR across the moderately normal canyons (Figure 4.26) is more consistent or evenly distributed, i.e. they exhibit a lower standard deviation value than the canyons grouped under high normality class. Across all the normality groups, highly normal canyons are more most deprived of solar insolation, and the mean insolation value is about 20% lower than that of moderately normal canyons.

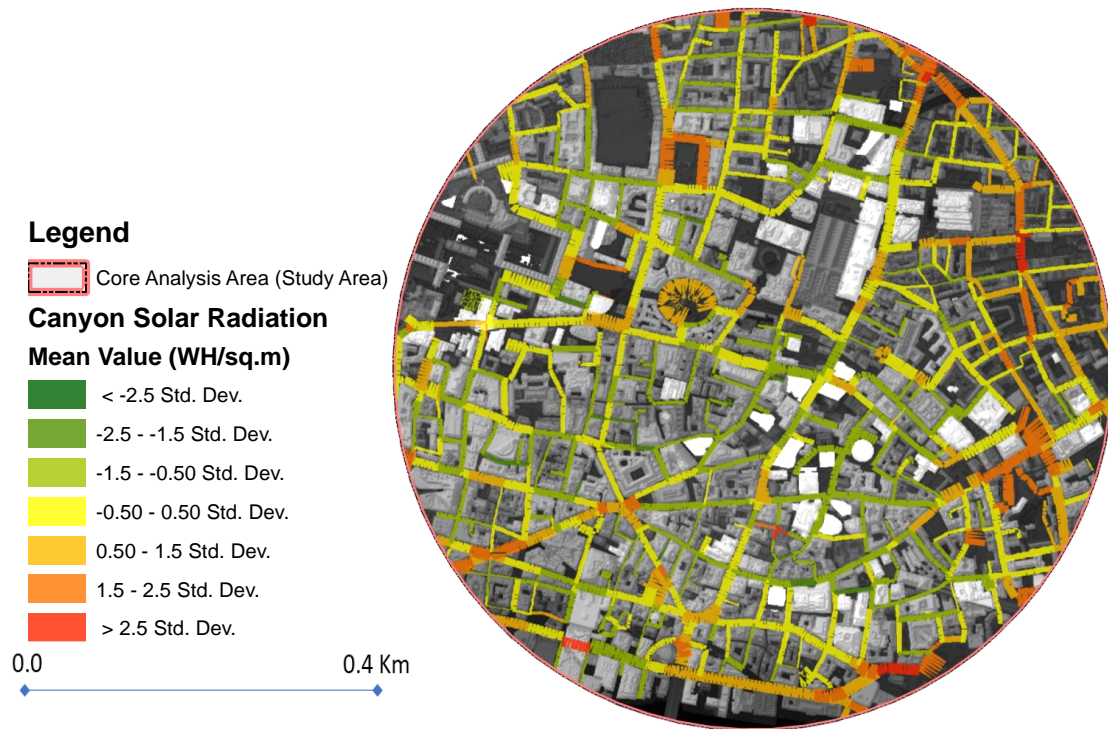


Figure 4.27. Canyon Solar Radiation Map

4.4.4.3 Wind Effect (WE – Direct)

The Wind Effect Index is calculated for a constant (mean) wind direction of 193.66° w.r.t. North as observed during the study period, June to December 2018. As illustrated in the figure below (Figure 4.28), the value of the wind effect in the study area ranges from 0.74 to 1.36. The spatial distribution of Wind Effect across the study area indicates that building roofs are more exposed than the street canyons. Vertically, the value of WE tends to rise with the rise in building heights while on the horizontal plane the WE value is higher for streets or canyons that are most aligned with the dominant wind direction which in this case is 193.66 degrees from North.

The WE value aggregates at the canyon level indicate that the overall exposure to the wind is lower in canyons of high normality class while the same tends to be higher for canyons of low normality. The overall mean value of WE across all the canyons is about 0.89.

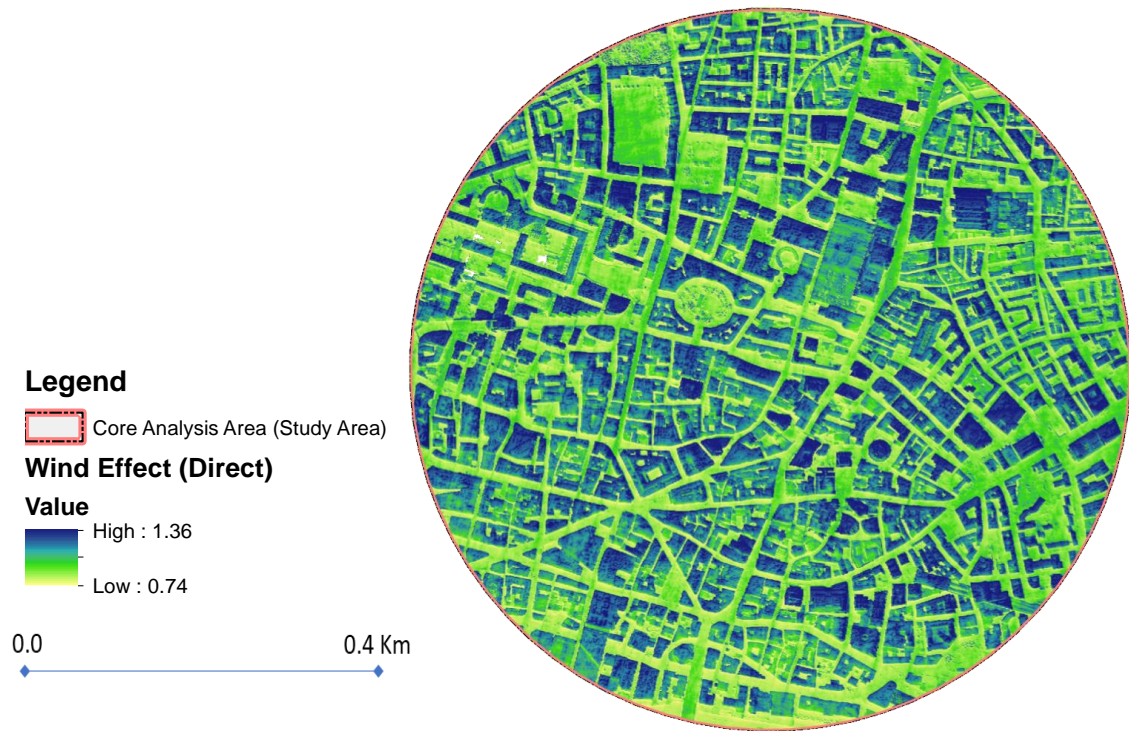


Figure 4.28. Wind Effect (Direct) Map



Figure 4.29. Wind Effect (direct) Map

4.5 Traffic Activity Intensity Hotspot

The traffic hotspot analysis indicates that across the study area, junctions are prominent hotspots. As *Figure 4.30* and *Figure 4.31* illustrate, that three major roads viz. Bishopgate Street (A1213 – A10), Upper Thame Street (A3211 – A100), and the London Wall Street (A1211) witnesses very high intensity of emissions activity. Internal roads are by and large classified as either non-significant or cold spots. Aggregating the Z-score value at the canyon level offers a more discrete understanding of the distribution of activity hotspots across the study area.

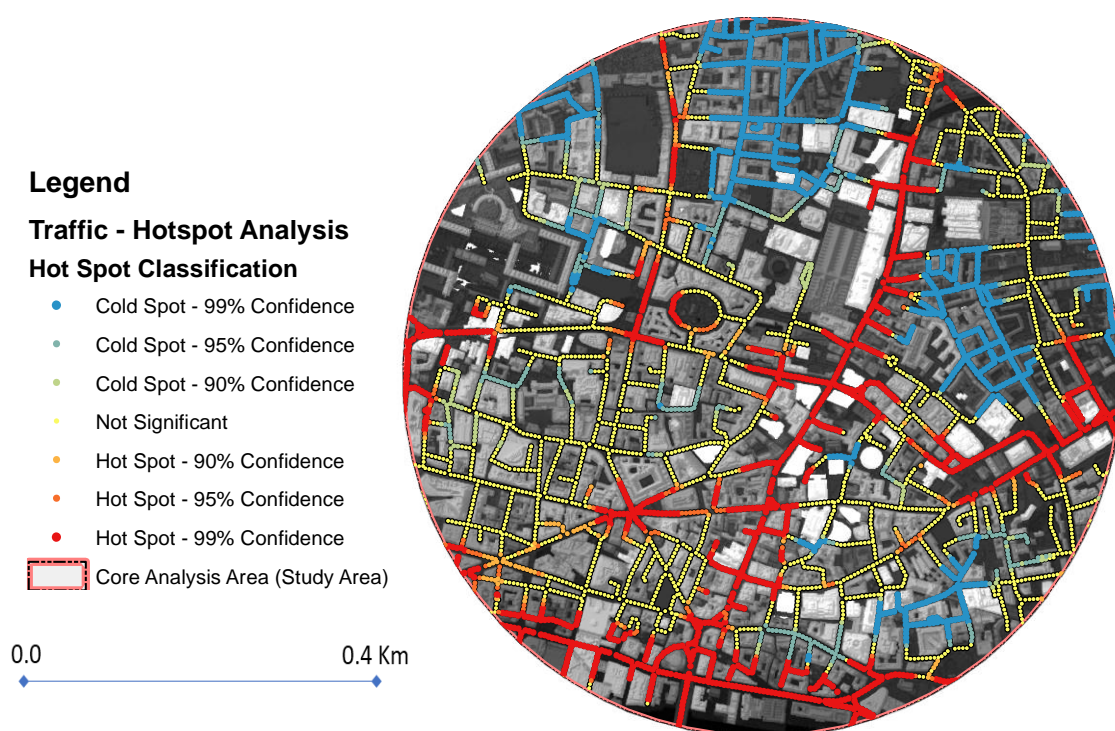


Figure 4.30. Traffic Hotspot Analysis Map

It can be inferred from the hotspot analysis that clusters 6,7a, 9, 4, and 10 of the air quality monitoring campaign, have most of their points in pockets classified as hotspots. This broadly substantiates for the high concentration values observed in these pockets of the cities. On the other hand, clusters 2, 7, and 8 have most of their observation points in pockets that are either classified as cold spots or non-significant with regards to the emission intensity activity.

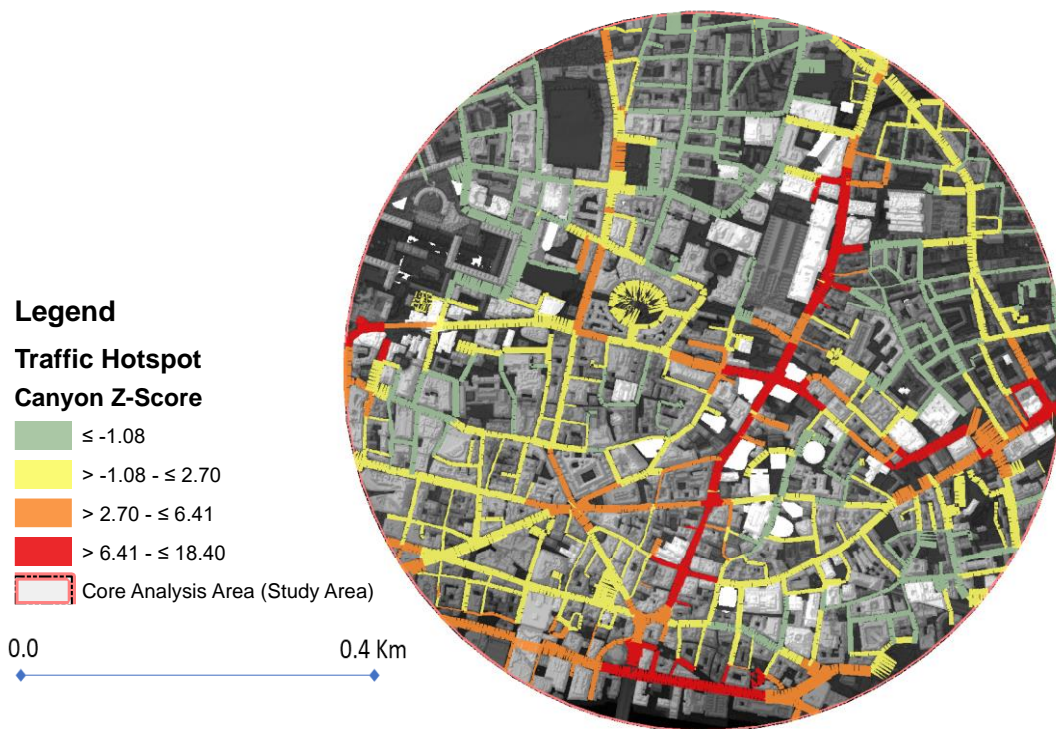


Figure 4.31. Traffic Hotspot Canyon Map (Z-score).

4.6 Wind Simulation and Metrics

Figure 4.32 illustrates the wind simulation output, i.e. spatially distributed wind vectors of varying speed and direction at 6m height around Bishopgate Street.

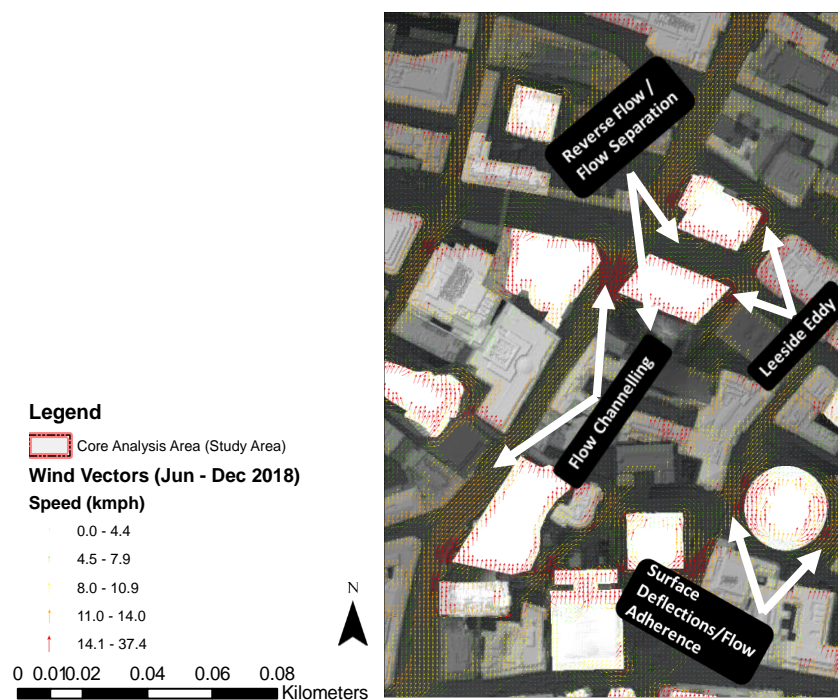


Figure 4.32. Wind simulation output (Wind Vectors).

It can be seen in the figure that while the model simulates wind speed variations effectively, it also identifies the formation of lee-side eddy, windward surface deflection and reverse flows and the channelling effect.

Table 4.16 and Table 4.17, present a statistical summary of the wind metrics derived using the simulation outputs obtained at 6 m and 12 m height.

Table 4.16. Wind metrics for 6m height.

Descriptors @ 6m	Normality Class	Statistical Parameters				
		Minimum	Maximum	Range	Mean	Std. Dev.
Wind Speed	High	0.00	11.77	11.77	5.30	1.86
	Medium	0.00	12.83	12.83	7.38	1.84
	Low	0.00	13.30	13.30	9.04	1.78
	ALL	0.00	13.30	13.30	7.19	2.47
Wind Direction	High	0.00	309.54	309.54	188.48	48.24
	Medium	0.00	265.02	265.02	195.12	33.96
	Low	0.00	231.16	231.16	192.06	19.33
	ALL	0.00	309.54	309.54	191.24	36.48
SD Speed	High	0.00	5.11	5.11	2.73	0.72
	Medium	0.00	5.43	5.43	2.49	0.82
	Low	0.00	6.17	6.17	2.59	0.80
	ALL	0.00	6.17	6.17	2.63	0.78
SD Direction	High	0.00	145.49	145.49	59.70	35.46
	Medium	0.00	133.04	133.04	27.25	22.07
	Low	0.00	110.78	110.78	16.06	13.58
	ALL	0.00	145.49	145.49	36.01	32.84
Turbulence Intensity	High	0.00	1.13	1.13	0.56	0.19
	Medium	0.00	0.84	0.84	0.36	0.15
	Low	0.00	0.92	0.92	0.30	0.13
	ALL	0.00	1.13	1.13	0.42	0.20
Wind Effect (Direct+Indirect)	High	0.82	1.25	0.44	0.93	0.06
	Medium	0.82	1.17	0.35	0.94	0.07
	Low	0.00	1.21	1.21	0.94	0.09
	ALL	0.00	1.25	1.25	0.93	0.07

Table 4.17. Wind metrics for 12m to 6m height.

Flux Descriptors (Vertical Gradient: 12m to 6m)	Normality Class	Statistical Parameters				
		Minimum	Maximum	Range	Mean	Std. Dev.
Wind Speed Flux	High	-0.707	0.429	1.136	-0.207	0.176
	Medium	-0.618	0.184	0.802	-0.238	0.107
	Low	-0.561	0.091	0.652	-0.238	0.087
	ALL	-0.707	0.429	1.136	-0.225	0.134
Wind Direction Flux	High	-15.156	13.457	28.613	-0.779	4.562
	Medium	-8.920	10.047	18.966	0.074	2.392
	Low	-3.325	5.389	8.714	-0.115	0.815
	ALL	-15.156	13.457	28.613	-0.345	3.160
SD Speed Flux	High	-0.297	0.385	0.682	0.027	0.108
	Medium	-0.140	0.355	0.495	0.067	0.069
	Low	-0.134	0.223	0.357	0.080	0.054
	ALL	-0.297	0.385	0.682	0.056	0.086
SD Direction Flux	High	-2.092	21.961	24.053	5.431	4.623
	Medium	-0.688	19.022	19.711	2.155	2.466
	Low	-0.508	12.500	13.007	1.101	1.429
	ALL	-2.092	21.961	24.053	3.069	3.824
Turbulence Intensity Flux	High	-0.119	0.122	0.242	0.018	0.032
	Medium	-0.044	0.055	0.099	0.017	0.013
	Low	-0.011	0.090	0.100	0.015	0.009
	ALL	-0.119	0.122	0.242	0.017	0.022

4.6.1 Wind Speed Metrics

For the chosen study period, the wind speed in the study area ranges from 0.143 to 27.75 kmph (Figure 4.33). In general, the building rooftops, wide streets and open spaces witness higher wind speeds. Across all the canyons in the study area, the mean wind speed is about 7.19 kmph. Canyons with high normality exhibit the lowest mean speed (5.3 kmph) while canyons with low normality have the highest mean wind speed (9.04 kmph). On the other hand, the wind speed deviation is higher in canyons that are highly normal to the wind flow while the same for moderately or mildly normal canyons remain relatively low.

Along the vertical plane, the least changes are observed in the canyons of high normality in comparison to the other two classes. This indicates that along the vertical plane, the wind environment remains relatively more consistent in canyons that are highly normal. This confirms the current understanding that canyons that have $HWR > 0.65$ and are perpendicular to the incident flow stay sheltered and entail weak winds and stable vortex which may be suitable for wind comfort but not conducive for ventilation and removal of pollutants (Erell, Pearlmutter and Williamson, 2015).

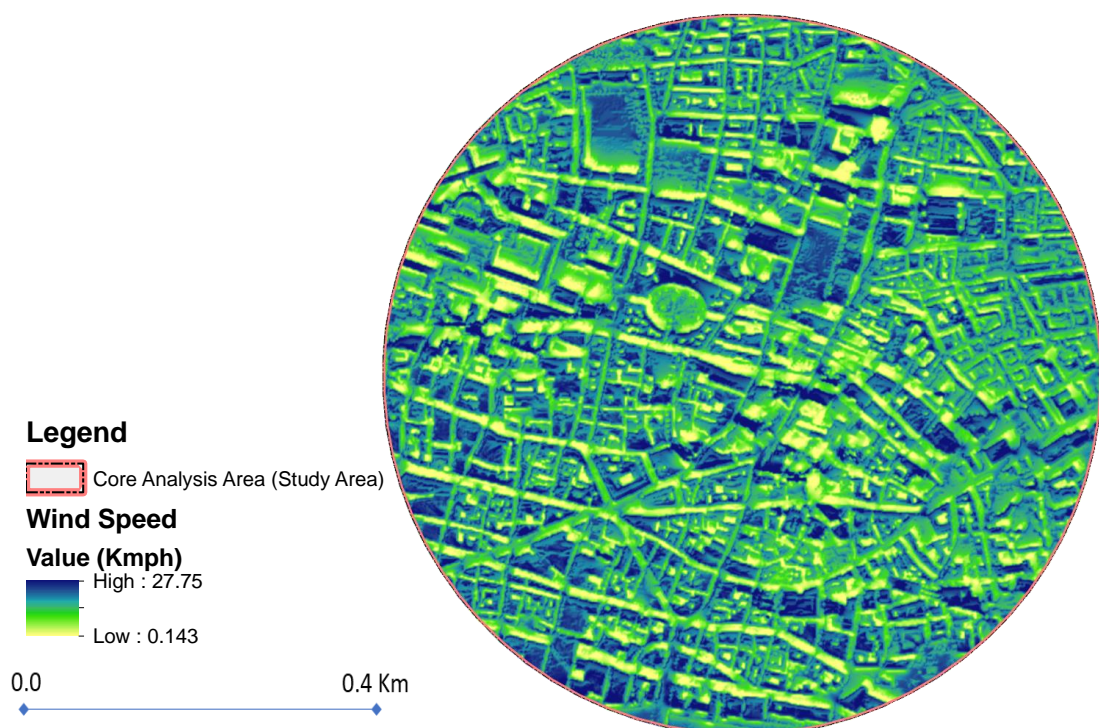
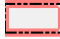








Figure 4.33. Wind Speed Map

Legend

 Core Analysis Area (Study Area)

Average Speed (Overall)

CanyonSpeed (kmph)


-  ≤ 1.00
-  $> 1.00 - \leq 3.48$
-  $> 3.48 - \leq 5.95$
-  $> 5.95 - \leq 8.42$
-  $> 8.42 - \leq 10.90$
-  $> 10.90 - \leq 13.30$

0.0 0.4 Km









Figure 4.34. Average Canyon Wind Speed Map

Legend

 Core Analysis Area (Study Area)

Vertical Speed Flux

Flux_Speed (kmph/m)

-  ≤ -0.44
-  $> -0.44 - \leq -0.30$
-  $> -0.30 - \leq -0.21$
-  $> -0.21 - \leq -0.10$
-  $> 0.10 - \leq 0.043$
-  $> 0.043 - \leq 0.43$

0.0 0.4 Km



Figure 4.35. Vertical Speed Flux Map

4.6.2 Wind Direction Metrics

The mean wind direction across all the mapped canyons in the study area is 191.66° with respect to North. This suggests that as the wind enters the study area, for the said study period, an overall southward deflection of 2.42° is observed in its trajectory (*Table 4.16 and Table 4.17*). Wind flow in highly normal canyons tends to lean more towards the South (188.48°), which indicates a strong presence of reverse flow. The mean wind flow in moderately normal canyons leans towards the South-SouthWest (195.12°) which implies deflection and channelling. The flow in canyons with low normality tends to align within the mean incident wind direction.

As expected, the change in wind direction along the horizontal plane is higher in highly normal canyons while the same remains relatively low in mildly normal canyons. A similar pattern is observed in the wind direction deviation along the vertical plane. In comparison to the other canyon classes, highly normal canyons observe more directional deviation –*indicating the formation of vortex, eddies or rotating cells*.

Figures below illustrate the directional properties of wind flow in the study area.

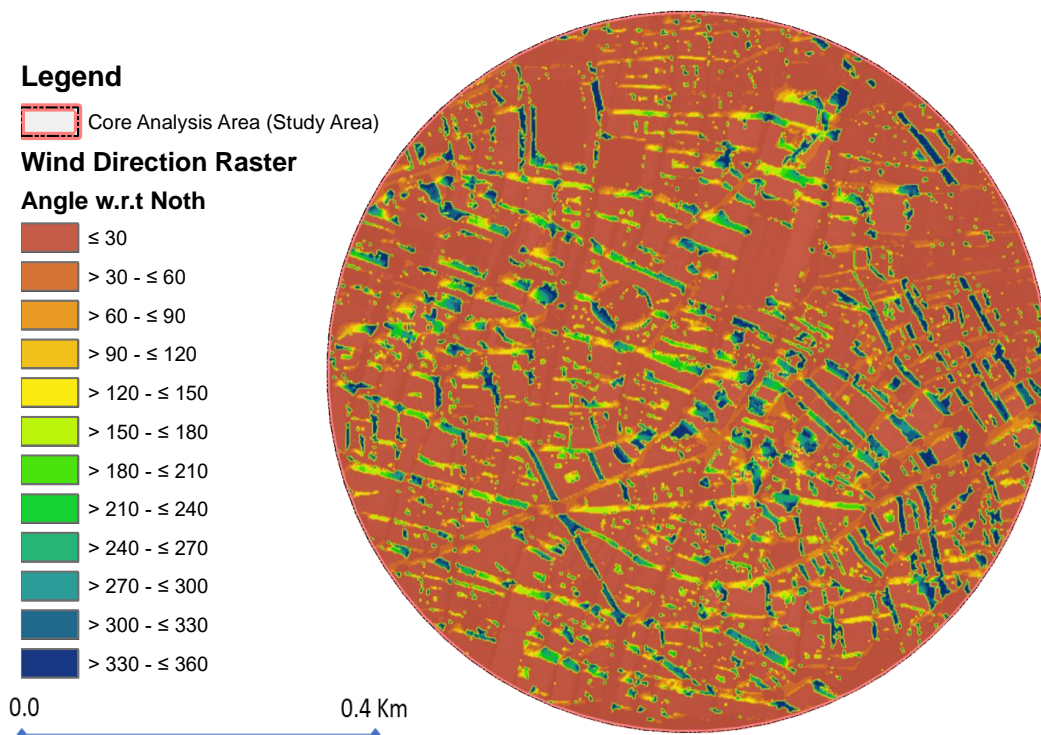


Figure 4.36. Wind Direction Raster Map



Figure 4.37. Vertical Direction Flux Map

4.6.3 Turbulence Intensity Metrics

The turbulence intensity - *along the horizontal plane* - is high in canyons that are highly normal to the wind flow while the same remains low for canyons with low normality. A similar pattern has been observed along the vertical plane. The turbulence intensity in highly normal canyons observes a more rapid change along the vertical plane in comparison to the other canyon classes. *Figure 4.38* below represents the spatial distribution of TI across all the canyons in the study area.

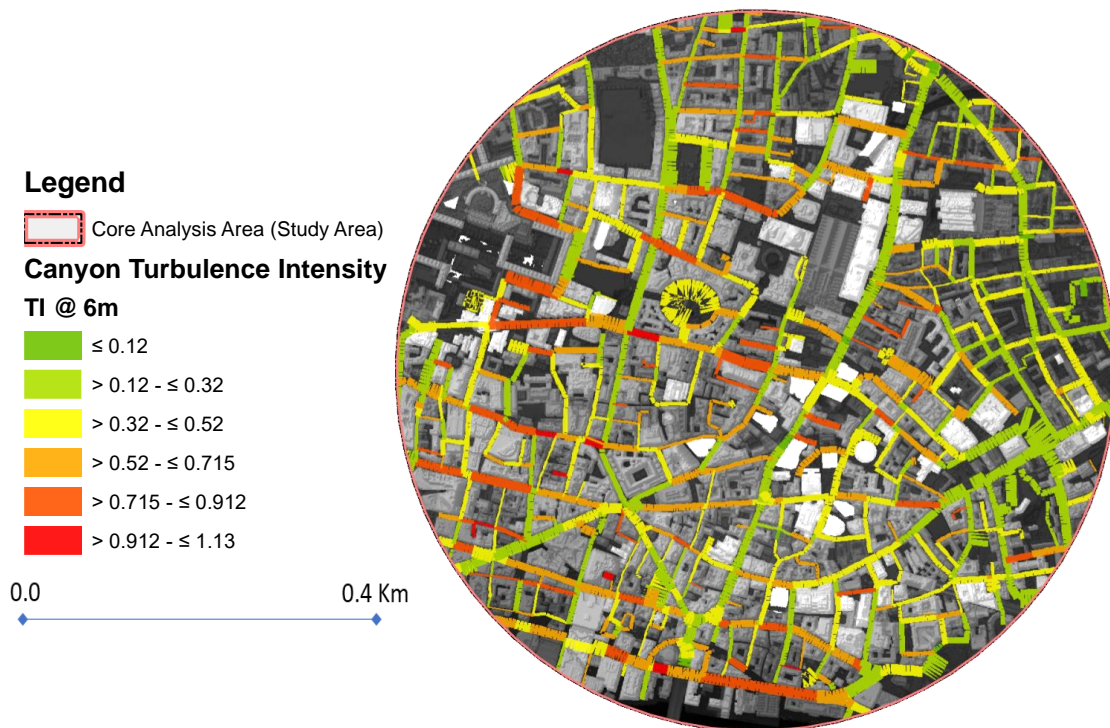


Figure 4.38. Canyon Turbulence Intensity Map

4.6.4 Wind Effect – Direct and Indirect (WEDI)

The WEDI Index is calculated using spatially distributed wind directions obtained post wind simulation. As illustrated in the figure below, the value of WEDI in the study area ranges from 0.74 to 1.36. Like WE, the spatial distribution of WEDI across the study area indicates that building roofs are more exposed than the street canyons. Vertically, the value of WE tends to rise with the rise in building heights, while on the horizontal plane the WE value is higher for streets or canyons that are most aligned with the dominant wind direction which in this case is 193.66 degrees from North.

The WE value aggregates at the canyon level indicate that the overall exposure to the wind is lower in canyons of high normality class while the same tends to be higher for canyons of low normality. The overall mean value of WEDI across all the canyons is about 0.93.

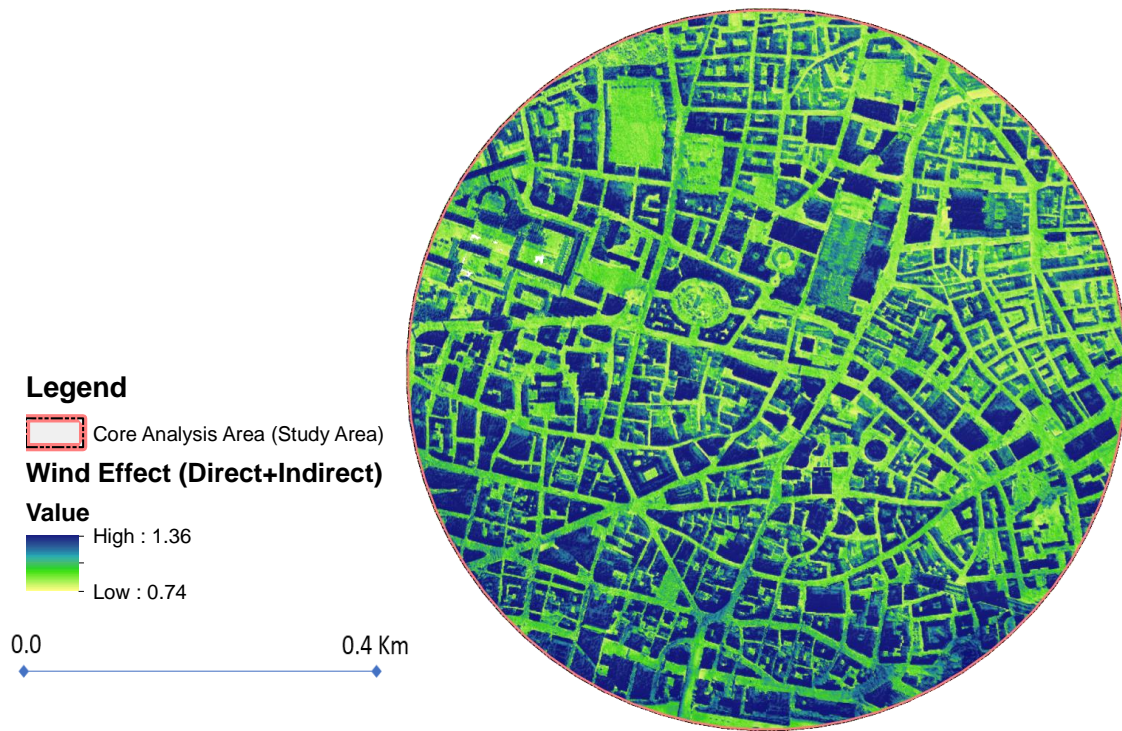


Figure 4.39. Wind Effect (Direct +Indirect) Map

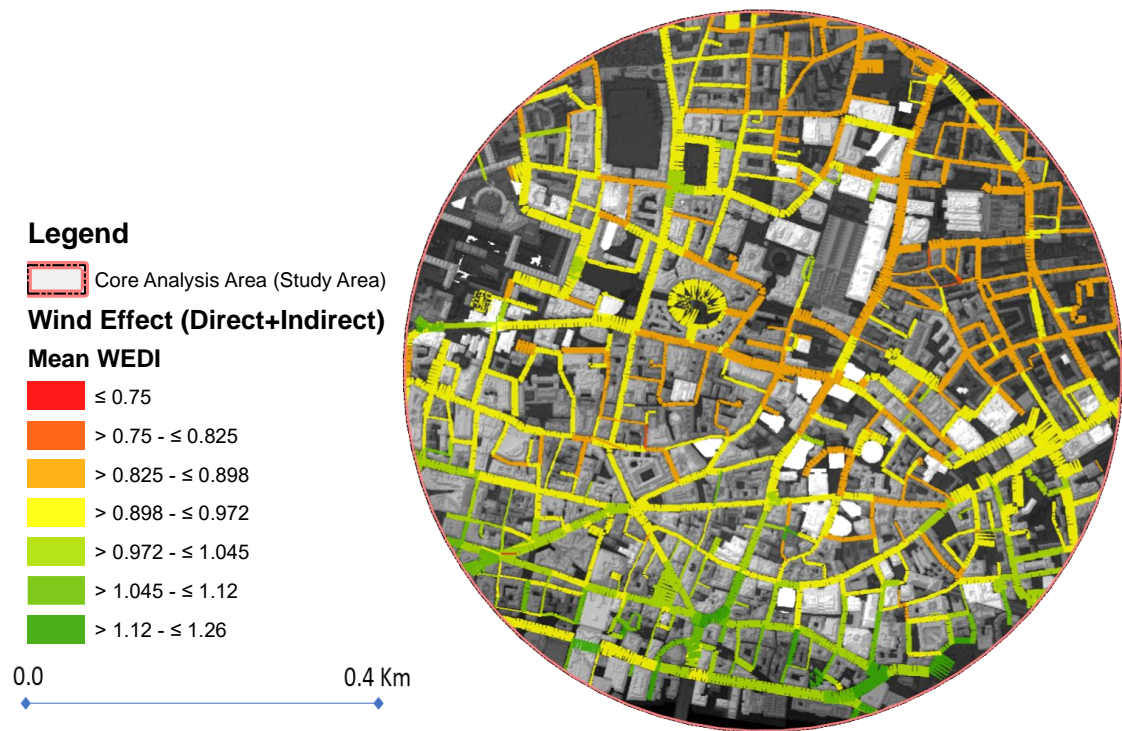


Figure 4.40. Wind Effect (Direct+ Indirect) (WEDI) Map

4.7 Exploratory Regression, Variable Significance and Correlation Matrix

4.7.1 Urban form and the Wind Environment

4.7.1.1 Ungrouped Canyons

The results below correspond to the exploratory regression analysis executed for canyons across the site using 42 explanatory variables to understand the interaction between urban form and the wind environment. A list explaining the variable abbreviations has been enclosed in *Appendix 9.1*.

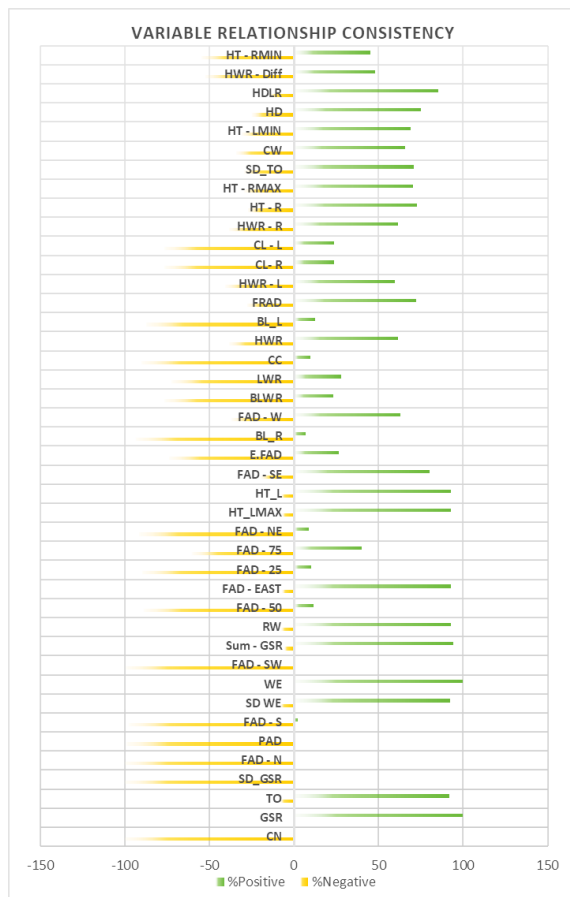


Figure 4.41. Variable relationship consistency (left)

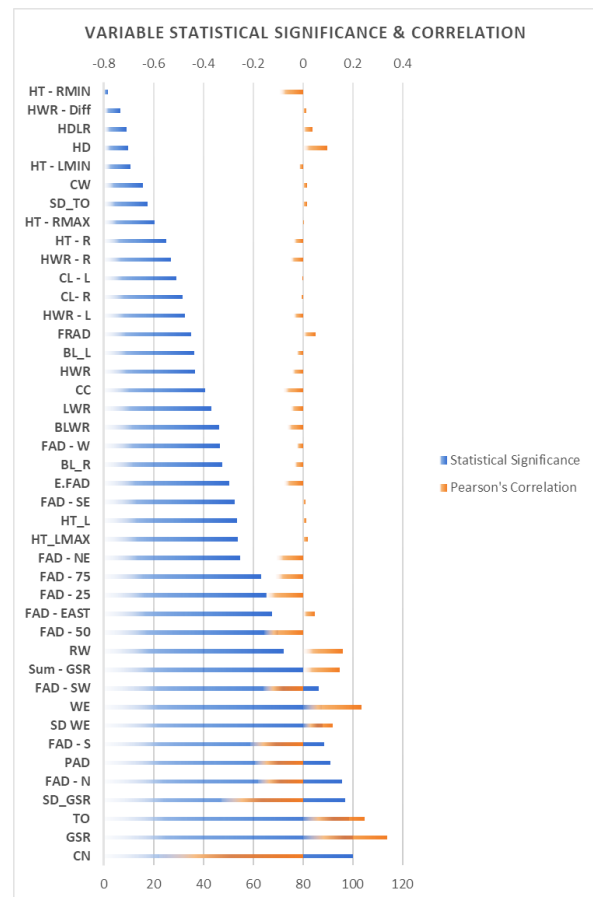


Figure 4.42. Variable statistical significance & correlation (right)

The variables in the illustrations above are presented in accordance to their significance as predictors of Wind velocity. The graph on the left (*Figure 4.41*) represents the consistency of the variable relationship while the one on the right (*Figure 4.42*) indicates the overall significance and strength of relationship using Pearson's correlation (R). out of the 42 variables deployed for this analysis, 22 were found to have a statistical significance of greater than 50%.

The newly incorporated metrics like Canyon Normality, Global Solar Radiation, Topographic Openness and Wind Effect, are found amongst the strongest predictors. Additionally, the use of surrounding FAD values (@25m) confirms that they strongly influence the wind environment of the point they enclose. In

this case, FAD-N (North), FAD- S (South), and FAD-SW (South-West) were found amongst the stronger predictors. Further, this also suggests that the nature of the relationship with surround FAD values need not be consistent across, i.e. while some surrounding FAD values may show a positive relationship with the dependent variable, others may differ.

FAD values for the study area have been computed at 25m resolution, however, in order to understand their representativity, they have been additionally aggregated to 50m and 75m resolutions. Out of these three resolutions, FAD-50m is found to exhibit a better relationship in comparison. Thus, for an intra-city comparison on urban form and wind speed, FAD values at 50m may be used.

PAD shows a strong negative influence on the wind environment. This indicates that an increase in PAD increases the surface roughness and canyon enclosure, thus dissipating the wind flow.

4.7.1.2 Canyons grouped by normality class

The figures below correspond to the outcomes of exploratory regression conducted by canyon normality class intended towards exploring the change in relationship, if any, between the explanatory and dependent variable which in this case is wind speed.

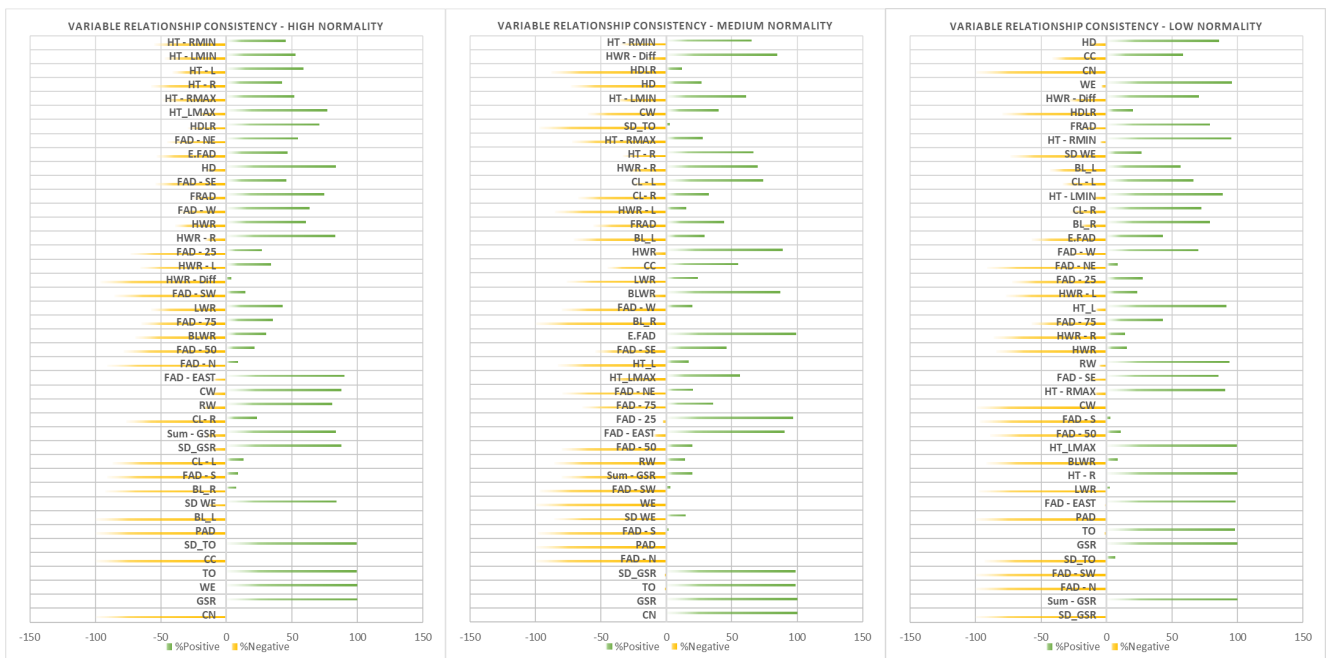


Figure 4.43. Variable relationship consistency – High Normality (left)

Figure 4.44. Variable relationship consistency – Medium Normality (middle)

Figure 4.45. Variable relationship consistency – Low Normality (right)

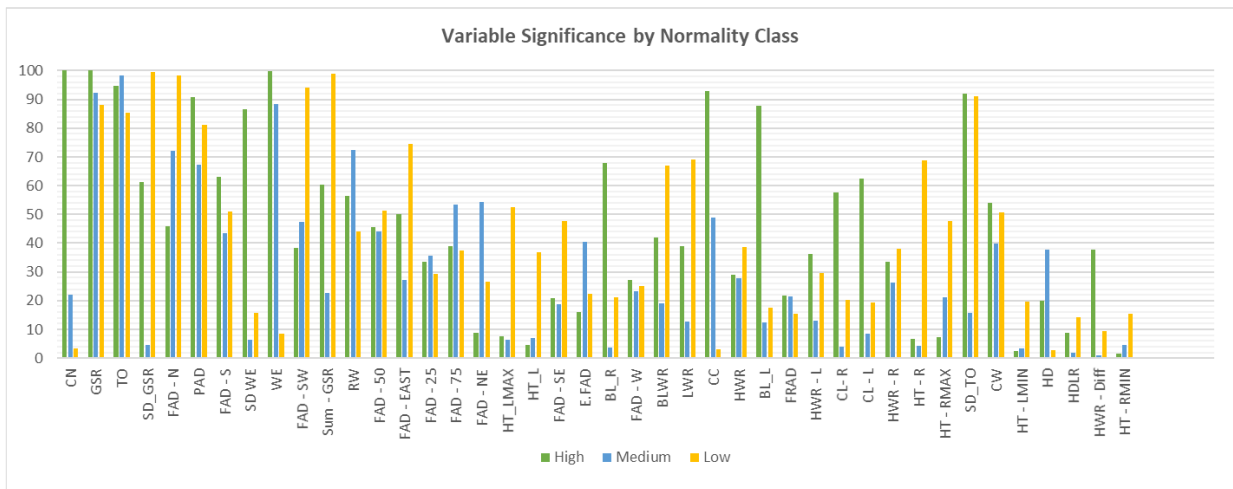


Figure 4.46. Variable Significance by Normality Class

It is observed that with changes in canyon orientation, the percentage significance as well as the nature of the relationship between some explanatory variables and the dependent variable changes. For instance, Canyon Coverage has a strong significance and influence on the wind speed in canyons of high normality. However, its influence and significance tend to decline with decreasing canyon normality. Similarly, Canyon Normality exhibits a strong significance and negative influence on the wind speeds in a highly normal canyon. While it still retains its significance on wind speed in moderately normal canyons, the nature of its relationship switches to highly positive. Although Global Solar Radiations (Insolation) continues to retain its significance and strong positive influence on wind speed across all canyon classes, its significance declines slightly in canyons with low normality, i.e. canyons that near parallel to the incident wind flow. A similar trend is observed in the case of topographic openness. This implies that when canyons align with the incoming wind, the influence of openness, which may provide additional access to deflected winds into the canyon, reduces. *Figure 4.46* demonstrates the changes in significance for all the 42 explanatory variables deployed for this assessment.

4.7.2 Air Quality, Urban Form and the Wind Environment

The illustrations below correspond to the exploratory regression analysis undertaken using 64 explanatory variables to explore the triadic relationship between air quality, the wind environment, and the urban form. This analysis, which is performed for 63 canyons with AQ observations, shows that out of the 64 variables deployed, 10 are found to have a statistical significance of greater than 50%. Some of the newly incorporated metrics feature amongst these top 10 predictors.

As anticipated, the proximity of the AQ observation points to emission intensity hotspots, expressed using Z-score and Node exposure (JN), has a strong positive influence on the AQ observations, i.e. AQ

worsens. Likewise, exposure to wind, expressed using WEDI and Std. Deviation of WEDI shows a strong negative influence on air quality, i.e. AQ improves with enhancing exposure to wind. Amongst neighbouring FAD metrics, FAD-Northwest and FAD-North have a strong negative influence on air quality. The Effective FAD, intended to capture the influence of surrounding frontal areas, is one of the most significant predictors and exhibits a strong negative influence on air quality.

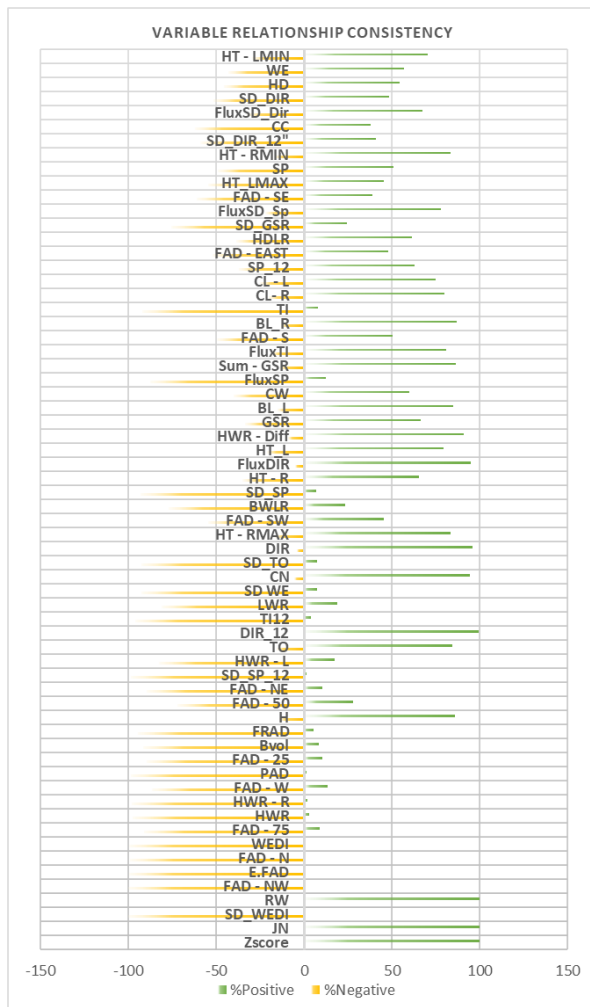


Figure 4.47. Variable relationship consistency (left)

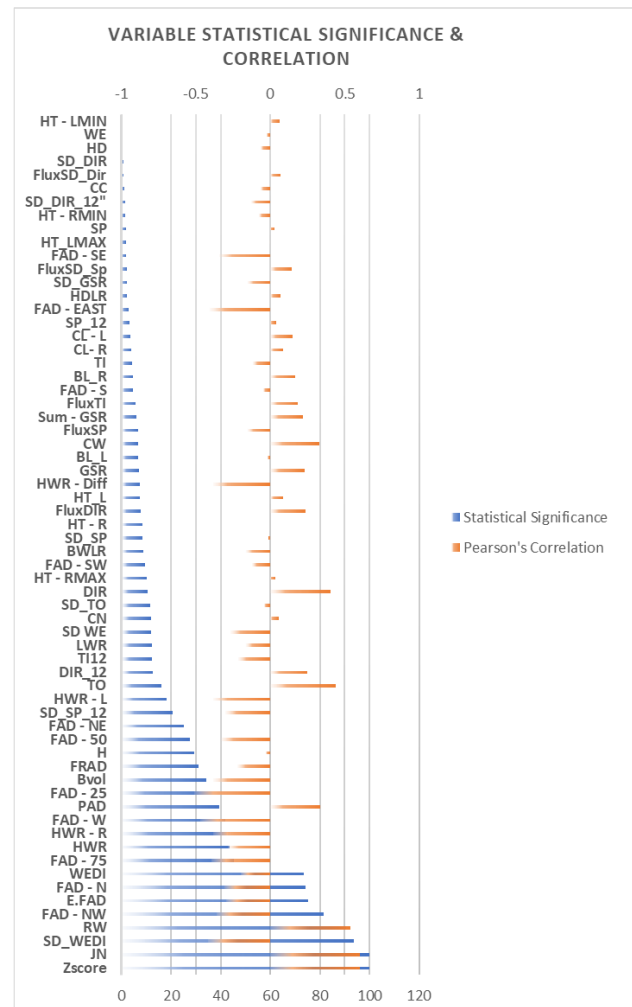


Figure 4.48. Variable statistical significance and correlation (right)

Although of relatively low significance, the wind metrics obtained at 12 m such as Turbulence Intensity and Std. Deviation of speed are better predictors of AQ than those obtained at 6m height.

The HWR of the right-side of canyons – which in most cases faces the windward direction - is one of the strongest predictors with a strong negative influence on AQ. This implies that the air quality may get better in areas where the HWR is high. However, this finding can be attributed to the location bias of the observation points intended to capture the impact of downdraft on air quality, i.e. some points in

the study area have been placed in pockets where downdraft of high urban winds takes place.

Although of statistically low significance, metrics like Topographic Openness and Global Solar Radiations that exhibit a strong positive influence on wind speed, indicate a negative relationship with air quality, i.e. AQ worsens with the increase in TO and GSR values. Similarly, PAD and Built Volume exhibit counter-intuitive outcomes wherein AQ tends to get better with the increase in PAD and Built Volume. However, some elements of this finding are misleading and thus are discussed further in the next section of the report.

The best OLS models passing the statistical criteria outlined in the methodology chapter are presented in the table below.

Table 4.18. The best OLS models

AdjR2	AICc	JB	K(BP)	VIF	SA	Model Predictors				
						Variable 1	Variable 2	Variable 3	Variable 4	Variable 5
0.67	477.4	0	0.77	7.06	0.19	-E.FAD	-FAD_SW	+FAD_E	+Z_Score	+JN
0.67	477.83	0	0.32	1.32	0.18	-FAD_NW	+Z_Score	+JN	-WEDI	-FLUX_SPEED
0.67	478.22	0	0.48	1.41	0.13	+Z_Score	+JN	-WEDI	-B_VOL	-FLUX_SPEED*

5 Discussion on Results and Reflections

This section of the dissertation report offers further discussions and reflections on the overall approach adopted and the results obtained in the preceding section. Towards the end of the chapter, the limitations of this study and the ways in which it may be further develop, have been highlighted.

5.1 Seasonal Variation in Air Quality

The seasonal variation in AQ data indicates that as the study area progress from summer to winter, the mean NO₂ concentration value witnesses a spike of 5.62%. This is in contradiction to the normally observed trend in the study region. The general trend in the study region suggests that while NO_x concentrations peak in winters, NO₂ concentrations peak in summer. The higher availability of sunlight driving photolysis of NO₂ alongside the greater extent of vertical convection is some factors contributing to this trend. (*Bohnenstengel et al., 2015; Derwent et al., 1995*). In the study area, the NO₂ concentration in Autumn spikes despite the overall increase in wind speed in the region. However, as discussed earlier, the wind direction leans towards the south in Autumn, which bring in about a change in the canyon normality and consequently leads to a reduction in the mean Frontal Area Density values in the study area by about 2%. Given the complex nature of urban form surrounding the AQ observation points, it can be argued that the seasonal changes in wind direction changes the way the wind moves and interacts with the study area morphology which further causes alterations in the ambient air quality. The seasonal changes in solar insolation values may further propel this change.

5.2 Influence of Canyon Orientation

Through existing literature, the behaviour of wind in canyons of varying orientations is well understood. However, none of the existing studies explores whether the change in orientation triggers a change in the influence of urban form metrics on either wind behaviour or air quality. This study, through the introduction of Canyon Normality and Normality Classes, has demonstrated that with changing canyon orientation, some urban form metrics may exhibit contrasting influence on the wind environment. Given the fact that the triadic relation of urban form, air pollution and the wind environment is a complex multidimensional problem, urban form metrics often display a weak statistical relationship with AQ and the wind environment in most of the studies observed on this matter. Thus, the varying influence of urban form metric on the wind environment with changing canyon orientations could be a reason for the weak statistical links. Therefore, it may be argued that the influence of canyon orientation should be incorporated in studies attempting to explore the interactions between urban form and the wind environment at street and intra-city levels.

5.3 Key Findings - Performance of Urban Morphological and Geometrical metrics

5.3.1 Canyon Normality (CN)

The introduction of Canyon Normality has facilitated in classifying the canyons and assigning them a score indicating their normality to the incident flow. Its performance as a predictor of wind speed has been significantly strong and thus may be used in future studies to gauge the wind behaviour in urban canyons. Its efficacy may be further enhanced if used in combination with other urban form metrics. Its performance as a predictor for air quality shows a relatively weak statistical significance and thus implies that its relevance to air quality may be indirect.

5.3.2 Effective FAD (EFAD)

The effective frontal area density which has been introduced to capture the positive or negative influence of the neighbouring frontal area densities turns out to be one of the strongest predictors for air quality. However, its performance as a predictor for wind speed has been of low statistical significance. Therefore, it may be understood that the metric tends to capture some non-tangible elements pertaining to the wind flow or pollution dispersion. It should, however, be noted that EFAD in the current study is computed for the mean incident wind direction during the study period, i.e. South-South-West. Further, the upwind and downwind neighbours have been identified instinctively. These may change with changing wind direction, and therefore the efficacy of the metric with regards to other wind direction is unknown at this stage. However, the consideration of neighbouring frontal area density values individually in the exploratory regression process has also facilitated in identifying the most influential neighbours. For instance, the FAD values of the neighbouring cell in the North-West has been identified as a more potent predictor. Thus, although EFAD has performed well, there is further scope for enhancement in its computation method.

5.3.3 Topographic Openness (TO)

Prior to this assessment, no other study has utilised topographic openness in the context of the urban area, and particularly in air pollution studies. As a metric defining multidirectional openness, TO has been identified as one of the strongest and most significant predictors of wind velocity in the study area canyons. However, its performance as a predictor of air quality was not just statistically of low significance, but it also exhibited a counter-intuitive relationship with the background air quality. Further investigation into this reveals that wide canyons apart from exhibiting high openness also tend to have high traffic activities, and thus high pollution concentration. However, as openness serves as a good predictor of wind speed, its indirect relevance to air quality is important.

5.3.4 Global Solar Radiations (GSR)

Global Solar Radiations (GSR) has been incorporated in the study to identify the influence of differential heating on canyon air quality. However, this metric has been identified as the strongest predictor of wind speed after canyon normality. Nevertheless, just like in the case of topographic openness, the counter-intuitive relationship between air quality and solar insolation has been observed. Solar insolation values are generally high for wide streets. However, wide street entails heavy traffic and thus poorer air quality, which misleads into concluding that higher solar insolation implies poorer air quality.

For simulating the wind behaviour within the study area, WindNinja has been used. Although with a simplified approach, WindNinja does consider the diurnal wind effect, which is a function of incident solar radiations. Thus, this may have been the reason for GSR exhibiting a strong positive influence on wind speed.

5.3.5 Wind Effect Index

As mentioned earlier, the Wind Effect Index is computed on two occasions. Firstly, using a constant direction and then using varying wind direction obtained through the wind simulation exercise. Wind Effect (WE – Direct), which is computed using a constant direction, has shown significance relevance with regards to serving as a predictor for wind speed. However, its performance as a predictor of air quality has been of very low statistical significance. On the other hand, WEDI, which takes into consideration the varying wind speed and direction values has been identified as one of the most statistically significant predictors of air quality in the study area. Although WEDI is a function derived using wind speed and direction, it exhibits a stronger significance and influence on air quality values in comparison to other metrics on the wind behaviours such as Speed, SD. Speed, Turbulence Intensity, etc. Thus, WEDI can be used as a single metric that can represent the wind behaviour in terms of both speed and direction.

5.3.6 Z-score and JN/Node Exposure

The traffic dynamics is often ignored in studies pertaining to exploring the relationship between urban form and air pollution at street level. However, traffic being the primary source of pollution in the study area, and the fact that several observation points are situated on main streets and nodes, it is of paramount importance to incorporate the emission activity element in the study. The addition of Z-score on the hot-spot analysis conducted in GIS and the assigning of Node exposure score is found to be the most influential predictors of air quality.

5.3.7 Road Width

Contrary to the understanding where wider roads allow for more air circulation and thus help in reducing pollution concentration, the outputs of this study suggest otherwise. Given the dense and busy nature of the city, wider streets only imply more traffic activity. Thus, as witnessed in the case of TO and GSR, Road width has been identified as a statistically significant predictor with a highly positive influence on the background AQ, i.e. air quality tends to get poorer as the road widens.

5.3.8 Plan Area Density (PAD)

PAD is one of the most common urban canopy descriptors used to indicate surface roughness. It has been observed to positively influence the NO_x concentrations in the studies undertaken earlier (*Edussuriya et al., 2014*). In the exploratory regression analysis undertaken in this study, it is identified as one of the most influential metrics for predicting wind velocity with a strong negative influence. On the contrary, with regards to its performance as a predictor for air quality, it has demonstrated a significant yet negative influence on air quality, i.e. AQ enhances with an increase in PAD. As cited earlier, this output has been found misleading and could be attributed to the resolution chosen for computing the PAD values across the study. As explained earlier, the urban canopy metrics have been computed at a resolution of 25 x 25 m grid (*Figure 5.1*). This fine resolution of computation render many of the grid cells covering only the canyon floor where the build area is virtually zero (green), but the air pollution is high.

On the other hand, in pockets away from the main roads, where buildings are closely spaced, high PAD values (red) is observed while the air pollution observed is low. This generates a false sense of PAD being negatively correlated to pollution concentration. However, this calls for re-evaluating the approach and resolution for deriving the canopy metrics for street-level studies.

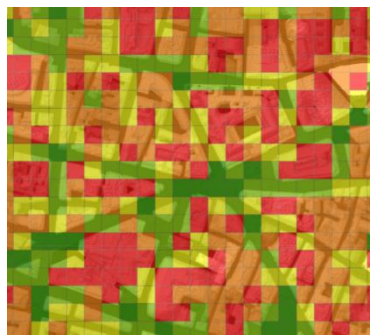


Figure 5.1. PAD map sampling

5.4 Limitations

- WindNinja is a tool meant for large scale simulation of wind. The application of this tool is rare in urban areas. However, with the use of fine-scale elevation data (0.5m), although the tool has performed quite well, it may have failed in simulating certain wind flow phenomenon. Further, due to the ongoing COVID-19 pandemic, the outputs of this model could not be validated through field observations, and thus, the entire analysis is based on non-calibrated simulations.
- In events where AQ observation points intersected with more than one canyon, especially around junctions, the mean canyon and canopy values of the respective streets are attributed to the observation points. This is owing to the complication in deciding which of the intersecting canyons is most influential under such circumstances. Since several AQ observation points are situated around nodes, attributing average canyon and canopy properties of multiple streets to one point may have led to smoothening or generalisation of data, which in turn might have artificially strengthened or weakened the statistical relationship between some of the analysed variables/metrics.
- The meteorological data used for this study corresponds stations that are situated at a distance ranging from 15 to 26 km from the study area. Given the highly heterogeneous nature of the city, the observations of these stations need not fully represent the study area. Further, no steps are taken in apportioning the data to the chosen study area.
- Cloud cover data used for wind simulation has been estimated using sunshine hours. This method is subject to errors, and thus the same might have propagated through the entire study.
- The air quality data composed of gaps which have been filled using statistical prediction. However, there is a possibility that the values have either been over or underestimated on certain occasions which potentially may have incurred more error into the study. Further, the air quality monitoring campaign is coarse in its temporal resolution, i.e. the data is collected once a month. Due to this, the study may have failed in capturing certain dynamics.
- The traffic activity data used for this study corresponds to the year 2016, which may not be fully representative of the study period traffic activities.
- Temporal scope of this study is limited to the period of June to December 2018.
- The findings of the study, especially the ones pertaining to air quality, are limited only to NO₂ and perhaps gases that are similar in nature.
- The ArcGIS based tools on Urban Canopy and Canyon mapping by CERC are used for this study. The accuracy of these tools has not been validated prior to using them for this study.

6 Conclusion

The triadic relation on urban form, air quality and the wind environment at street level in a dense setting of the City of London is investigated through detailed characterisation of the urban form, wind simulation and statistical analysis in conjunction with AQ data observations for the period June – December 2018. While there are a plethora of broad level indicators describing urban morphology and form at neighbourhood and city levels, this study has taken a detailed approach towards identifying the street level canyon and canopy related metrics that influence the urban wind environment and ambient air quality. While it has tried out some of the existing metrics, the study has also introduced a set of new parameters that may further aid in understanding the triadic relation. For over 826 canyons mapped in the study area, the study has analysed about forty-two (42) urban form and morphological metrics to understand the influence of urban form on the wind environment.

Additionally, for sixty-three (63) canyons with AQ observations, sixty-four (64) wind and urban form related metrics were analysed for their statistical significance as predictors using the exploratory regression approach. Out of the 42 metrics used to investigate the influence of urban form on wind pattern, twenty-two (22) are found to have a statistical significance of greater than 50%. Moreover, out of the sixty-four (64) variables used towards investigating the role of wind and urban form metrics on AQ, ten (10) are found to exhibit a statistical significance of greater than 50%.

Amongst the newly introduced parameters Canyon Normality, Topographic Openness, Global solar Radiation, Effective Frontal Area, Wind Effect, Node Exposure and traffic Z-score are identified as statically significant predictors with a strong influence on the wind environment and consequently, the ambient air quality.

7 Recommendation for future studies

The study has undertaken a detailed characterisation of the urban form within the study area and thus has paved a solid foundation for further studies to investigate the subject in detail. Towards this end, the following studies are proposed:

1. **Comprehensive Urban Ventilation Index:** This study has demonstrated that Topographic Openness, Solar Insolation, Wind Effect and Proximity to Traffic hotspots are significant predictors of air quality and wind behaviour in the study area. Thus, a comprehensive ventilation index based on the IPCC Exposure (*Traffic*), Sensitivity (*Lack of Openness*) and Adaptive Capacity (*Wind Effect*) Framework is proposed for further evaluation.
2. **Simulation-based sensitivity analysis of urban form:** Based on the existing characterisation of the urban form, some key canyons or neighbourhoods may be identified for scenario-based simulations exploring the changing interaction between urban form, solar insolation and wind, and their consequent implications on the ambient air quality.
3. **Logistic regression-based hotspot mapping:** A logistic regression-based hotspot prediction model may be developed. Towards this end, the urban geometrical and morphological metrics developed in this study may be deployed in conjunction with the field-based AQ observations, and thus a probabilistic model that may be applied towards identifying air pollution hotspots in the city with regards to either existing or proposed urban developments.
4. **Role of Edge and Corner Density:** This study has used metrics like turbulence intensity and flux to capture the eddy-like behavioural pattern of wind. However, built form metrics like edge and corner density may be worth exploring.
5. **In-depth study exploring the seasonal variations:** Section 5.1 of this report broadly argues that change in seasonal wind directions changes the way urban form interacts with it, and thus this may have some implications on pollution dispersion. Towards this end, a simulation-based study exploring the pollution concentration distribution with changing wind directions would facilitate in fostering this understanding.

8 Bibliography

1. Badach, J., Voordeckers, D., Nyka, L. & Van Acker, M. (2020) A framework for Air Quality Management Zones - Useful GIS-based tool for urban planning: Case studies in Antwerp and Gdańsk. *Building and Environment*. 174 (February), 106743.
2. Boehner, J., Antonic, O. (2009). Chapter 8 Land-surface parameters specific to topoclimatology'. in: Hengl, T., Reuter, H. (Eds.): 'Geomorphometry - Concepts, Software, Applications'. Developments in Soil Science, Volume 33, p.195-226, Elsevier. Available from: <http://www.sciencedirect.com/science/article/pii/S0166248108000081>.
3. Bohnenstengel, S.I., Belcher, S.E., Aiken, A., Allan, J.D., Allen, G., Bacak, A., Bannan, T.J., Barlow, J.F., Bedddows, D.C.S., Blossss, W.J., Booth, A.M., Chemel, C., Coceal, O., Di Marco, C.F., Dubey, M.K., Faloon, K.H., Flemiming, Z.L., Furger, M., Gietl, J.K., et al. (2015) Meteorology, air quality, and health in London: The ClearfLo project. *Bulletin of the American Meteorological Society*. 96 (5), 779–804.
4. Cambridge Environmental Research Consultant (2014). Urban Canopy Tool, User Guide. Cambridge. Available from: https://www.cerc.co.uk/environmental-software/assets/data/doc_userguides/CERC_Urban_Canopy_User_Guide.pdf [Accessed: June 2020].
5. Cambridge Environmental Research Consultant (2015). Street Canyon Tool, User Guide. Cambridge. Available from: https://www.cerc.co.uk/environmental-software/assets/data/doc_userguides/CERC_Street_Canyon_Tool_User_Guide.pdf [Accessed: June 2020].
6. Cárdenas Rodríguez, M., Dupont-Courtade, L. & Oueslati, W (2016). Air pollution and urban structure linkages: Evidence from European cities. *Renewable and Sustainable Energy Reviews*. 53, pp.1-9. Available from: 10.1016/j.rser.2015.07.190.
7. Carrington, D. (2019). Air pollution falling in London but millions still exposed. *The Guardian - UK*.
8. Chatzipoulka, C., Compagnon, R. & Nikolopoulou, M. (2016). Urban geometry and solar availability on façades and ground of real urban forms: using London as a case study. *Solar Energy*. 13853–66.
9. Chatzipoulka, C. & Nikolopoulou, M. (2018) Urban geometry, SVF and insolation of open spaces: London and Paris. *Building Research and Information*. 46 (8), 881–898.

10. Chatzipoulka, C. & Nikolopoulou, M. (2018). Urban geometry, SVF and insolation of open spaces: London and Paris. *Building Research & Information*. 46(8), pp.881-898. Available from: 10.1080/09613218.2018.1463015.
11. Chen Lu & Yi Liu, (2016). Effects of China's urban form on urban air quality. *Urban Studies*. 53(12), pp.2607.
12. City of London Corporation (2019). *Air Quality Strategy - Delivering healthy air in the City of London*. City of London.
13. Clark, L.P., Millet, D.B. & Marshall, J.D (2011). Air Quality and Urban Form in U.S. Urban Areas: Evidence from Regulatory Monitors. *Environmental Science & Technology*. 45(16), pp.7028-7035. Available from: 10.1021/es2006786
14. Dempsey N, Brown C, Raman S, Porta S, Jenks M, Jones C, Bramley G (2010) Elements of urban form. In: Jenks M, Jones C (eds) *Dimensions of the sustainable cities*. Springer, London, pp 21–51. Available at: https://link.springer.com/chapter/10.1007/978-1-4020-8647-2_2 . [viewed March, 2020].
15. Derwent, R.G., Middleton, D.R., Field, R.A., Goldstone, M.E., Lester, J.N. & Perry, R. (1995) Analysis and interpretation of air quality data from an urban roadside location in Central London over the period from July 1991 to July 1992. *Atmospheric Environment*. 29 (8), 923–946.
16. Edussuriya, P., Chan, A. & Malvin, A. (2014) Urban morphology and air quality in dense residential environments: Correlations between morphological parameters and air pollution at street-level. *Journal of Engineering Science and Technology*. 9 (1), 64–80.
17. Emmanuel, R. & Steemers, K. (2018). Connecting the realms of urban form, density and microclimate. *Building Research & Information*. 46(8), pp.804-808. Available from: 10.1080/09613218.2018.1507078.
18. Erell, E., Pearlmutter, D., Williamson, T. (2015). *Urban Microclimate: Designing the Spaces Between Buildings*. New York, Routledge.
19. ESRI (2020). Exploratory Regression using ArcGIS. [Online].[Accessed April 2020]. Available from: <https://desktop.arcgis.com/en/arcmap/latest/tools/spatial-statistics-toolbox/exploratory-regression.htm>
20. Fellini, S., Ridolfi, L. & Salizzoni, P. (2020) Street canyon ventilation: Combined effect of cross-section geometry and wall heating. *Quarterly Journal of the Royal Meteorological Society*. (March), 2347–2367.
21. Foresight Government Office for Science, UK (2014), *Urban form and infrastructure: a morphological review*. Future of cities: working paper. Foresight Government Office for

- Science, London, UK. [viewed Feb, 2020]. Available from: https://assets.publishing.service.gov.uk/government/uploads/system/uploads/attachment_data/file/324161/14-808-urban-form-and-infrastructure-1.pdf
22. Forthofer, J.M., Butler, B.W., Mchugh, C.W., Finney, M.A., Bradshaw, L.S., Stratton, R.D., Shannon, K.S. & Wagenbrenner, N.S (2014). A comparison of three approaches for simulating fine-scale surface winds in support of wildland fire management. Part II. An exploratory study of the effect of simulated winds on fire growth simulations. *International Journal of Wildland Fire*. 23(7), pp.982-994. [viewed June, 2020]. Available from: 10.1071/WF12090.
 23. Futch J (under publication). 'Urban Lab City' Investigating the Role of Built Form on levels of Air Pollution at a Microscale Level; *The City of London Pilot Study Preliminary Findings of Air Quality and Daytime Air Temperature Measured Survey*.
 24. Gokhale, S. (2011) Traffic flow pattern and meteorology at two distinct urban junctions with impacts on air quality. *Atmospheric Environment*. 45 (10), 1830–1840.
 25. Gillham, B. (2000) *Case Study Research Methods*. Continuum, London.
 26. Hoyt, D. V. (1977) Percent of Possible Sunshine and the Total Cloud Cover. *Monthly Weather Review*. 105 (5), 648–652.
 27. Jareemit, D. & Srivanit, M. (2019) Effect of Street Canyon Configurations and Orientations on Urban Wind Velocity in Bangkok Suburb Areas. *IOP Conference Series: Materials Science and Engineering*. 690 (1), .
 28. Krüger, E.L., Minella, F.O. & Rasia, F. (2011). Impact of urban geometry on outdoor thermal comfort and air quality from field measurements in Curitiba, Brazil. *Building and Environment*. 46(3), pp.621-634. Available from: 10.1016/j.buildenv.2010.09.006.
 29. Marquez, L.O. & Smith, N.C. (1999). A framework for linking urban form and air quality. *Environmental Modelling and Software*. 14(6), pp.541-548. Available from: 10.1016/S1364-8152(99)00018-3.
 30. Met Office (2019): MIDAS Open: UK mean wind data, v201901. Centre for Environmental Data Analysis, 01 March 2019. [viewed Dec, 2019].. Available from doi:10.5285/11c15f2640f541d4847d4fe9be1bb90a. <http://dx.doi.org/10.5285/11c15f2640f541d4847d4fe9be1bb90a>
 31. Næss, P (2014). Urban Form, Sustainability and Health: The Case of Greater Oslo. *European Planning Studies*. 22(7), pp.1524-1543. Available from: 10.1080/09654313.2013.797383.
 32. Neslen, A (2019). Europe's most deprived areas 'hit hardest by air pollution'. *The Gaurdian* - UK.

33. Oke, T.R., Mills, G., Christen, A. & Voogt, J.A (2017). *Urban climates*. Cambridge: Cambridge University Press.
34. Patel, S. (2015). [Online] Available at: <http://salmapatel.co.uk/academia/the-research-paradigm-methodology-epistemology-and-ontology-explained-in-simple-language> [Accessed April 2020].
35. Stewart D. & Oke T. R. 2012. Local Climate Zones For Urban Temperature Studies. *Bulletin of the American Meteorological Society*. 93(12), pp.1879-1900. Available from: 10.1175/BAMS-D-11-00019.1.
36. The World Bank, (2019). Urban Development. Available from: <https://www.worldbank.org/en/topic/urbandevelopment/overview>.
37. United Nations, 2015 United Nations Sustainable Development Goals - Knowledge Platform. Available from: <https://sustainabledevelopment.un.org/sdg11>.
38. Urban Morphology and Complex System Institute (2013). Urban Form Matters. [viewed Feb, 2020]. Available from: <http://www.urbanmorphologyinstitute.org/urban-form-matters/>.
39. UK Air Information Resource (2005). National air quality objectives and European Directive limit and target values for the protection of human health. Available at https://ukair.defra.gov.uk/assets/documents/Air_Quality_Objectives_Update.pdf (Accessed: April 2020).
40. Williams K, Burton E, Jenks M (2000) *Achieving sustainable urban form*. E & FN Spon, London. Available at: <https://books.google.co.uk/books?hl=en&lr=&id=gVnoeny1wG4C&oi=fnd&pg=PA1&ots=REpOfg6ss3&sig=iHxExMhMY5esKcZVIFLIXQC0xiM&redir> [viewed March, 2020].
41. Wong, M.S. & Nichol, J.E. (2013) Spatial variability of frontal area index and its relationship with urban heat island intensity. *International Journal of Remote Sensing*. 34 (3), 885–896.
42. Yang, J., Shi, B., Shi, Y., Marvin, S., Zheng, Y. & Xia, G. (2020) Air pollution dispersal in high density urban areas: Research on the triadic relation of wind, air pollution, and urban form. *Sustainable Cities and Society*. 54 (November 2019), 101941.
43. Yang, J., Shi, B., Zheng, Y., Shi, Y. & Xia, G. (2020) Urban form and air pollution disperse: Key indexes and mitigation strategies. *Sustainable Cities and Society*. 57 (November 2019), 101955.
44. Yin, R., K. (2014). *Case study research: Design and methods*. Los Angeles, CA: Sage.
45. Yokoyama, R., Shirasawa, M. & Pike, R.J. (2002) Visualizing topography by openness: A new application of image processing to digital elevation models. *Photogrammetric Engineering and Remote Sensing*. 68 (3), 257–265.

9 Appendices

9.1 List of Metrics and Abbreviations

BL_L	Built Length - Left
BL_R	Built length width Ratio
Bvol	Built Volume Density
BWLR	Built Length-Width Ratio
CC	Canyon Coverage
CL - L	Canyon Length - Left
CL- R	Canyon Length - Right
CN	Canyon Normality
CW	Canyon Width
DIR	Avarage Wind Direction
DIR_12	Wind Direction @ 12m
E.FAD	Effective Frontal Area Density
FAD - 25	Frontal Area Density @ 25m
FAD - 50	Frontal Area Density @ 50m
FAD - 75	Frontal Area Density @ 75m
FAD - EAST	Frontal Area Density - East
FAD - N	Frontal Area Density - North
FAD - NE	Frontal Area Density - North East
FAD - NW	Frontal Area Density - North West
FAD - S	Frontal Area Density - South
FAD - SE	Frontal Area Density - South East
FAD - SW	Frontal Area Density - South West
FAD - W	Frontal Area Density - West
FluxDIR	Flux Direction
FluxSD_Dir	Flux - Standard Deviation - Wind Direction
FluxSD_Sp	Flux - Standard Deviation - Wind Speed
FluxSP	Flux Speed
FluxTI	Flux- Turbulence Intensity
FRAD	Frontal Advantage
GSR	Global Solar Radiation

H	Average Canopy Height
HD	Height Difference
HDLR	Height Difference – Left to Right
HT - LMIN	Minimum Height- Left
HT - R	Average Height - Right
HT - RMAX	Maximum Height - Right
HT - RMIN	Minimum Height- Right
HT_L	Average Height - Left
HT_LMAX	Maximum Height- Left
HWR	Height Width Ratio
HWR - Diff	Height Width Ratio - Difference
HWR - L	Height Width Ratio - Left
HWR - R	Height Width Ratio - Right
JN	Junction / Node Exposure
LWR	Length Width Ratio
PAD	Plan Area Density
RW	Road Width
SD WE	Standard Deviation - Wind Effect (Direct)
SD_DIR	Standard Deviation - Wind Direction
SD_DIR_12	Standard Deviation - Wind Direction @ 12m
SD_GSR	Standard Deviation - Global Solar Radiation
SD_SP	Standard Deviation - Wind Speed
SD_SP_12	Standard Deviation - Wind Speed @ 12m
SD_TO	Standard Deviation - Topographic Openness
SD_WEDI	Standard Deviation Wind Effect (direct and indirect)
SP	Average Speed
SP_12	Average Speed @ 12m
Sum - GSR	Global Solar Radiation
TI	Turbulence Intensity
TI12	Turbulence Intensity @ 12m
TO	Topographic Openness
WE	Wind Effect
WEDI	Wind Effect- direct and indirect
Zscore	Traffic Hotspot Score

9.2 Predictors used for filling data gaps

Cluster no	Monitoring Section	Observation Points	Predictors	Coefficient of Correlation
Cluster10	R5	S10-16	S10-04	0.8741
	R6	S10-05	S10-03	0.9195
	R6	S10-07	S10-01	0.9577
	R7	S10-09	S10-02	0.9058
	R7	S10-11	S10-02	0.9139
	R8	S10-01	S10-07	0.9577
	R9	S10-04	S10-03	0.8248
	R9	S10-13	S10-16	0.8301
Cluster 9	R5	S09-03	S09-04	0.843
	R5	S09-06	S09-01	0.8771
Cluster 7-8	R6	S08-06	S09-04	0.8777
	R7	S08-03	S07-b	0.6574
	R7	S08-07	S08-01	0.8976
	R7	S08-08	S08-02	0.7841
	R8	S08-03	S07-b	0.6574
	R8	S08-04	S07-b	0.7625
Cluster 7	R5	S07a-7a	S07-05	0.5149
	R6	S07-04	S07-05	0.942
	R6	S07-a	S07-b	0.5313
	R6	S07a-7b	S07-06	0.9329
	R10	S07-02	S07-04	0.8641
Cluster 7-6	R5	S06-05	S07-05	0.9335
	R6	S06-05	S07-05	0.9335
	R10	S06-02	S07a-02	0.641
	R10	S06-03	S07a-02	0.6245
Cluster 4	R8	S04-03	S04-04	0.7252
	R9	S04-09	S04-10	0.7368
Cluster 2	R5	S02-03	S02-02	0.2889
	R5	S02-11	S02-30	0.8795
	R6	S02-14	S02-05	0.8877
	R6	S02-30	S02-08	0.9859
	R7	S02-02	S02-22	0.5352
	R10	S02-06	S02-07	0.9249
	R10	S02-08	S02-04	0.8741

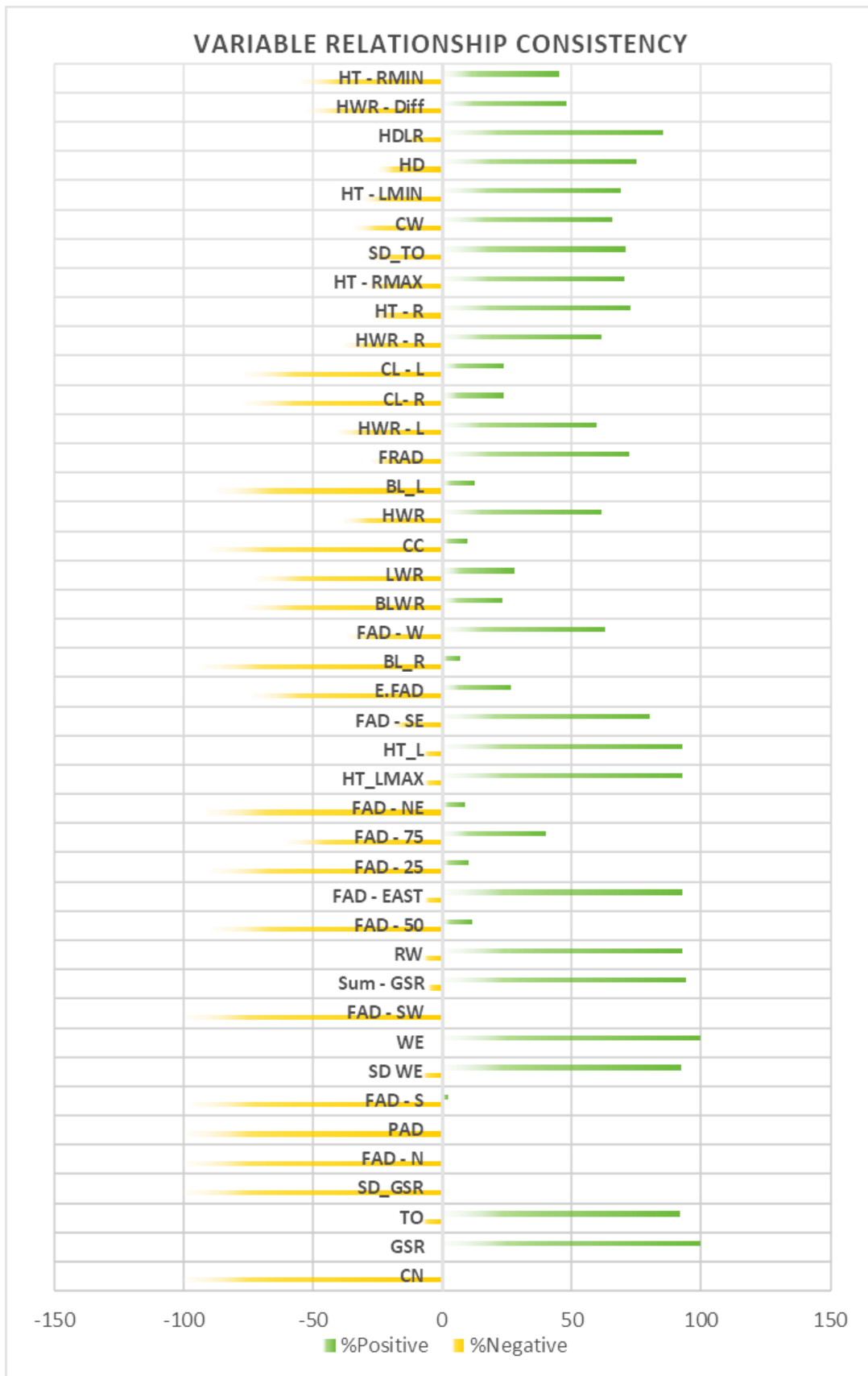
9.3 Air Quality Observations - Data Used for the Study

Code	Station Name	Summer (June-August)			Autumn (September - November)			Average			Cluster Average
		R5	R6	R7	R8	R9	R10	Summer	Autumn	Overall	
S04-01	1 WORSHIP ST	38.82	42.71	32.03	42.94	47.71	46.22	37.85	45.62	41.74	62.21
S04-03	3 WORSHIP ST (W)	40.55	40.81	36.23	51.04	44.90	55.18	39.20	50.37	44.78	
S04-04	4 Worship St	39.80	45.29	41.73	56.81	57.51	59.35	42.27	57.89	50.08	
S04-08	8 Bishopsgate	58.46	80.97	67.10	69.66	75.94	74.18	68.84	73.26	71.05	
S04-09	9 210 Bishopsgate	52.30	76.57	62.58	80.79	67.59	79.72	63.82	76.04	69.93	
S04-09a	9a Bishopsgate	69.79	77.65	53.41	68.42	63.71	67.97	66.95	66.70	66.82	
S04-10	10 Top of Bishopsgate	54.79	80.18	58.36	74.29	65.07	67.98	64.44	69.11	66.78	
S04-07	7 Liverpool St	80.15	109.94	80.67	78.16	82.39	87.76	90.25	82.77	86.51	
S07a-01	1 Junction (N)	72.67	124.79	86.32	90.10	79.64	84.44	94.59	84.73	89.66	80.51
S07a-02	2 Junction (W)	83.82	127.62	75.17	77.82	73.62	77.56	95.54	76.33	85.94	
S07a-04	4 Bishopsgate	78.90	109.23	83.63	85.39	73.34	92.40	90.59	83.71	87.15	
S07a-05	5 Bishopsgate (SS)	77.29	112.12	81.57	36.34	79.13	85.75	90.33	67.07	78.70	
S06-02	2 63 Camomile St	80.95	75.57	54.55	64.87	64.76	63.51	70.35	64.38	67.37	
S06-03	3 Camomile St	71.16	76.00	62.04	60.90	67.54	65.29	69.73	64.58	67.15	
S06-05	5 Camomile St	95.94	95.56	91.17	85.19	74.20	83.59	94.22	81.00	87.61	
S07-02	2 ST MARY AXE CUSTER (S)	40.67	53.29	42.22	42.31	50.71	46.78	45.39	46.60	46.00	
S07-04	4 BURY ST (S)	34.12	27.98	34.72	41.61	50.71	44.73	32.27	45.68	38.98	
S07-05	5 BURY ST (N)	31.83	30.39	36.27	43.75	50.13	45.22	32.83	46.37	39.60	
S07-06	6 ST MARY AXE (N)	38.20	41.34	36.89	41.29	46.95	44.80	38.81	44.35	41.58	
S07-a	7-a Lime Street (ZOFC)	47.74	47.51	54.99	40.24	40.64	55.26	50.08	45.38	47.73	
S07-b	7-b Lime Street (ZOFC)	35.44	38.65	34.26	38.47	49.37	34.89	36.11	40.91	38.51	
S07a-7a	7a (7) Gracechurch	82.82	85.35	73.93	83.14	65.81	69.64	80.70	72.86	76.78	
S07a-7b	7b 3 Bishopsgate	70.45	67.33	73.79	68.92	60.96	60.62	70.52	63.50	67.01	
S08-01	1 ROOD LANE	31.08	33.86	39.71	37.45	42.36	41.83	34.88	40.54	37.71	43.68
S08-02	2 ROOD LANE	41.91	48.53	42.82	49.64	54.13	56.88	44.42	53.55	48.98	
S08-03	3 PHILPOT LANE (N)	44.83	38.08	32.31	34.50	62.90	47.23	38.41	48.21	43.31	
S08-04	4 Philpot Lane (S) (ZOFC)	39.02	34.59	36.06	36.92	53.51	40.10	36.56	43.51	40.04	
S08-06	St mary-at-Hill	57.57	42.83	33.40	33.74	46.08	37.94	44.60	39.25	41.93	
S08-07	Eastcheap S	32.73	42.74	53.59	47.38	64.44	53.37	43.02	55.06	49.04	
S08-08	Eastcheap N	41.38	46.05	41.93	44.22	45.31	49.51	43.12	46.35	44.73	
S09-01	1 Old Watermans Walk	35.28	31.38	34.08	39.13	49.62	41.83	33.58	43.52	38.55	
S09-02	2 OLD WATERMANS WALK	39.35	35.23	31.66	34.30	49.33	41.83	35.41	41.82	38.62	
S09-03	3 OLD WATERMANS WALK	63.55	49.51	42.59	51.90	54.82	50.03	51.89	52.25	52.07	
S09-04	4 LOWER T STREET	80.70	66.81	53.19	63.59	69.83	61.64	66.90	65.02	65.96	
S09-05	09-05 Lower Thames St	83.54	80.33	67.66	71.71	78.73	58.49	77.18	69.64	73.41	
S09-06	9-05a Monument St	49.64	49.10	46.52	53.00	59.38	52.78	48.42	55.05	51.74	

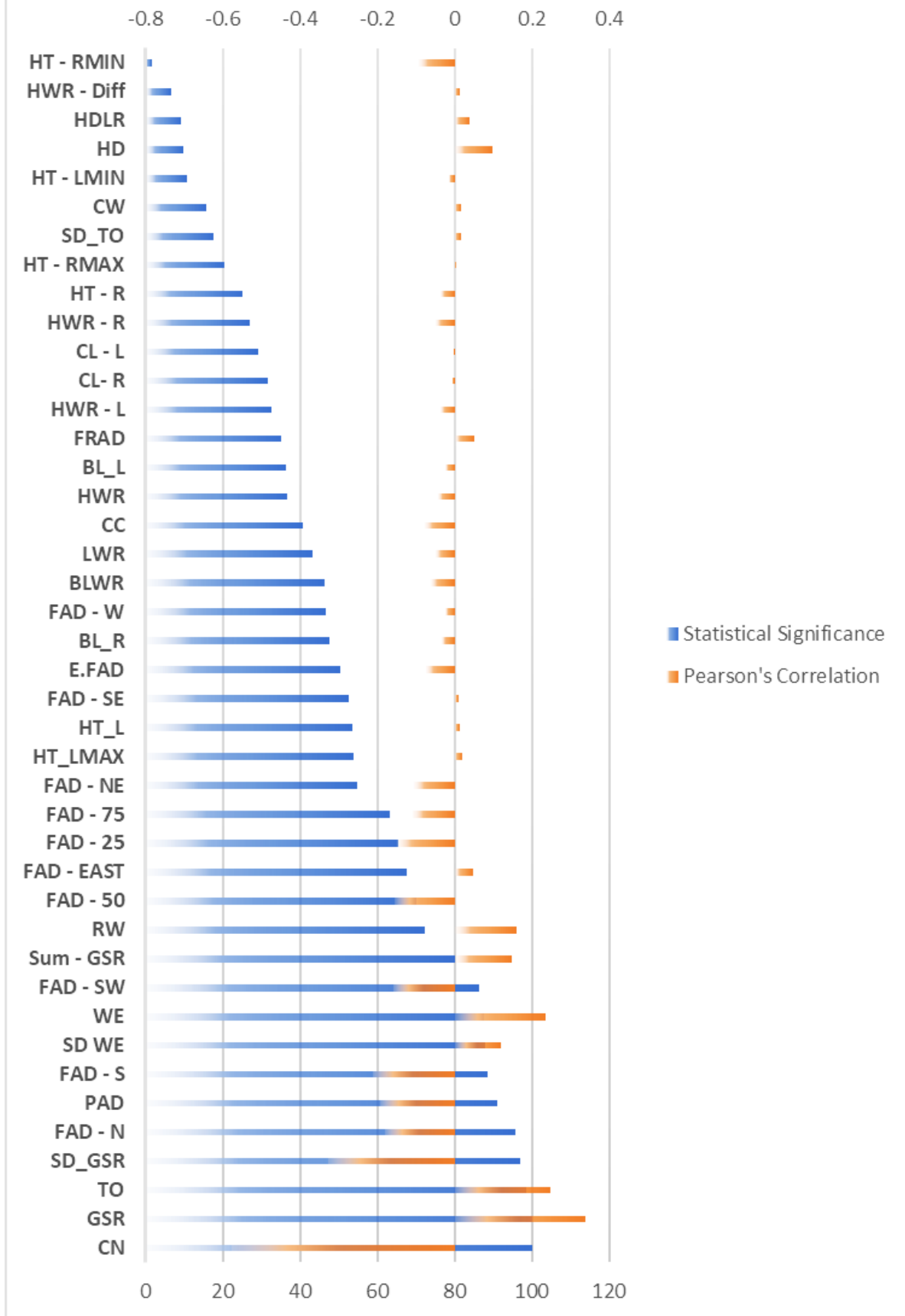
S10-01	1 THREADNEEDLE ST (W)	83.47	92.84	73.63	78.61	78.18	67.75	83.31	74.84	79.08	69.10
S10-02	2 PRINCES ST (S)	64.30	76.14	79.47	86.14	87.49	83.77	73.30	85.80	79.55	
S10-03	3 PRINCES ST (N)	54.22	72.98	67.90	78.19	73.66	91.94	65.03	81.26	73.15	
S10-04	4 MOORGATE (S)	64.19	69.81	72.26	85.17	76.22	87.64	68.75	83.01	75.88	
S10-05	5 LOTHBURY (N)	48.83	59.16	53.03	65.79	59.27	69.50	53.68	64.85	59.27	
S10-06	6 THROGMORTON (W)	33.87	42.51	45.48	43.92	50.19	71.38	40.62	55.16	47.89	
S10-07	7 THREADNEEDLE ST (E)	75.09	91.52	63.68	68.65	68.31	49.17	76.76	62.04	69.40	
S10-09	9 LOMBARD ST	57.40	60.95	64.59	66.55	70.77	67.54	60.98	68.29	64.63	
S10-10	10 MANSION HOUSE (E)	68.19	80.15	84.41	80.38	90.34	93.42	77.58	88.05	82.81	
S10-11	11 ROYAL EXCHANGE	50.36	61.15	61.69	63.11	68.58	65.59	57.73	65.76	61.75	
S10-12	10-12 28 Throughmortons	38.04	37.53	39.61	38.90	42.71	47.99	38.39	43.20	40.80	
S10-13	10-13 Moorgate	66.29	56.50	58.48	69.77	52.20	66.18	60.42	62.71	61.57	
S10-14	10-14 Moorgate 69	114.52	111.10	123.99	137.64	113.91	94.37	116.54	115.31	115.92	
S10-15	10-15 Moorgate	74.21	58.74	69.30	71.97	70.60	55.53	67.42	66.03	66.72	
S10-16	10-16 Moorgate	51.68	57.66	54.14	66.62	51.57	66.47	54.49	61.55	58.02	

S02-09	9 MOORGATE	76.84	77.71	69.65	87.86	82.15	76.84	74.73	82.28	78.51	53.65
S02-19	19 Moorgate (2)	75.63	82.74	78.36	83.91	90.49	71.92	78.91	82.11	80.51	
S02-21	21 South Place Mid Island	52.10	60.99	51.87	56.16	59.61	60.39	54.98	58.72	56.85	
S02-22	22 Near Wilson St	49.51	69.00	49.48	59.08	58.21	65.66	56.00	60.98	58.49	
S02-04	4 ROPEMAKER (N)	35.35	42.25	37.62	47.39	49.39	46.58	38.40	47.79	43.10	
S02-02	2 South Place	50.87	64.37	39.91	48.55	47.63	55.25	51.72	50.47	51.09	
S02-03	3 ROPE MAKER	48.57	43.99	46.45	53.99	45.03	47.44	46.34	48.82	47.58	
S02-05	5 MILTON ST	36.40	38.24	36.87	48.55	44.42	48.03	37.17	47.00	42.08	
S02-06	6 ROPEMAKER (W) (N)	41.35	38.79	34.69	43.41	56.72	52.14	38.28	50.76	44.52	
S02-07	7 MOOR LN (M)	38.68	36.68	31.11	41.13	47.25	45.22	35.49	44.53	40.01	
S02-08	8 Ropemaker (E)	40.45	43.06	38.09	46.70	46.96	45.55	40.53	46.40	43.47	
S02-09	9 MOORGATE	76.84	77.71	69.65	87.86	82.15	76.84	74.73	82.28	78.51	
S02-11	11 BREWERY BEACH ST	49.76	59.49	43.59	58.87	56.78	57.29	50.95	57.65	54.30	
S02-14	14 Ropemaker	44.43	43.84	40.97	52.20	47.45	53.62	43.08	51.09	47.09	
S02-16	16 City Point	46.28	45.10	36.09	50.74	46.45	51.32	42.49	49.51	46.00	
S02-30	Finsbury St (W) (M)	42.99	46.14	37.02	51.74	52.72	47.11	42.05	50.52	46.29	

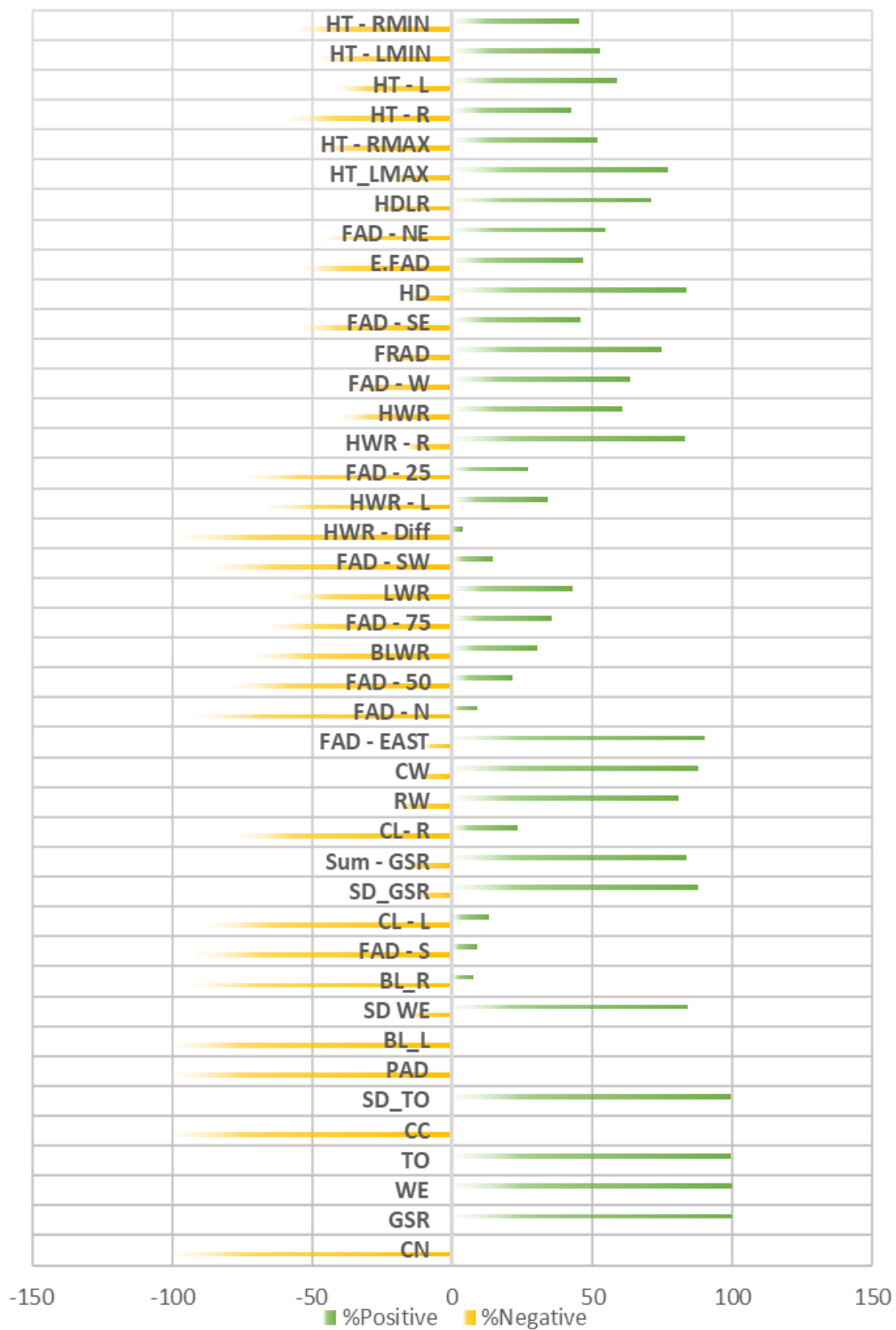
9.4 Urban form and the Wind Environment



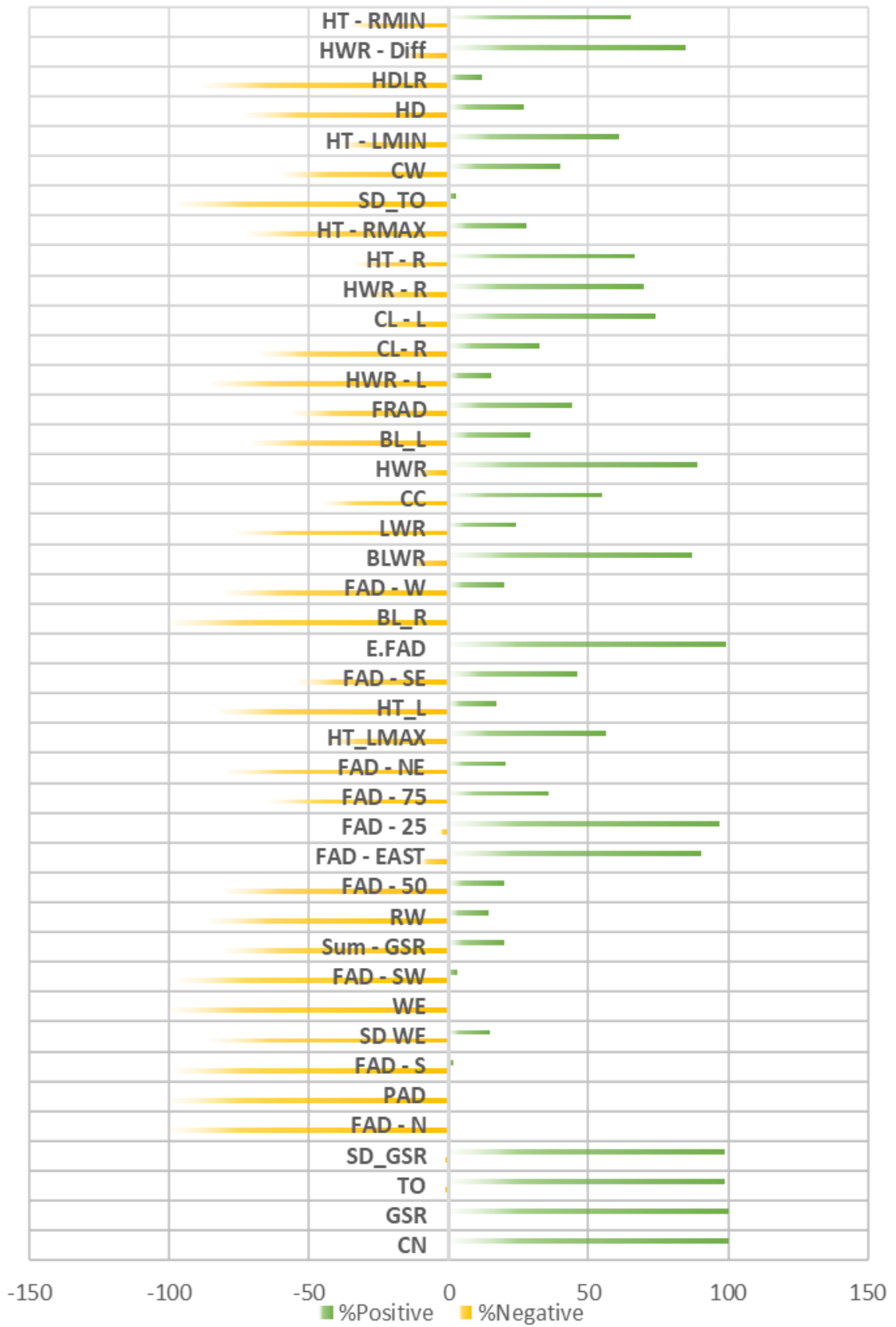
VARIABLE STATISTICAL SIGNIFICANCE & CORRELATION



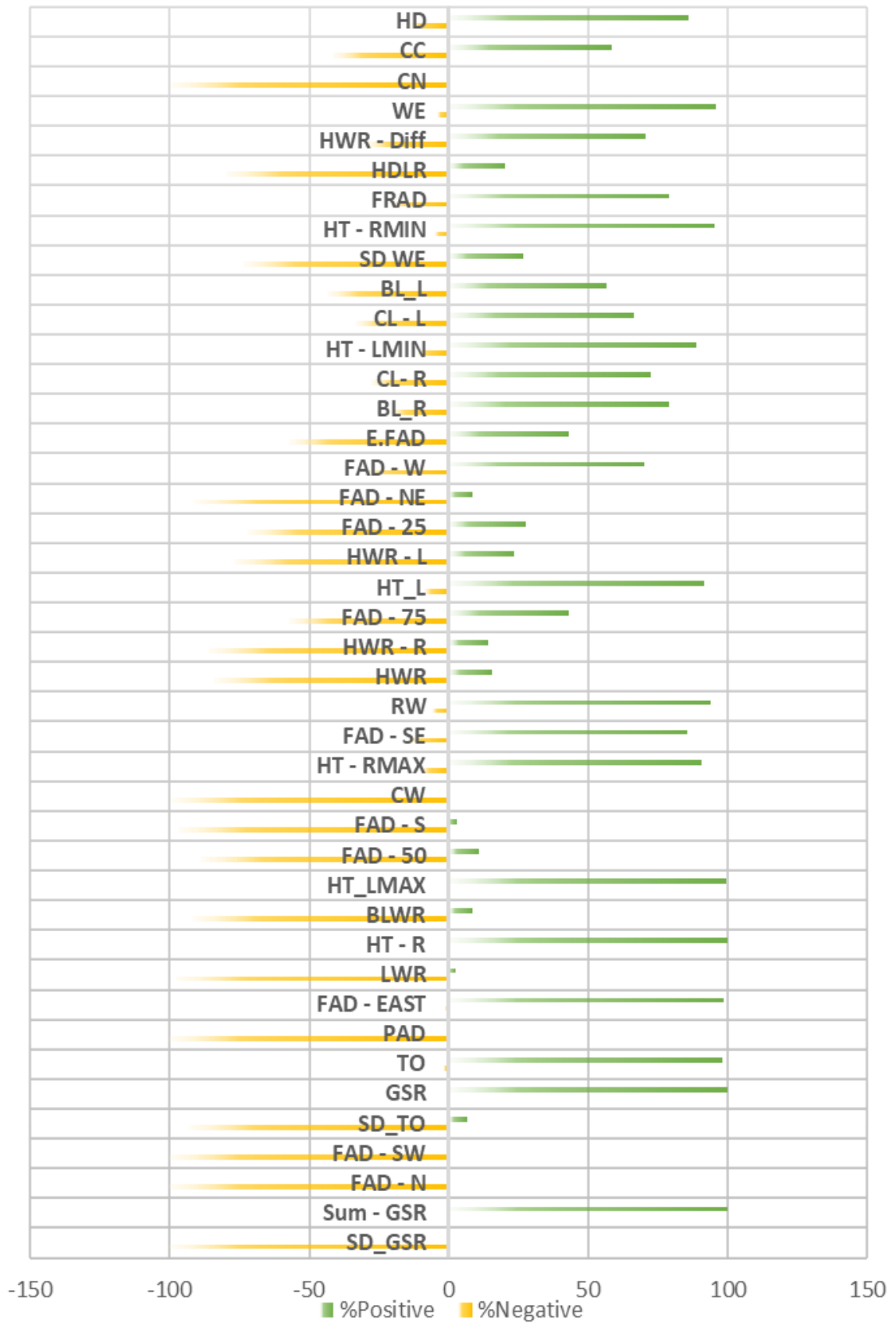
VARIABLE RELATIONSHIP CONSISTENCY - HIGH NORMALITY



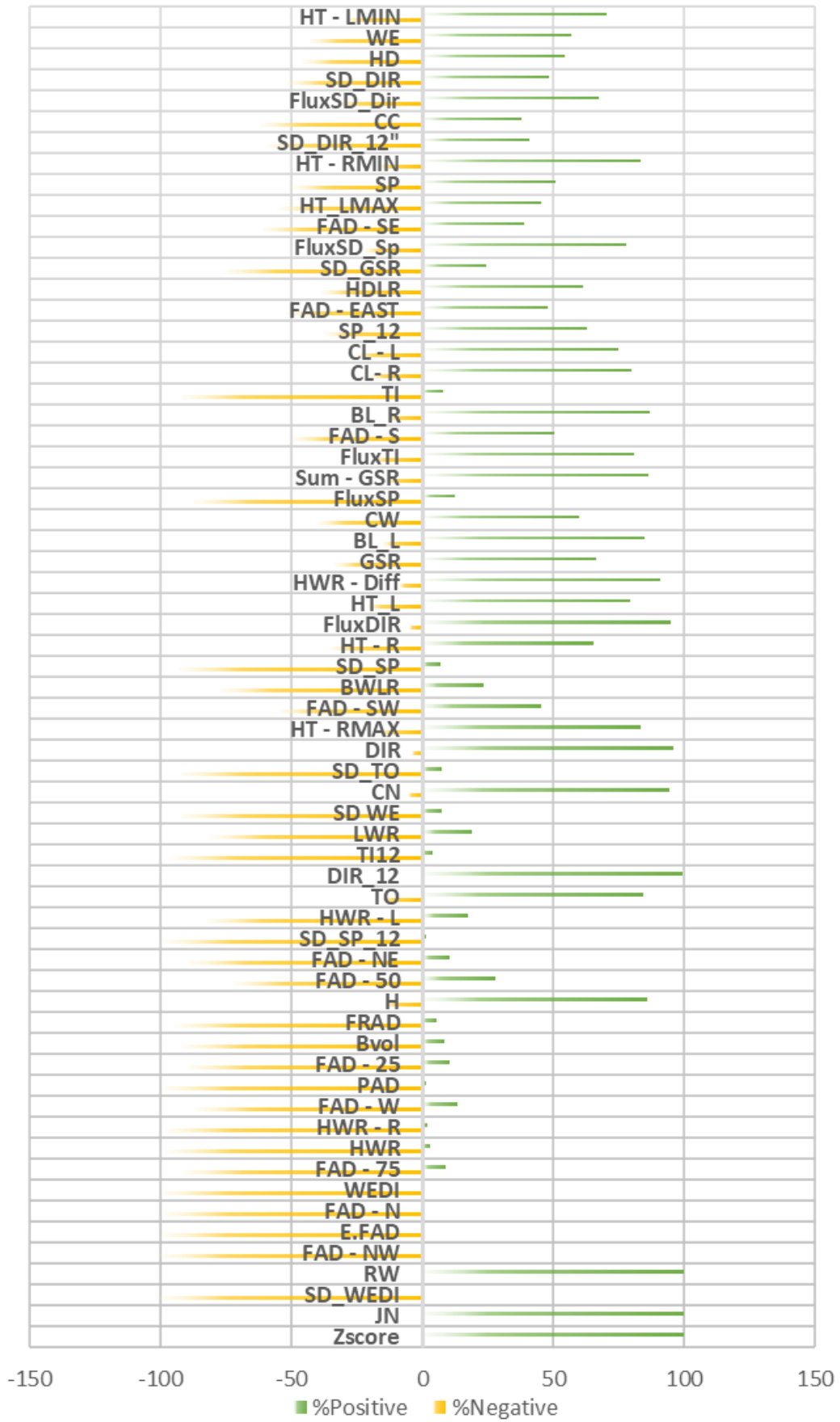
VARIABLE RELATIONSHIP CONSISTENCY - MEDIUM NORMALITY



VARIABLE RELATIONSHIP CONSISTENCY - LOW NORMALITY



VARIABLE RELATIONSHIP CONSISTENCY



VARIABLE STATISTICAL SIGNIFICANCE & CORRELATION

